Modelling collective motion and obstacle avoidance to assess avian collision risk with wind turbines

Simon Anthony Croft

PhD

University of York

Biology

September 2014

Abstract

Hazardous obstacles are a prominent feature of all natural environments and moving animals must demonstrate a robust avoidance response in order to prevent collisions. Whilst the study of collective motion has yielded many models for simulating animal movements, comparatively few have considered interactions with such obstacles. This thesis outlines a framework for incorporating obstacles into existing models of collective motion and uses these models to explore the impact of social interactions on collision risk.

The findings presented show that in the case of obstacle avoidance, where navigational information can be contradictory, the collective decisions of homogeneous groups often results in increased collision risk due to conflicting information between individuals. The introduction of heterogeneous social networks, which gives preference to particular individuals, acts as a natural mechanism by which these conflicted decisions may be averted, thereby facilitating coherent avoidance manoeuvres. However, this comes at the cost of cohesion, and groups must balance staying together against the benefits of more effective decision making.

The insights provided by models are applied to assess avian collision risk with wind turbines. This is an increasingly important ecological problem and has received wide attention. The difficulties in obtaining accurate empirical data at the individual level require that accurate and robust modelling solutions are developed. The models presented in this thesis provide a powerful tool in which collision risk can be assessed taking into account site- and species-specific factors. The key observation is that both social factors such as flock size, and spatial factors such as array design, significantly affect avoidance rates and consequently collision risk. Therefore the established methods of risk assessment, which assume a general avoidance rate and apply this to each individual independently, are argued to be inadequate.

List of contents

4 Obstacle avoidance in social groups: new insights from asynchronous models   **88**

5 Investigating the effect of obstacle layout and representation on collision risk with wind turbines   **121**

List of figures

List of tables

List of additional material

Supplementary films 1-4: simulations with underlying social network provided on compact disk.

Acknowledgements

There are lots of people I need to thanks for getting me through the last 4 years. Firstly, my supervisors Dr Jon Pitchford, Dr A. Jamie Wood and Richard Budgey. Whilst I may not have always been the easiest student to mentor I can assure them that their advice and "words of wisdom" have been invaluable and I am sure will serve me well in the future. As members of my thesis advisory panel Prof. Chris Thomas and Dr Dan Franks have helped to shaped my research, always managing to identify the next difficult questions to ask.

I gratefully acknowledge funding for this work from the University of York and the Food Environment Research Agency through a Department for Environment, Food and Rural Affairs Seedcorn grant.

Thanks go to my friends and family, particularly for all of the beers while I try to explain why birds fly into things. I want to say a special thanks my parents, for their love and support, both financial and emotional.

Finally, to my girlfriend Sarah, without your unwavering confidence in me even when I had lost my own, this thesis would not have been possible. I will be eternally grateful.

Author's declaration

I hereby declare that this submission is entirely my own work, except where due acknowledgement is given. This work has not been presented for an award at this, or any other, university.

Figure 1.2 is taken from "P. Plonczkier and I.C. Simms. Radar monitoring of migrating pink-footed geese: behavioural responses to offshore wind farm development. *Journal of Applied Ecology*, 49(5):1187–1194, 2012". Permission to reuse this figure has been granted by the publisher John Wiley and Sons under license.

The additional empirical data presented in Figure 3.7 was collected and supplied by Richard Budgey.

Chapters 2 and 4 have been published in peer-review journals and are presented as they appear in print with minor revisions to comply with examiners' comments. Details of these revisions are included in a preface section at the beginning of each chapter together with a brief section summarising the work in the general context of the thesis at the end. Full references for these publications are provided below and at the beginning of each chapter.

S. Croft, R. Budgey, J.W. Pitchford, and A.J. Wood. The influence of group size and social interactions on collision risk with obstacles. *Ecological Complexity*, 16: 77–82, 2013

S. Croft, R. Budgey, J.W. Pitchford, and A.J. Wood. Obstacle avoidance in social groups: new insights from asynchronous models. *Journal of The Royal Society Interface*, 12(106):20150178, 2015

Chapter 1

General introduction

1.1 Thesis motivation

The environments in which many animals live are cluttered with hazardous obstacles. These obstacles present a challenge to navigation, and moving individuals must possess robust avoidance behaviours in order to prevent collisions. Whilst animals appear to have evolved this behaviour in response to natural obstacles, such as trees and cliffs, collisions with man-made structures can be commonly observed. This is particularly evident in birds, to the extent that some scientists have claimed mortality as a result of these collisions is the largest unintended cause of avian fatalities worldwide (Banks, 1979; Klem Jr et al., 2004). As man-made structures begin to spread away from densely packed urban areas into the more remote environments occupied by a large numbers of bird species, it becomes increasingly important to understand the causes of collisions in order to develop sustainable mitigation strategies.

Initial studies have suggested that bird collisions may occur as a result of the limited changes in flight speed and manoeuvrability associated with maintaining flight (Bevanger, 1998; Janss and Ferrer, 2000; Drewitt and Langston, 2008). More recently arguments have be made that, in addition to these physical limitations, the visual perception of obstacles can have a significant impact on which avoidance response (Martin, 2011). However, as yet no studies have considered the role of social interactions in collision risk. Many species of bird exhibit social tendencies, for example moving together in large flocks or foraging in family groups. The purpose of this thesis is to outline a framework in which the interactions between groups and obstacles can be assessed. This involves combining the increasingly sophisticated field of collective motion with the ecological need to predict and understand collisions. In particular, the insights provided by such models will be applied to investigate the collision risk of birds with wind turbines used for power generation.

1.2 Collective motion in animals

The aggregation of animals can be observed at all scales of the natural world, from familiar human crowds and bird flocks, to fish schools, and even unicellular organisms like bacteria (Grégoire and Chaté, 2004). Several theories have been offered to explain this behaviour, these include, but are not limited to: social dependence; increased mating success; enhanced foraging capabilities; and dilution of predation risk (Abrahams and Colgan, 1985; Parrish and Edelstein-Keshet, 1999; Krause and Ruxton, 2002; Sumpter, 2006).

The study of collective motion attempts to categorise and explain the way in which these groups of animals move. Movement is an important animal capability; individuals are required to move in order to disperse, to find food or to escape predators. Often the movements within animals groups demonstrate a high degree of organisation (Bajec and Heppner, 2009; Viscido et al., 2005). This organisation can manifest in numerous different forms from the rigid v-shaped formations of migrating geese to the swirling vortices of sardines in response to attacks from predators. Murmurations of starlings swooping across the evening sky are a particularly striking example, where individuals appear to turn synchronously (Ballerini et al., 2008b). This led early scientists to hypothesise that they must be communicating telepathically (Selous, 1931).

Perhaps the most significant observation in the study of collective motion is that despite the limited sensory capabilities of individuals the size of groups displaying complex coordinated movement appears to be unbounded (Sumpter, 2006; Rackham, 1933; Buhl et al., 2006). Such groups containing many individuals can show a large degree of synchronisation over huge distances, for example a single shoal of herring can extend as far as 17 miles (Scheffer, 1985). At these distances even high levels of sensory perception would be unlikely to allow individuals to have knowledge of the motion of the group as a whole. Consequently, scientists have hypothesised that collective motion is likely to occur as a result of local interactions between neighbours (Aoki, 1980; Reynolds, 1987). Many numerical models have tried to investigate the

14

mechanisms underlying this behaviour. These numerical models have been developed to study collective motion in groups of animals including birds, fish, ants, bats, dolphins and locusts to name a few, (Kawasaki, 1978; Aoki, 1982; Huth and Wissel, 1992; Vicsek et al., 1995; Edelstein-Keshet et al., 1998; Czirók et al., 1999; Mogilner and Edelstein-Keshet, 1999; Couzin et al., 2002, 2005; Topaz et al., 2006; Eftimie et al., 2007; Codling et al., 2007; Bode et al., 2010a; Hildenbrandt et al., 2010; Hemelrijk and Hildenbrandt, 2011; Bode et al., 2011a, 2012a; Leonard et al., 2012). However, it is unclear whether the rules for interaction outlined in these studies have a clear empirical basis to merit their use in the movement models for other species (Cavagna et al., 2008).

1.2.1 Empirical studies of collective motion

Collective animal behaviour has been observed for over 2000 years (observations by Pliny in 200BC, translated by Rackham (1933)). Bird flocking is an eye-catching example of this that can be seen by a casual observer. However, the limitations of available technology to analyse this behaviour meant that initial scientific studies were capable only of qualitative assessment (Bajec and Heppner, 2009). Early studies attempting to quantify collective motion filmed or photographed animals, predominantly fish, in laboratory experiments (Aoki, 1980; Cullen et al., 1965; Partridge et al., 1980). This provided a closed, controllable environment allowing the trajectories of individual fish to be observed using positional data over time. The investigation by Aoki (1980) extracted critical data about group behaviour from these observations such as speed distributions, distance to nearest neighbours, turning events, internal structure and alignment of individuals. These key metrics are still used in studies today.

It is not necessarily possible to apply empirical data obtained from studies of fish to models of bird flocking because although they share some behaviours, there are other patterns that are present in one case and not in the other (Krause and Ruxton, 2002). For example, there are differences in the mechanisms of sensory perception

available to each taxa, birds primarily rely upon vision to determine motion whereas fish also have the capacity to use mechanical stimuli perceived via the lateral line, a system of sensory organs found in aquatic vertebrates which can detect vibrations in the surrounding environment. It has been argued that the latter causes the shape of sensory zones in fish to be more elliptical. The resulting motion of fish typically forms stable oblong shaped groups (Hemelrijk and Kunz, 2005). In contrast the constraints of flight behaviour, requiring birds to maintain a minimum speed, produces more variable and less stable structures (Hemelrijk and Hildenbrandt, 2012) The importance of distinguishing general characteristics from those that are situation specific has been highlighted by Ballerini et al. (2008b). This study also notes that experiments in the laboratory, and in confined spaces, may influence some features of groups such as their shape and dynamics.

Studies of collective motion in bird flocks present a greater experimental challenge since they can only be observed in real-world environments. Similarly to fish studies, the first attempts to track the movements of birds involved measurements in two dimensions (Sugg, 1965; Van Tets, 1966). These studies used a single photographic technique to estimate flock densities. As photographic techniques evolved it became possible to reconstruct trajectories for each individual in three dimensions. The approach described by Major and Dill (1978) captured the relative positions of individuals using single images from multiple cameras allowing them to successfully reconstruct the three-dimensional position of individual birds within small flocks (25–76 individuals). While this approach was useful for establishing the internal structure of specific flocks it cannot be used to investigate general flock dynamics (Pomeroy and Heppner, 1992). A non-stereo three-dimensional photographic technique, the orthogonal method, was proposed by Pomeroy and Heppner (1992) to study turning movements in flocks of Rock Doves. This technique allowed individual bird trajectories to be distinguished and provided information on group considerations during turning manoeuvres. Building on the work of Major and Dill, Budgey (1998) was able to reconstruct three-dimensional trajectories of various bird species using similar

stereoscopic techniques. This study was able to calculate nearest neighbour distances and link this variable to wing span. However, the flock sizes were limited to 61 individuals.

The use of small flocks in all these studies may have implications for the applicability of their findings to other situations, for example use in numerical models; there are boundary effects associated with there being larger numbers of individuals at the extremities of the flock and fewer in the centre (Ballerini et al., 2008a; Cavagna et al., 2008). Larger, more compact flocks were not studied because computational methods had not yet been developed to allow the analysis of the image data. The scarcity of similar studies and the time span of this work illustrates the difficulty associated with the collection of high quality, three-dimensional data (Ballerini et al., 2008b).

With advances in technology, stereometric and computer vision techniques were used in a landmark study by Ballerini et al. (2008a) which was able to measure the three-dimensional positions of individuals in flocks of up to 2600 birds. This represented an increase of two orders of magnitude in the flock size compared with previous studies, and a huge step forward for empirical observation of collective motion. It was the first study to provide insights into the hidden mechanisms underlying collective motion within large flocks. The findings showed that flocks maintain cohesion even when sparsely distributed and when under intense stimuli, but also that it seems sensible that the interactions between individuals will decay as the distance between them increases. This leads to a discussion of the most appropriate measure of distance over which interactions with neighbours can occur.

The majority of models at this time used metric distance to define the strength of interactions (e.g. Couzin et al., 2005). While this seems reasonable these models predict that when groups or individuals break apart sufficiently they would not regroup; this is not what is observed in nature. An alternative is to use topological distance, which would predict that it is the number of intermediate individuals separating the birds that determines the strength of interaction, rather than the distance between them. Observations of flocks at different densities (Ballerini et al., 2008a) revealed

that the topological range of interactions in the studied flocks was approximately constant, suggesting that on average individuals interacted with a fixed number of neighbours regardless of flock density. The number of individuals with which one bird would interact in this study was shown to be 6–7. There are previous studies whose results would seem to support the findings of Ballerini et al. (2008a). A study by Emmerton and Delius (1993) showed that pigeons can recognise distinct sets of objects so long as each set contains fewer than 7 objects. Tegeder and Krause (1995) found that fish have a perceptual limit of 3–5 neighbours. The work of Ballerini et al. (2008a) has changed the way in which some models parametrise the range over which interactions can occur.

A further complication is that animals have been to shown to display "personalities"; observations reveal that individuals exhibit behavioural differences that are consistent over time and in various contexts (Kurvers et al., 2009). One such personality trait is that of leadership influencing movement order. Beauchamp (2000); Dumont et al. (2005); Harcourt et al. (2009) show that movement order is consistent suggesting that some individuals will be leaders and others will follow. The concept of leadership and the reasons why certain individuals emerge as leaders has been the subject of several theoretical investigations (e.g. Couzin et al., 2005; Conradt et al., 2009; Bode et al., 2012a). Some of these suggest that, whilst personality may have a bearing on an individual's propensity to lead, it may in fact be a more transient property depending on situation-specific factors (Vicsek and Zafeiris, 2012). For example, initial work by Couzin et al. (2005) proposed that leaders emerge as a result of greater ability to perform a specific task, in this case knowledge of a given target location representing a food source or roosting site. Other studies have instead theorised that leadership occurs as a result of "need", with individuals for whom reaching a particular target location is most critical, for instance those motivated by food deprivation, changing their behaviour in order to influence group movements (Conradt et al., 2009). In such cases individuals must consider a "consensus cost" foregoing their own optimal behaviour in favour of retaining the benefits offered by

group movement (King et al., 2008).

To explore these ideas empirically, studies now can take advantage of GPS tracking as well as more advanced video tracking, computer vision and associated algorithms to study the interactions of animals in a group more thoroughly. For example, in a recent study these techniques have been used to investigate the leadership and dominance in groups of pigeons (30 individuals) by tracking their behaviour on the ground and in flight (Nagy et al., 2013). It was shown that social dominance while feeding does not correlate with leadership in flight. This may be due to the difference in interaction, because aggressive interactions in flight will not aid navigational decisions, or that other individual attributes (such as local experience and route fidelity) are more relevant than dominance (Flack, 2012; Freeman et al., 2011). Individuals at the front of a group are the first to arrive at new food sources and so have first access to nourishment, but being on the extremities of the group increases their risk of predation (Krause, 1994; Stankowich, 2003). The benefits and penalties for leadership and the fact that movement order is consistent gives weight to the idea that leaders may be fundamentally different from followers. This type of leadership as a consequence of social networks is a concept that is only recently being investigated in numerical models (Bode et al., 2012a).

With the advancements in computing in the late twentieth century, focus shifted from empirical studies to numerical modelling of collective behaviour. This is in part responsible for the decreased emphasis on empirical data but also for the development of the type of models we use today. It is still true that without essential empirical data there is no "ground-truthing" for models and it is difficult to know what model, rules and parametrisations are appropriate (Ballerini et al., 2008b).

1.2.2 Mathematical models for collective motion

Mathematical models of collective motion can be classified into two distinct types: Eulerian (or continuum) (Eftimie et al., 2007; Kawasaki, 1978; Mogilner and Edelstein-Keshet, 1999; Topaz et al., 2006) and Lagrangian (or individual-based) (Aoki, 1982;

Couzin et al., 2002; Huth and Wissel, 1992; Vicsek et al., 1995). Eulerian models determine motion using partial differential equations describing the mean-field density of groups (Parrish and Edelstein-Keshet, 1999). In such models rules for interaction are defined and implemented either locally (Edelstein-Keshet et al., 1998), or globally (Eftimie et al., 2007; Topaz et al., 2006). Typically, this approach is used to simulate the movements of large dense groups, such as swarms of insects, where finer individual-level detail is unnecessary and can be computationally expensive. In contrast, a Lagrangian approach is applied to simulate smaller groups with distinguishable individuals. In a similar way to Eulerian models rules for interaction are defined but are always applied locally. Using these rules for interaction, movement trajectories can be described continuously over time using precise, coupled ordinary differential equations (Niwa, 1996) though these can be difficult to resolve numerically (Parrish and Edelstein-Keshet, 1999). Instead, most Lagrangian models choose to dispense with equations entirely and determine motion over discrete time steps according to an algorithmic implementation of interaction rules from which collective motion can emerge (Reynolds, 1987; Czirók et al., 1999; Couzin et al., 2002; Codling et al., 2007).

These models are commonly referred to as individual-based models and this has become the most popular approach for simulating animal collective motion with each interaction rule providing an intuitive link to identifiable social or biomechanical behaviour, for example, avoidance of predators. Typically behavioural rules include repulsion, alignment and attraction, although not all models use all of these rules, for example arguing that alignment is unnecessary (Strömbom, 2011). The way in which these core rules are implemented differs greatly across studies depending on the situation that is being simulated.

Most models determine group motion by combining the response to each sensory stimulus as a weighted average. The response towards neighbours can be classified into three zones of interaction; repulsion, alignment and attraction. Figure 1.1 illustrates how these zones are organized. Generally models apply rules in a hierarchy, giving the highest priority to repulsion. In cases where repulsion is necessary, i.e. an imminent

collision, all other interactions are ignored (Couzin et al., 2005; Codling et al., 2007).

An early study by Couzin et al. (2002) investigated the effect of varying the level of alignment within groups. Where only attraction and repulsion are applied the result is a group with high levels of cohesion but low levels of polarization and low angular momentum, in other words a disorganized swarm such as that exhibited by insects (Figure 1.1(b)(i)). When the alignment zone is small compared to the attraction zone the resulting group moves in a toroidal pattern similar to the structure observed in shoals of fish during attack from predators (Parrish and Edelstein-Keshet, 1999) (Figure 1.1(b)(ii)). Increasing the radius of the alignment zone further, groups become highly polarized and well aligned such as the familiar behaviour of flocking birds (Figure 1.1(b)(iii)). This goes some way to demonstrate that simple rules of interaction can reproduce the different types of group behaviour seen in nature (Wood and Ackland, 2007).

As demonstrated above, when considering interaction zones a distance over which these interactions occur must be defined. Generally models use a metric system to limit the zones but following the work of Ballerini et al. (2008a) some models have chosen to use an alternative measure of distance. As a result of the empirical data showing that birds interact with a distinct number of nearest neighbours models have applied a limit on interactions topologically. This modifies the zones of interaction to consider only a fixed number of neighbours (Hildenbrandt et al., 2010; Hemelrijk and Hildenbrandt, 2011; Codling and Bode, 2014).

The majority of models assume that individuals are identical (Bode et al., 2010a). In some models there is a degree of heterogeneity introduced by varying the amount of information that individuals possess, that is whether they are an informed individual or not (Couzin et al., 2005; Leonard et al., 2012). In nature, when moving in groups there may be only a few individuals that have information about the location of a food source or a migratory route (Swaney et al., 2001; Franks et al., 2002; Seeley et al., 1985). Using a simple model Couzin et al. (2005) showed how a few informed individuals can facilitate successful motion within groups even when there is no perceivable
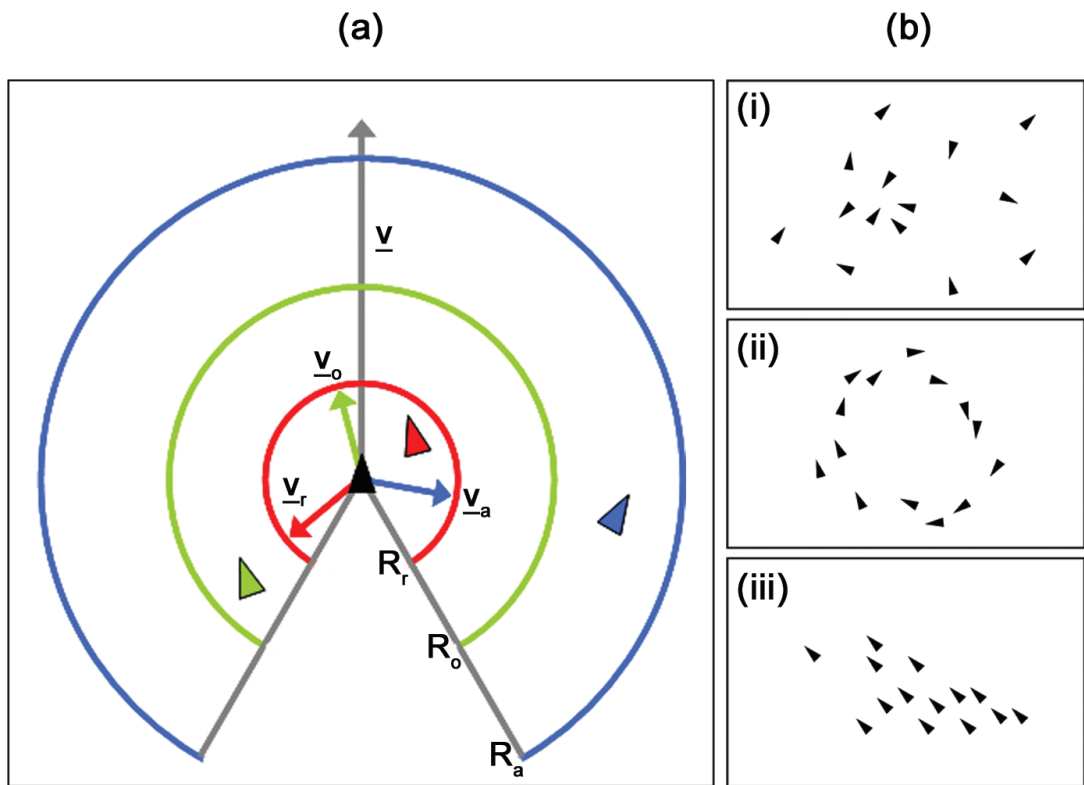
Figure 1.1: An illustration outlining the basic rules for simulating social movement with examples of characteristic patterns seen in nature which can be reproduced under different parameterisation of the zones of interactions (redrawn from Couzin et al. (2002)). (a) shows the social response of an individual (black) to neighbours located within each of the distinct zones of interaction: repulsion (red); alignment (green); attraction (blue). (b) shows ; (i) disorganised motion produced when only attraction and repulsion is applied; (ii) toroidal motion produced when a small alignment zone is added; (iii) highly polarised motion produced when the zone of alignment is further increased.

distinction between informed and uninformed group members. This study also showed that the larger the group the smaller the proportion of informed individuals necessary to enable successful navigation. Other models introduce heterogeneity by introducing noise to represent imperfect sensing or movement abilities (e.g. Codling et al., 2007). In both cases the variability in information or ability does not affect the stability of group structure or ability to move as a group. By averaging throughout the group information is passed between individuals, balancing out individual deficiencies and maintaining a stable and cohesive group. A consequence of the robust nature of group structure and stability of collective motion in this approach is that it is difficult to distinguish the effects of individual rules (Bode et al., 2012a).

Scientists have tried to match models to empirical data by simulating particular features, for example limiting neighbours to a fixed number as discussed above. Similarly, most models apply a constant homogeneous speed (e.g. Couzin et al., 2002) but there are some (e.g. Aoki, 1982) that use variable speeds based upon the observed speed distributions in empirical studies. However, by applying constraints such as these, the emergent nature of collective motion can be difficult to recreate.

Initially proposed as a method to investigate and understand the mechanisms that produce the varied speed distributions seen by Aoki (1980), Bode et al. (2010a) suggest a new asynchronous update scheme. In previous models, during every time step all individuals react to their local stimuli and update their positions and orientations together – that is synchronously. In Bode et al. (2010a) instead individuals are selected at random each time step. This means some individuals may update more than once and others not at all. This method of updating produces speed distributions similar to those seen in nature without the need for a priori assumptions or the addition of stochastic noise. In order to maintain cohesion it was found that a higher speed of attraction was required; approximately double that of other behaviours. As part of this work laboratory studies were conducted to record speed and nearest neighbour distributions from fish under varying levels of perceived threat. This showed that variations in the frequency at which model updates occur reproduced

these distributions, with faster updates corresponding to increased levels of threat. This would appear to reproduce behaviours seen in nature where individuals attempt to avoid being morphologically or behaviourally distinctive relative to other group members when threat is perceived (Ward et al., 2008). The details of this modelling approach, and it's computational implementation, are discussed in more detail in Chapter 5.

Further developments of this modelling approach (Bode et al., 2011a) have incorporated the use of random sensory zone sampling. Rather than responding to all neighbours within a fixed distance an individual instead chooses a single neighbour to interact with. The probability of selecting a particular neighbour is weighted inversely with distance. Using this approach it was possible to reproduce emergent topological properties within groups consistent with the empirical observations of Ballerini et al. (2008a).

The impact of social networks has been explored in Bode et al. (2011b) using the same model as previous studies (2011a) but applying an underlying preference for particular neighbours according to an interaction matrix. A "social network" represents the preferences of individuals to associate or interact with other individuals within a group. Studies of animal groups have shown that individuals may show preferences for familiar individuals or those with certain characteristics and that structures may emerge as a result of these preferences (Krause et al., 2014). Empirical observations of groups are used to assess the preferences displayed and to construct an interaction matrix. In some cases this is done by weighting connections between individuals according to the number of times interactions are observed. An alternative approach determines a connection to be significant if the interaction is observed more than a fixed number of times, a minimum threshold. No further distinction is made between the connections determined to be significant; no weighting is applied, connections are either significant or they are not (Croft et al., 2008). Once constructed network analysis techniques can be used to identify non-random characteristics, such as clustering, which may explain behaviours at a population level (Newman, 2010).

Defining social networks empirically remains a challenge for ecologists and careful consideration must be given to the context in which interactions occur (Wey et al., 2008); in the absence of context, which is typical in cases where direct observation is difficult, it is often assumed that all members of a group are interacting and part of the same social network, an assumption also known as "the gambit of the group" (Whitehead and Dufault, 1999). It is far easier to observe where individuals are part of a group than to assess which individuals are interacting with each other. Advancement of empirical methods, i.e. GPS technology, allows ecologists to observe individual movements in more detail and infer social interactions. For example by comparing relative changes in direction and alignment of individuals, information about social interactions and networks can be inferred. Bode et al. (2011b) assert that the addition of social networks into their model could explain the hierarchical dynamics observed by Nagy et al. (2010) in flocks of pigeons.

One of the particular benefits of the modelling approach used by Bode et al. (2011a) is the emergence of stochastic noise from the algorithmic implementation. Noise is often added to models to represent imperfect decision-making or sensory capabilities. As models become more complex, for example with the inclusion of social networks, it becomes more difficult to identify a suitable noise term. Whilst previous studies (Aoki, 1982; Hildenbrandt et al., 2010) have shown that models can reproduce specific empirical observations, the constraints necessary to achieve this limit their general applicability. The three studies by Bode et al. (2010a; 2011a; 2011b) show that an asynchronous modelling approach begins to bridge the gap between the collective motion observed in empirical studies and that reproduced by numerical models.

1.2.3 Obstacle avoidance in models of collective motion

Considering the wide range and scope of studies investigating collective motion it is surprising that few include mechanisms for the avoidance of obstacles. This is perhaps a reflection of the difficulties involved in representing obstacles simply, and in defining

rules that reflect the visual perception of them.

One of the most notable studies of collective motion which includes obstacle avoidance is the "boids" model developed by Reynolds (1987). The motivation of this study was to develop a robust alternative to scripted collective behaviour in computer animations. The methods for representing obstacles in this model are based on early computer graphics techniques. These define a set of basic geometric shapes which can be used to construct complex obstacles. Whilst it was shown that general behavioural rules could be applied to interact with obstacles (Reynolds, 1988), a particular drawback was that each shape possessed distinct geometric properties requiring different computational processes.

As technology has evolved computers have become faster and more powerful allowing vast amounts of data to be processed. The demand for realistic real-time computer graphics in games and motion pictures has led to the development of many sophisticated techniques for modelling objects. One of the most popular methods uses an approach which describes objects using a technique known as polygon meshing (Botsch et al., 2010). Using this technique a solid surface can be reconstructed by a finite set of interconnecting polygons, usually triangles, each of which is defined by an ordered set of vertices and a normal vector describing its relative orientation in space. By reducing the size of polygons highly accurate three-dimensional shapes can be represented. Whilst this approach has been applied successfully to many applications in computer science, such as facial recognition software (Lu et al., 2004) and three-dimensional reconstructions of objects using stereoscopic vision techniques (Hartley and Zisserman, 2003), it has yet to be adopted in models of collective motion. The methods of obstacle representation used in this thesis develop some of the key ideas from Reynolds (1987), while allowing for both computational efficiency and more realistic interactions between birds and obstacles.

Obstacle avoidance in simulations of collective motion has also been developed for applications in other areas of artificial systems, such as robotics (Lindhe et al., 2005). Whilst informative, similar to Reynolds (1987) the primary motivation for such studies

has been to provide a framework for "perfect" avoidance, i.e. to render collisions impossible, and behavioural rules have therefore been implemented to conform to this. It is clear that obstacle avoidance is not perfect in the real world (Banks, 1979; Martin, 2011), and so the general applicability of these existing models to biological systems is not necessarily justified. However, some of the approaches which have been developed for perfect avoidance may be applicable after careful modification.

In biological systems obstacle avoidance has been considered in models of collective motion to investigate escape dynamics of human crowds (Helbing et al., 2000; Frank and Dorso, 2011). These models use a force-based approach to determine the direction of motion. Individuals experience repulsive or curb-crawling responses to obstacles, such as walls, providing a mechanism to explore smoke filled environments and discover nearby exits. Further extensions of this work dispense with a distinct obstacle avoidance response, instead encoding this information into a floor field which influences the navigational route of individuals (Bode et al., 2014). Whilst these methods for simulating behavioural response are suitable for situations in closed environments, such as buildings, they are perhaps less applicable for applications where more open and unrestricted motion is possible. In such environments long distance pre-emptive avoidance strategies may occur resulting in a less extreme response than that required at close distances. Additionally, for birds the use of repulsion in force-based models can be problematic as conflicts have the potential to slow the movement reducing an individuals ability to maintain flight (Reynolds, 1987).

1.3 Birds and wind farms

1.3.1 Renewable energy in the UK

There is growing pressure on governments to implement immediate mitigation strategies to offset the effects of unsustainable greenhouse gas emissions and to stem climate change. Advancements in renewable technologies to generate energy provide a significant part of the proposed strategy. In Europe, members of the EU have

committed to a substantial shift towards renewable energy, imposing a target of sourcing 20% of energy from renewable technologies by 2020 (Commission of the European Communities, 2007). The current technologies that present a viable option to contribute to this increased demand include solar power, hydropower, geothermal energy and wind power. Of these, wind power is predicted to provide one of the more significant contributions (Larsson, 1994). This observation was validated in a recent review of renewable energy in the UK, identifying wind power, and in particular offshore wind power technologies, as key growth areas for development. This report anticipated that by 2030 wind power could potentially provided as much as 75% of renewable energy and nearly 50% of all energy in the UK (Committee on Climate Change, 2011). Statistics provided by Renewable UK, formally BWEA, demonstrate this commitment to the development of the wind power industry in the UK with plans to double the number of operational wind farms from 306 to 563 with further plans for an additional 283 wind farms (UK Renewables, 2012).

1.3.2 The impact of wind power on birds

As with all energy generation technology, there are economic, social and environmental impacts associated with wind farm developments. The rapid deployment of wind power has made it difficult for environmental assessment methodologies to maintain pace (Drewitt and Langston, 2008). While wind farms present clear benefits to the UK carbon budget, there are concerns that the wind farm developments are likely to impact negatively on the distribution and abundance of wildlife, particularly birds (Elphick, 2008).

Potential impacts of wind farms on bird populations can be categorized into three types: direct mortality of individuals as a result of collision with turbines and infrastructure; modification of the physical habitat as a consequence of the footprint of the turbines and associated structures; and behavioural responses of birds to turbines (Fielding et al., 2006; Fox et al., 2006). The latter considers the possibility that wind farms could form a barrier to movement with birds choosing to avoid them entirely

(Masden et al., 2009). Whilst this response reduces the risk of collisions with wind farm structures it could have significant energetic costs as birds are required to travel greater distances. Though the impact that this may have on populations is yet to be fully assessed migration studies have suggested that energetic efficiency can be related to the survival fitness of birds (Pennycuick, 2008).

1.3.3   Empirical estimates of collision risk

In order to quantify the levels of mortality as a result of collisions, impact studies have been conducted globally both pre and post construction (Desholm and Kahlert, 2005; Drewitt and Langston, 2008; Cook et al., 2012; Plonczkier and Simms, 2012). Direct observation of fatalities is limited to terrestrial sites (onshore) where a method of corpse retrieval can be employed (Barrios and Rodriguez, 2004; Langston and Pullan, 2003). In general, these studies have indicated that collision rates are low, though quantitative estimates are subject to significant observational error with corpses removed by scavengers or simply not detected (Morrison, 2002). As a result it is likely that actual collision rates could be significantly higher.

Estimating collision risk at marine sites (offshore) presents a much greater challenge and the majority of studies have instead focused on estimating avoidance rates around wind farms using remote sensing techniques such as Thermal Animal Detection Systems (TADS) and radar surveillance (Desholm et al., 2006; Plonczkier and Simms, 2012). These studies have shown that the activity of birds within the footprint of wind farms is significantly reduced (Desholm and Kahlert, 2005) confirming the notion that wind farms act as a barrier to movement (Masden et al., 2009). For migratory birds, such as geese, estimates indicate that between 50 and 70% of all groups show avoidance behaviour (Cook et al., 2012). Of those birds which enter the wind farm footprint, only around 10% pass close enough to a wind turbine (approximately 50 metres) to risk any chance of collision (Desholm and Kahlert, 2005). In addition to these observations a recent long-term radar study which mapped the movement patterns of geese over a number of years both pre- and post- construction, summarised in figure

1.2, has revealed that flocks displayed a growing tendency for avoidance behaviour (Plonczkier and Simms, 2012).

1.3.4 Modelling collision risk

Modelling provides a method of prediction without the need for extensive site surveys by using basic pre and post construction data to determine risk over a wide range of environmental and engineering scenarios. The most widely accepted Collision Risk Model (CRM) is that described by Band (2000). The methodology consists of a two-stage probabilistic approach that combines aspects of data describing the structure and operation of a wind turbine with attributes of bird physiology and flight in order to predict mortality. The first stage of the process estimates the number of birds that pass through the rotor blades or "risk window". The second stage of the process calculates the probability of a bird passing through the risk window being struck by a rotor blade. The approach uses data describing the structure and operation of the turbines: number of blades; maximum chord width and pitch angle of blades; rotor diameter; and rotation speed; and of bird size and flight: body length; wingspan; flight speed; flapping; or gliding flight, to derive a probability of collision. Mortality is then estimated by multiplying the collision probability by the number of birds passing through the area at risk height.

Crucially, however, this initial model assumes that an individual bird takes no avoiding action when encountering a turbine, so an adjustment must also be made for avoidance behaviour. This was addressed in the revised version of the model (Band et al., 2005) through the addition of an avoidance factor which scales the determined collision probability. However, this modification has since come under significant scrutiny due to the inaccuracies involved in estimating suitable values. These values are reliant upon empirical data combining the avoidance rates from remote studies (macro avoidance) with collision rates observed at terrestrial sites (micro avoidance) to generate a single estimate for each species of bird (Cook et al., 2012), for example current advice for wintering geese calculates the rate of avoidance to be approximately
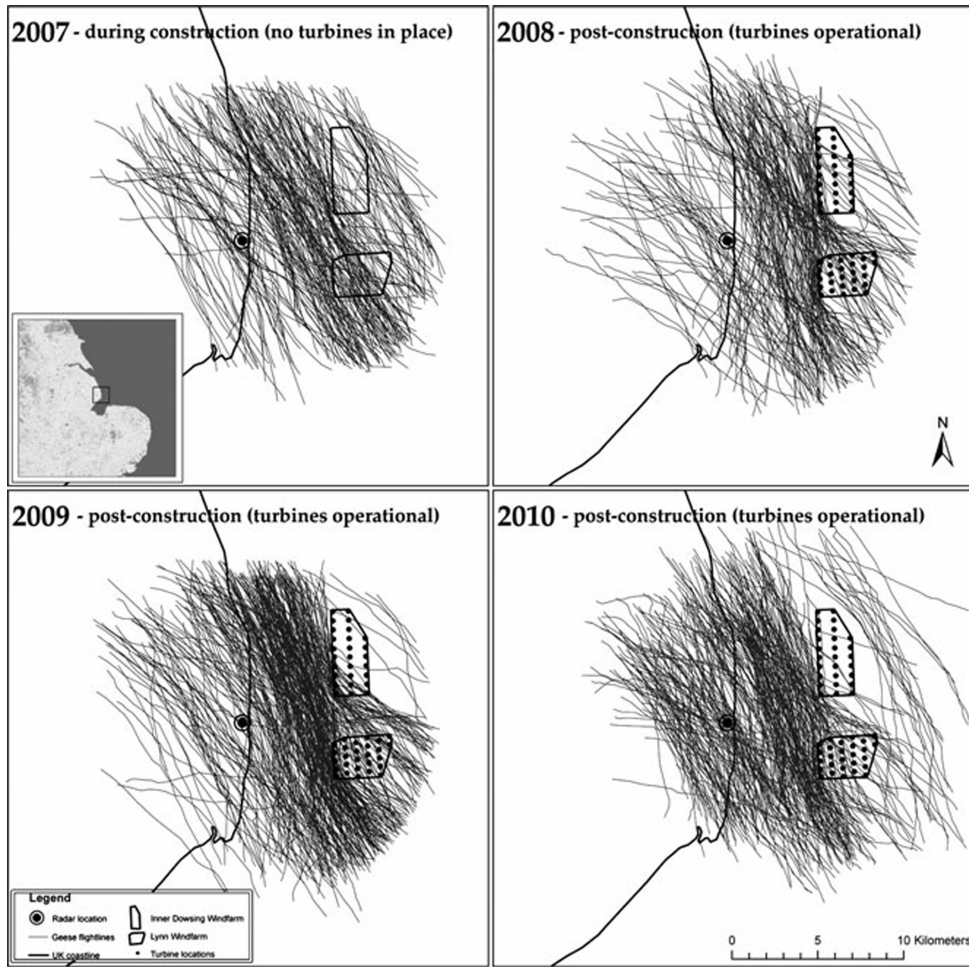
Figure 1.2: An example of goose flock movement patterns recorded by radar studies. Taken from Plonczkier and Simms (2012), this figure shows the change to these patterns over sequential years (2007 – 2010), from wind farm construction to operation.

99.8% (Pendlebury, 2006). It has been demonstrated through sensitivity analysis that even small errors in these estimated rates can have large effects on predicted mortality rates making accurate quantitative assessment difficult (Chamberlain et al., 2006).

Recently modelling studies have begun to explore ways in which more accurate avoidance rates can be determined by considering implicit factors such as the spatial configuration of turbines. In particular, the statistical model presented by Masden et al. (2012) has been used to show that the spacing between turbines and number of turbines in each column or row have a significant impact on avoidance rates. The aim of these studies is to provide a tool for industry which can shape wind farm layouts for both optimal power generation and minimal environmental impact. However, these models do not consider the movements of individuals but instead only simulate groups as a single entity. Studies of collective motion have shown that the decisions, and thus movements, of a groups can be considerably different depending on the degree of social interaction and variation of navigational information (Couzin et al., 2005; Codling et al., 2007; Leonard et al., 2012). In order to gain a better understanding of the factors driving avoidance it is therefore important that these considerations be taken into account.

1.4 Thesis structure

This thesis develops a method for the inclusion of obstacle avoidance in collective motion models which can be used to assess the collision risk of birds with wind turbines. This provides a framework to reinterpret existing predictive models in the light of group dynamics, and furthermore to explore the potential role of social networks on navigation and avoidance. Chapter 2 outlines a general approach for representing obstacles and implements this using an established individual-based model. Mechanisms for possible avoidance behaviours are proposed and tested, with findings discussed in the context of existing collision risk modelling techniques. Chapter 3 assesses the feasibility of using a popular stereoscopic vision technique to observe and analyse the movements of geese interacting with a fixed static obstacle.

The discussion outlines the limitations of this approach and suggests improvements which could be used in future study. The results of this work together with additional data from a previous study (Budgey, 1998) are analysed to identify key parameters. Chapter 4 develops an recent asynchronously updating model for collective motion to investigate the movement of social groups around obstacle arrays. In particular, different network structures are simulated to study their effect on decision-making within groups and the potential impact this could have on collision risk. Finally, Chapter 5 applies the model outlined in Chapter 4 to explore the impact various aspects of wind farm design have on avoidance in order to identify potential mitigation strategies that could be implemented pre-construction. Further justification of the model development is also presented with particular focus on the inclusion of bird specific behaviours. Overall, this work provides a robust basis upon which future collision risk models can be built and applied to real-world problems.

Chapter 2

The influence of group size and social interactions on collision risk with obstacles

Published manuscript

2.1 Preface

As stated previously in the Thesis Declaration this chapter has been published in a peer-review journal. It is presented as it appears in print with the following revisions:

1. Minor grammatical and referencing errors have been corrected to improve clarity.

2. Referencing to relevant discussion elsewhere in the thesis has been incorporated.

3. Technical language and mathematical notation has been changed to be consistent with that used throughout the remained of the thesis (Chapters 4 and 5). For example, obstacle "nodes" are now referred to as "vertices".

4. Additional figures 2.1, 2.2 and 2.3 omitted from the published manuscript have been included to supplement the methodology by providing a graphical illustration of key concepts.

5. Comment has been added to justify the use of equal weighting between alignment and attraction behavioural responses in Equation 2.2.

6. Comment has been added regarding interactions with non-linear obstacles.

7. Comment has been added to clarify the definition and generation of the vectorial noise $w_e\hat{\underline{\xi}}$ (formerly $\sigma\underline{\xi}$).

8. Comment has been added to explain the omission of a sensory error when detecting the target navigational direction.

9. Comment has been added to define how a collision is determined.

10. Comment has been added to discuss the choice of parameter value relating to obstacle interactions.

11. The simulation algorithm described in Section 2.4.3 has been updated following discovery that the application of the warm-up routine documented in the

published manuscript, which was designed to form groups into a representative stable configuration, did not behave as anticipated. Instead, group configuration remained effectively random and therefore can be considered indistinguishable from the initial random placement step.

12. Comment has been added to retrospectively justify the choice of target weighting following more recent work by Codling and Bode (2014).

Significant additions to the text are presented in *italics* delineated by square brackets.

2.2 Abstract

In the UK there has been dramatic growth in the number of proposed wind farms, and the impact on wildlife of this expansion is largely unknown. Avian collisions with wind turbines have received wide attention but reliable predictions remain elusive. Existing predictive models consider behavioural factors such as group movement only implicitly and require accurate site-specific data to produce predictions, making them difficult to translate between locations. Here we introduce an individual-based modelling approach to describe group interactions with obstacles that incorporates aspects of collective motion to simulate and quantify likely avoidance behaviour. We quantify the effect of group size on the probability of an individual colliding with a fixed obstacle, and investigate the roles of both navigational efficiency and group cohesion. We show that, over a wide range of model assumptions and parametrisations, social interactions have a significant and potentially large effect on collision risk; in contrast to previous models, collision risk is typically a non-linear function of group size. These results show that emergent behaviour induced by social interactions can have important effects on the metrics used to inform management and policy decisions.

2.3 Introduction

Individual-based models have become a popular solution to simulating animal collective motion, providing a natural link to identifiable social, biomechanical and environmental forces (Reynolds, 1987; Vicsek, 2001; Couzin et al., 2005; Codling et al., 2004, 2007; Wood and Ackland, 2007; Bode et al., 2010a,b, 2011a). While providing a rigorous set of modelling methods, these studies have not explicitly considered the implications of group social behaviour on risk of collision with hazardous obstacles. This is an increasingly important application for models of this type, for example

offering an avenue by which the impact of wind turbines on moving groups, and migrating birds in particular, can be assessed *in silico*.

Wind power is one of a host of rapidly developing solutions to enable governments to implement sustainable energy strategies. In Europe, members of the EU have committed to a substantial shift towards renewable energy, imposing a target of sourcing 20% of energy from renewable technologies by 2020 (Commission of the European Communities, 2007). However, some countries such as Scotland have imposed a more rapid shift, setting a target of 100% electricity generation from renewable sources by 2020. A recent review of renewable energy in the UK identifies wind power, and in particular off-shore wind power technologies, as key growth areas for development. It suggested that by 2030 wind power could potentially provide as much as 75% of renewable energy and nearly 50% of all energy in the UK (Committee on Climate Change, 2011). To achieve such a contribution of wind power energy would require a large-scale expansion in the number of wind farms. Statistics provided by Renewable UK, formally BWEA, suggest that current and proposed developments will increase the existing number of wind farms in the UK two-to-three fold in the near future (UK Renewables, 2012).

Despite this confidence in the role of wind power there are concerns that wind farm developments are likely to impact negatively on the distribution and abundance of wildlife, particularly birds. Potential impacts of wind farms on bird populations can be categorized into four types: collision, disturbance (particularly during construction), barrier effects (exclusion) and habitat modification (Fielding et al., 2006; Fox et al., 2006). Of these, collisions have a direct effect on avian mortality and have received wide attention. Impact studies have been conducted at several wind farm sites both pre- and post-construction to record the avian activity in the area and to monitor collisions with turbines (Garthe and Hüppop, 2004; Desholm and Kahlert, 2005; Pearce-Higgins et al., 2012). These studies use a number of different approaches such as radar, thermal imagery, human observation and carcass retrieval. The data obtained reveal that avian collisions with turbines can vary greatly across sites and

species. However, wind farms are often positioned in remote locations, especially those offshore, and it is not practical to conduct empirical studies.

Modelling has the potential to provide a reliable method of prediction without the need for extensive pre- and post-construction site surveys. The most widely used Collision Risk Model (CRM) is that described by Band (2000). The methodology consists of a two-stage probabilistic approach to predict mortality by combining a description of the structure and operation of a wind turbine with attributes of bird physiology and flight. The model first estimates the number of birds that pass through a "risk window" (turbine blades), and secondly calculates the probability of a bird passing through the risk window being hit by a rotor blade. Mortality is then estimated by multiplying the collision probability by the number of birds passing through the area at risk height. Crucially, the model assumed that an individual bird takes no avoiding action when encountering a turbine. This omission was addressed in a revised version of the model (Band et al., 2005) through the addition of an avoidance factor which scales the determined collision probability. This avoidance factor incorporates an implicit dependence on parameters such as the average number of individuals that pass through a "risk window" simultaneously. However, it has been demonstrated through additional sensitivity analysis that even small errors in this parameter can have large effects on predicted mortality rates. Therefore, no matter how robust the estimates of collision risk in the absence of avoiding action, the final predicted mortality is unreliable until "species-specific and state-specific avoidance probabilities can be accurately established from observation and empirical evidence" (Chamberlain et al., 2006).

The study of collective motion provides a new avenue of investigation in which specific avoidance probabilities no longer need to be imposed, but instead emerge from a set of behavioural rules (Grégoire and Chaté, 2004; Couzin et al., 2002). Individual-based models apply rules in a hierarchy based on proximity following the observation that individuals within a group remain synchronised despite having no knowledge of the group as a whole (Sumpter, 2006; Rackham, 1933; Buhl et al., 2006),

instead relying on local interactions with nearest neighbours to navigate (Reynolds, 1987). This methodology has allowed the recreation of complex flocking behaviour with a high degree of success and provided a deeper understanding of the mechanics involved in collective motion. For example, models of this type (Bode et al., 2010a; Hildenbrandt et al., 2010) have shown emergent properties such as the idea that individuals interacting with a fixed number of neighbours can explain complex real-world observations (Ballerini et al., 2008a). Models also predict that whilst there are navigational benefits to moving within a group this is not always the case (Codling et al., 2007; Guttal and Couzin, 2010). Here we describe an individual-based model of collective motion and obstacle avoidance, and use this to determine the effect of group size on collision risk for a single obstacle under a range of ecologically plausible parametrisations. These results elucidate important directions for future research, and are likely to be of direct relevance to the construction of wind farms in sensitive environments.

2.4 Methods

2.4.1 Modelling framework

The model is adapted from that outlined by Couzin et al. (2005) in which a group of individuals attempt to navigate toward a distant target. Individuals exist in a two-dimensional environment. Each individual is represented by a position ($\underline{\mathbf{x}}$) and an orientation ($\underline{\hat{\mathbf{v}}}$). At discrete time intervals (τ) there is a "turning event" in which each individual (indexed by i in the equations below) assesses the position and/or orientation of other individuals (indexed by j) or objects within a given proximity, and calculates a new heading according to a set of behavioural rules. The individual then moves in this direction at a constant speed (v_0). This process is repeated until all individuals reach a specified termination condition (or "target"). The behavioural rules used in this model form a two-tier hierarchy which considers three non-overlapping zones of interaction; collision (R_r), alignment (R_o) and attraction (R_a). The highest

priority is given to collision avoidance where individuals attempt to steer away from other individuals or objects (Equation 2.1, Equation 2.3). If not performing an avoidance manoeuvre individuals combine a balance of directional vectors relating to three behavioural cues; social behaviour $(\underline{\mathbf{v}}_i^s)$ where individuals are attracted to distant group members and align with neighbours (Equation 2.2), obstacle avoidance $(\underline{\mathbf{v}}_i^o)$ (Equation 2.4) and target seeking $(\hat{\underline{\mathbf{v}}}_t)$. We define these vectors in turn below before combining them to determine a new direction of motion.

If an individual j is closer than R_r to an individual i then collision avoidance is prioritised as follows,

$$\underline{\mathbf{v}}_i^s = -\sum_{\substack{j \neq i}}^{j \in R_r} \frac{\underline{\mathbf{x}}_j - \underline{\mathbf{x}}_i}{|\underline{\mathbf{x}}_j - \underline{\mathbf{x}}_i|} \tag{2.1}$$

If not, then the social interaction serves both to align to the closest individuals, and to attract the individual towards the perceived centre of the group (Equation 2.2). [*Consistent with the method outlined by Couzin et al. (2005), this implementation considers all neighbours within the sensory zone of an individuals to contribute equally to the resultant direction of motion regardless of relative distance or the particular zone of interaction, alignment or attraction, in which they appear. However, as indicated below, it is noted that alternative approaches have been proposed in similar models which consider the interplay between alignment and attraction behaviours differently. For instance, both Couzin et al. (2002) and Codling et al. (2007) only considers attraction responses if there are no neighbours within the repulsion or alignment zones. Whilst the latter approach was considered, hierarchical equality of alignment and attraction behaviour was required in this case to provide a comparable structure in which to incorporate obstacle based interactions.*]

$$\underline{\mathbf{v}}_i^s = \sum_{\substack{j \neq i}}^{j \in R_o} \hat{\underline{\mathbf{v}}}_j + \sum_{\substack{j \neq i}}^{j \in R_a} \frac{\underline{\mathbf{x}}_j - \underline{\mathbf{x}}_i}{|\underline{\mathbf{x}}_j - \underline{\mathbf{x}}_i|} \tag{2.2}$$

The reader is directed elsewhere for details of similar models, e.g. Couzin et al. (2002, 2005); Wood and Ackland (2007).

41
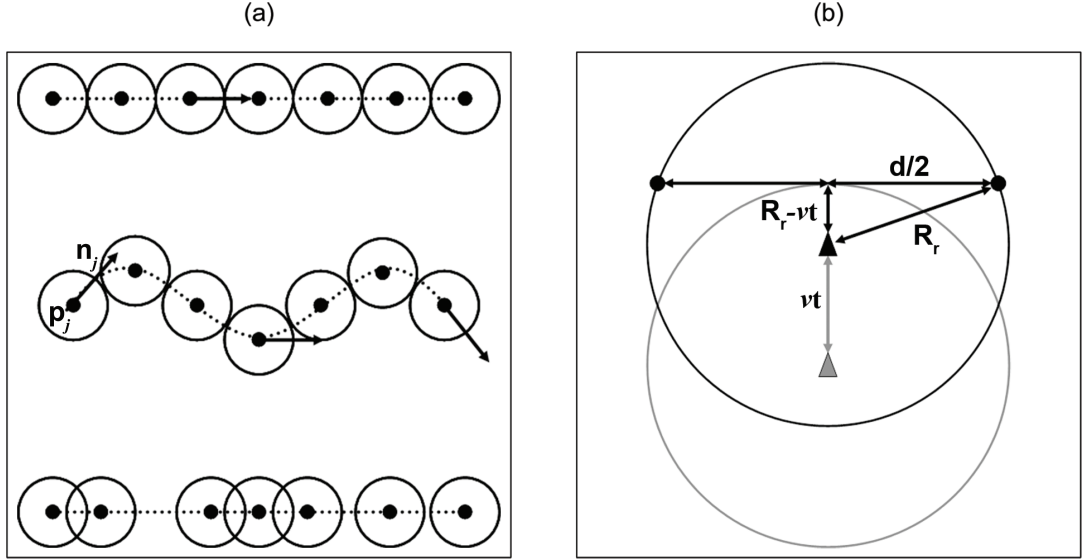
Figure 2.1: An illustration of the method for obstacle representation. Obstacles consists of a finite set of vertices represented by a point $\underline{\mathbf{p}}_j$ and a tangential surface vector $\underline{\mathbf{n}}_j$ (by convention these follow a clockwise direction around the surface). In addition each vertex is defined with a circle of fixed radius which is used to determine collisions. (a) shows three example representations of obstacles using this approach (from top to bottom): a line with even spacing as is used in all simulations throughout this chapter, a curve with even spacing, and a line with uneven spacing. This demonstrates the flexibility to approximate any shape. The spacing between vertices effects the error associated with this approximation and especially the detection of collisions as circles may no longer overlap. (b) outlines a method for calculating the minimum spacing between vertices (or granularity), d, to ensure that even at short distances (R_r) individuals cannot move directly towards an obstacle without detecting at least one vertex within the appropriate zone of interaction (hence showing the correct behavioural response). For an individual moving with speed (v_0) over an update step τ, the minimum distance can be calculated using basic trigonometry as $d = 2\sqrt{2R_r v_0 \tau - (v_0 \tau)^2}$.

In our model we introduce a one-dimensional obstacle, mimicking a single wind turbine, which is placed such that the flock must interact with it in order to reach the given target. Obstacles are constructed as a set of vertices (indexed by k in the following equations), each of which has a fixed position ($\underline{\mathbf{p}}$) and an associated unit vector ($\underline{\mathbf{n}}$) parallel to the obstacle surface (illustrated in Figure 2.1(a)). The density of points is chosen to minimise the granularity errors associated with representing a solid object by a set of points (shown in Figure 2.1(b)).

The description of an obstacle as a set of discrete points emulates the interaction framework between individuals as described above, allowing similar interaction mechanics to be employed. This representation allows for an emergent relationship between proximity to, and reaction to, obstacles. As an individual moves toward an obstacle more vertices lie within the zones of interaction, thereby inducing a larger reaction. We choose here to implement a short range repulsion, exactly paralleling the interaction with other group members, combined with a longer range aligning interaction (an illustration of these behavioural rules is presented in Figure 2.2).

This is based on the notion that the most efficient way to move around an obstacle is to align with the surface towards the closest perceived end point. [*Although not considered here it should be noted that this concept does not necessarily hold for interactions with more general non-linear obstacles, such as those forming convex or concave shapes. For these interactions it may be more appropriate to apply a similar alignment behaviour instead based on the one-dimensional projection, or silhouette, of an obstacle as proposed by Reynolds (1987). The avoidance mechanism outlined in later chapters is a simplified implementation of this approach.*] We therefore introduce a new interaction weighting with this obstacle computed as follows.

If an obstacle vertex k is closer than R_r to an individual i then collision avoidance is prioritised,

$$\underline{\mathbf{v}}_i^o = - \sum_{k=0}^{k \in R_r} \frac{\underline{\mathbf{p}}_k - \mathbf{x}_i}{|\underline{\mathbf{p}}_k - \mathbf{x}_i|} \tag{2.3}$$

Otherwise, an individual is seeks to move away from vertices in a direction parallel
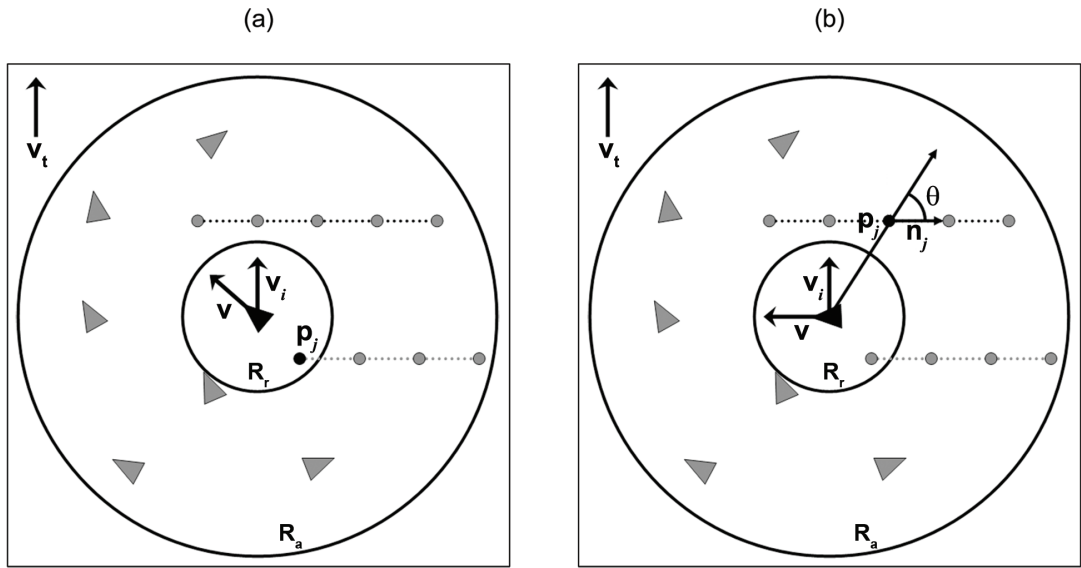
Figure 2.2: An illustration of the behavioural rules for obstacle avoidance. Each panel illustrates the directional response ($\hat{\underline{v}}$) of an individual (black triangle), with positions $\underline{x}_i$ and heading $\hat{\underline{v}}_i$, to the highlighted obstacle vertex (black circle), with position $\underline{p}_j$ and tangential vector $\underline{n}_j$, located within: (a) the zone of repulsion (R_r); and (b) the zone of surface alignment (R_a). The marked angle θ is used to determine direction of surface alignment, if the angle is acute (i.e. less than $\pi/2$ radians) then, according to Equation 2.4, the individual aligns with a vector directly opposite $\underline{n}_j$ (moving along the surface in an anti-clockwise direction).

to the obstacle surface,

$$\underline{\mathbf{v}}_i^o = \sum_{k=0}^{k \in R_o \cup R_a} \text{sgn}\left(\cos^{-1}\left(\left(\frac{\underline{\mathbf{p}}_k - \underline{\mathbf{x}}_i}{|\underline{\mathbf{p}}_k - \underline{\mathbf{x}}_i|}\right) \cdot \underline{\mathbf{n}}_k\right) - \frac{\pi}{2}\right)\underline{\mathbf{n}}_k \tag{2.4}$$

where sgn denotes the sign function.

If not performing an avoidance manoeuvre an individual also orientates towards a fixed target direction which remains constant across all individuals at all time steps ($\hat{\underline{\mathbf{v}}}_t$) corresponding to a fixed target represented as a point at infinity. This is in contrast to alternative models which apply a more general approach where the target is fixed in space and hence the target direction is allowed to vary across individuals (Codling et al., 2004, 2007). In addition we apply uniform vectorial noise $w_e\hat{\underline{\boldsymbol{\xi}}}$ [*a unit vector generated using a random angle drawn from a uniform distribution on the range $(0, 2\pi)$ radians applied with a relative weighting w_e*] for each individual at each time step. For simplicity we use a single error term to account for imprecision in movement and sensing ability which is common in collective motion studies (Grégoire and Chaté, 2004). However, studies that consider separate error terms have shown that the interplay between sensing and movement error can be quite complex (Codling et al., 2007). [*To explore the relationship between social and obstacle interactions in isolation, "perfect" navigation is required in all simulations for consistency to ensure that any avoidance, or apparent reduction in collision risk, is as a result of behaviour rather than a failure to navigate. It should be noted that error is only included to introduce a minimal level of disturbance and is not designed to have a significant effect on movement. Furthermore, the relative effect of varying levels of error on movement is not explored and remains constant in throughout.*] The new direction of individual i at a new time step can then be calculated as follows.

If an individual detects a collision threat [*defined as a neighbour or obstacle vertex within R_r*] then,

$$\hat{\underline{\mathbf{v}}}_i = \frac{w_s\underline{\mathbf{v}}_i^s + w_o\underline{\mathbf{v}}_i^o}{|w_s\underline{\mathbf{v}}_i^s + w_o\underline{\mathbf{v}}_i^o|} + w_e\hat{\underline{\boldsymbol{\xi}}} \tag{2.5}$$

45

and otherwise,

$$\hat{\underline{\mathbf{v}}}_i = \frac{w_s\underline{\mathbf{v}}_i^s + w_o\underline{\mathbf{v}}_i^o + w_t\underline{\mathbf{v}}_t}{|w_s\underline{\mathbf{v}}_i^s + w_o\underline{\mathbf{v}}_i^o + w_t\hat{\underline{\mathbf{v}}}_t|} + w_e\hat{\underline{\boldsymbol{\xi}}} \tag{2.6}$$

The parameters w_s, w_o and w_t represent the relative preference of each individual for social, obstacle avoidance and target directions respectively. We constrain the angle to which an individual's orientation can change in any one time step by implementing a maximum angular turning rate. Finally, the new orientation vector is renormalised and the individual's position updated accordingly.

Note that the above formulation (Equation 2.5, Equation 2.6) makes an assumption that the components corresponding to social interactions and obstacle avoidance are not individually normalised before they are combined (hereafter designated Model I). This is a reasonable assumption; each detectable point in the system is considered on an equal footing, in order not to provide individuals with global information about the system. It could, however, be argued that the social weighting may unrealistically overwhelm the interactions with obstacles at large group sizes. For this reason, our results are also calculated for an equivalent model (Model II) as follows where the vectors corresponding to social and obstacle avoidance vectors are each normalised before being combined (Equation 2.7, Equation 2.8). [*Further discussion of the differences between these model implementations, specifically with regard to the idea that a single obstacle could present multiple yet equally merited avoidance strategies and that this may lead to indecision, is presented in Section 5.2.3.*]

If an individual detects a collision threat then,

$$\hat{\underline{\mathbf{v}}}_i = \frac{w_s\hat{\underline{\mathbf{v}}}_i^s + w_o\hat{\underline{\mathbf{v}}}_i^o}{|w_s + w_o|} + w_e\hat{\underline{\boldsymbol{\xi}}} \tag{2.7}$$

and otherwise,

$$\hat{\underline{\mathbf{v}}}_i = \frac{w_s\hat{\underline{\mathbf{v}}}_i^s + w_o\hat{\underline{\mathbf{v}}}_i^o + w_t\underline{\mathbf{v}}_t}{|w_s + w_o + w_t|} + w_e\hat{\underline{\boldsymbol{\xi}}} \tag{2.8}$$

where $\hat{\underline{\mathbf{v}}}_i^X = \frac{\underline{\mathbf{v}}_i^X}{|\underline{\mathbf{v}}_i^X|}$.

As will be seen below, both models have consistent large-scale behaviour and produce qualitatively identical results in terms of the predicted obstacle collision risk.

2.4.2 Parametrisation

We initially parametrise our model to simulate a group of individuals attempting to negotiate a single obstacle, using values based on previous theoretical animal collective motion studies (Couzin et al., 2002, 2005; Codling et al., 2007). In order to investigate the specific scenario of birds interacting with a single wind turbine we nominally consider a flock of pink-footed geese (*Anser brachyrhynchus*) moving either between roosting and feeding sites or on a longer term migration. The model could be adapted for any social species of bird, geese are chosen here because they can be observed throughout the UK and provide a reliable species for fieldwork observations in order to validate this model. We use existing literature and expert knowledge, together with our own observations from video analysis of flocks of geese to choose parameter values. Where parameters are unknown values are taken from previous theoretical studies, and whilst they have been scaled using realistic values they remain arbitrary and do not have any biological meaning. [*For example, due to the limited availability of empirical data relating to obstacle interactions we assume, consistent with the concept that each obstacle vertex is considered similar to a conspecific, the same parameterisation defining the relative zones of interaction. However, it would not be unreasonable to anticipate that responses to large obstacles, relative to the size of a conspecific, may require a larger collision radius. We therefore suggest that the results of this study can only be used to inform a theoretical understanding of interactions with obstacles and that accurate real-world predictions, which may be used to inform policy, would require additional empirical evidence to justify such parameter choices.*] More precise estimates of parameter values could be derived from analysis of stereoscopic video data (Cavagna et al., 2008); this is addressed in Chapter 3. The magnitude of the "error" vector is essentially an arbitrary choice at this stage; its value is taken from that used by Couzin et al. (2005) and the effect of this choice was

47

Table 2.1: Typical parameter values used in the simulation models. The reader should note that the values for interaction zones are scaled from those outlined in existing theoretical studies by the average size of an individual. The range of values given for social preference and obstacle avoidance represent those used across both models.

Description	Symbol	Value	Reference
Number of individuals	N	1-100	(Couzin et al., 2002;
			Codling et al., 2007)
Zone of collision (metres)	R_r	1.5	Couzin et al. (2002, 2005);
			Codling et al. (2007);
			Ogilvie (2011)
Zone of orientation (metres)	R_o	15	Couzin et al. (2002, 2005);
			Codling et al. (2007);
			Ogilvie (2011)
Zone of attraction (metres)	R_a	37.5	Couzin et al. (2002, 2005);
			Codling et al. (2007);
			Ogilvie (2011)
Time step increment (sec)	τ	0.1	Couzin et al. (2002, 2005)
Speed (metres/second)	v_0	5	Ogilvie (2011)
Max. turning rate (deg/sec)		45	Couzin et al. (2002, 2005)
Magnitude of noise vector	w_t	0.05	Couzin et al. (2002, 2005)
Initial centre mass of group	(I_x, I_y)	(0, 1000)	
Centre of obstacle	(O_x, O_y)	(0, 750)	
Width of obstacle (metres)	O_z	50	Siemens AG (2012)
Target direction	$\hat{\underline{\mathbf{v}}}_t$	(0, -1)	
Social preference	w_s	0-100	
Obstacle avoidance	w_o	0.1-100	
Target preference	w_t	1	
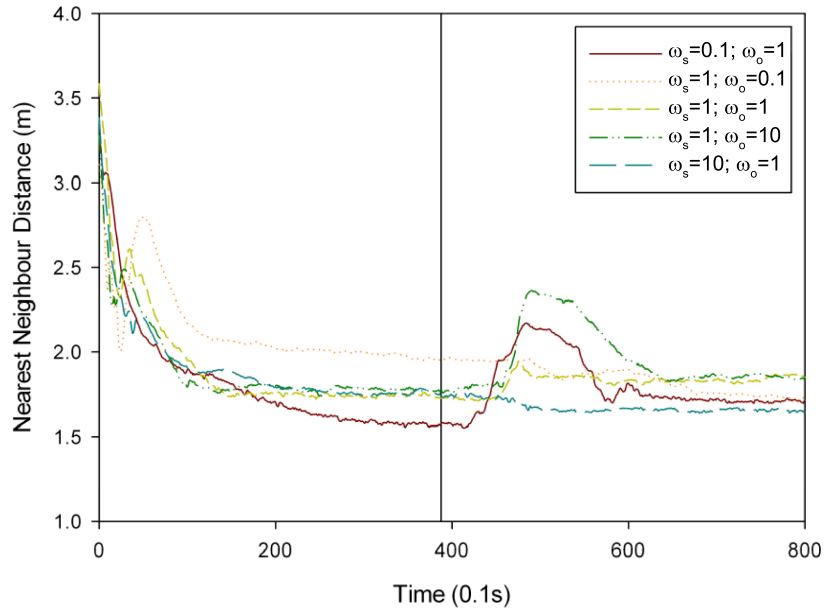
Figure 2.3: Plot of Nearest Neighbour Distance (NND) (average of 100 independent simulation runs) as a function of simulation time for various parametrisations of social and obstacle preference. The vertical line (grey) marks the minimum time at which a group can begin interacting with the obstacle. The pattern shows that when groups are released there is an initial restructuring which reduced NND. However, it can be observed in that groups reach a stable equilibrium prior to interacting with the obstacle.

explored prior to our simulations so when social interactions are present collisions with the obstacle may occur.

2.4.3 Simulations

The goal of this study is to examine the impact of group size on the risk of collision with an obstacle. We therefore construct a simple environment with a single obstacle placed directly ahead of, and a large distance from, the initial group of individuals. For each group size, and for each set of social interaction parameters, we run 100 independent simulation runs. Each run consists of the following steps:

1. The individuals are created with random initial positions and heading.

2. The group is then rotated so that the group is, on average, heading in the target direction $\hat{\underline{\mathbf{v}}}_t$, the centre of the group is placed at (I_x, I_y) 250 metres (approximately 500 time steps) away from the centre of the obstacle which is located at (O_x, O_y). The target direction preference is now turned on, with an arbitrary weighting of 1 relative to the social and obstacle avoidance weightings. [*The value of target weighting was set in an attempt to ensure that accurate navigation towards the obstacle was maintained for all combinations of social and obstacle preference weighting (this may not have been the case and the implications are discussed further in Section 6.1). Since publication of this study, work by Codling and Bode (2014) has suggested that only a relatively small target weighting is required to achieve accurate navigation – approximately 6%. Whilst it may therefore appear that the weighting chosen here may be unnecessarily large it should be noted that the implementation of target navigation differs between these models, and consequently direct comparison of this parameter value is difficult. Here, the proportion of direct target navigation contributing to movement is not soley reflected by the value of w_t but instead relative to that of w_s and w_o and, in the case of Model I, by the number of neighbours and obstacle vertices which appear within an individuals sensory zone). As a result the actual contribution to the direction of motion is significantly smaller and may in fact be quantitatively similar to the value suggested above.*]

3. The group then moves towards, and interacts with, the obstacle and reaches a new equilibrium after passing the obstacle. The number of collisions of individuals with the obstacle is recorded.

The transit distance of the individuals prior to interacting with the obstacles allows burn in time for the group dynamics and ensures that the configuration is coherent. [*Figure 2.3 confirms that the relative distance between the initial group position and the obstacle is sufficient to ensure that following initial release groups reach a stable state prior to any interactions with the obstacle. Therefore, any differences in group structure prior to interaction may be compared with that after an interaction has*

occurred in order to assess the cost of avoidance.]

Collisions in our model [*defined as being when an individual moves within a set distance of an obstacle vertex – set at R_r (see Figure 2.1)*] are assumed always to be "fatal". We do, however, permit the colliding individual to react to the presence of the obstacle immediately prior to its demise, i.e. prior to its removal from the simulation. This is so that the information about the presence of the obstacle is implicitly transmitted back through the group. Groups are not constrained to remain coherent and individuals are free to select any trajectory around the obstacle independent of the actions of the majority. The relative weighting of the preference parameters is unknown and we therefore make a large scale search of this 2-dimensional state space. Our goal is to illustrate the potential for social interaction to influence collision risk so we select parameters to show the full range of behaviour in this pilot. This means varying relative weights by orders of magnitude.

2.5   Results

Figure 2.4 plots the number of collisions against group size, for a model in which social interactions are switched off. The approximately linear dependence of collision risk on group size therefore simply reflects the fact that each individual acts entirely independently. These results correspond to the predictions of a model such as Band et al. (2005), as anticipated, and form a null model against which any changes in collision risk due to social interactions may be judged.

The principal results from our study are shown in Figure 2.5 in which we plot the average number of collisions for different combinations of social and obstacle avoidance parameters, across a range of group sizes from 1 to 100 individuals. The first column refers to the model as presented in equations 2.5 and 2.6 (Model I). The second column shows the alternative formulation presented in equations 2.7 and 2.8 where the vectors corresponding to social and obstacle avoidance factors are each normalised before being combined to produce a resultant direction (Model II). The key finding appears in the first row of Figure 2.5, which quantifies the role of social preference
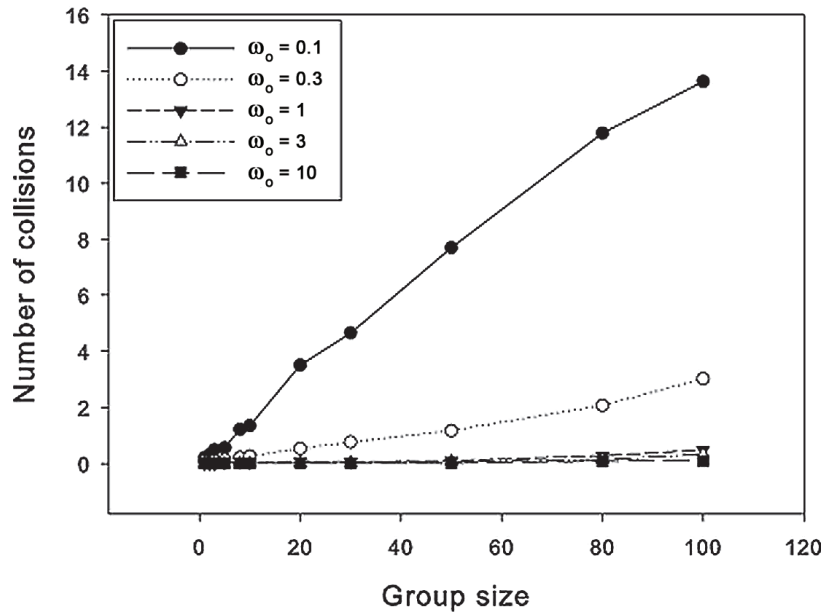
Figure 2.4: The number of collisions against group size for an asocial group (i.e. $w_s = 0$) with varying levels of obstacle avoidance (w_o) generated using Model I. The magnitude of the error vector is fixed at $w_t = 1$. We used a higher error value in these simulations so that sufficient collisions occur to be able to construct a complete plot of the asocial case. The qualitative differences between asocial and social cases remain unchanged. [*We note that in this asocial case w_o simply represents the trade-off between obstacle avoidance and target navigation, which in the defined scenario conflict with increased target navigation reducing avoidance and vice versa.*]
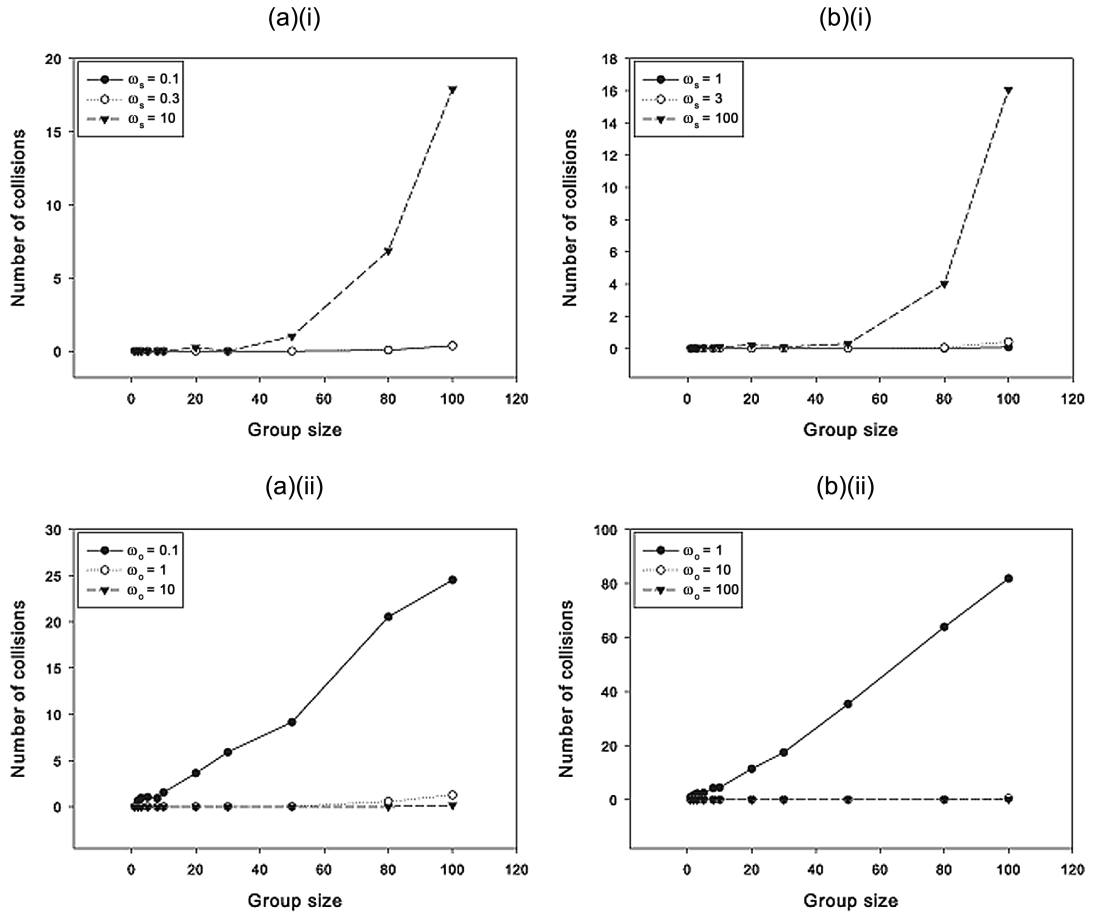
Figure 2.5: The number of collisions against group size for different sets of parameter values generated using: (a) Model I; (b) Model II; varying: (i) levels of social preference (w_s) with fixed obstacle avoidance (Model I: $w_o = 1$ and Model II: $w_o = 10$); (ii) levels of obstacle avoidance (w_o) with fixed social preference (Model I: $w_s = 1$ and Model II: $w_s = 3$). In all simulations target preference (w_t) is fixed at $w_t = 1$.
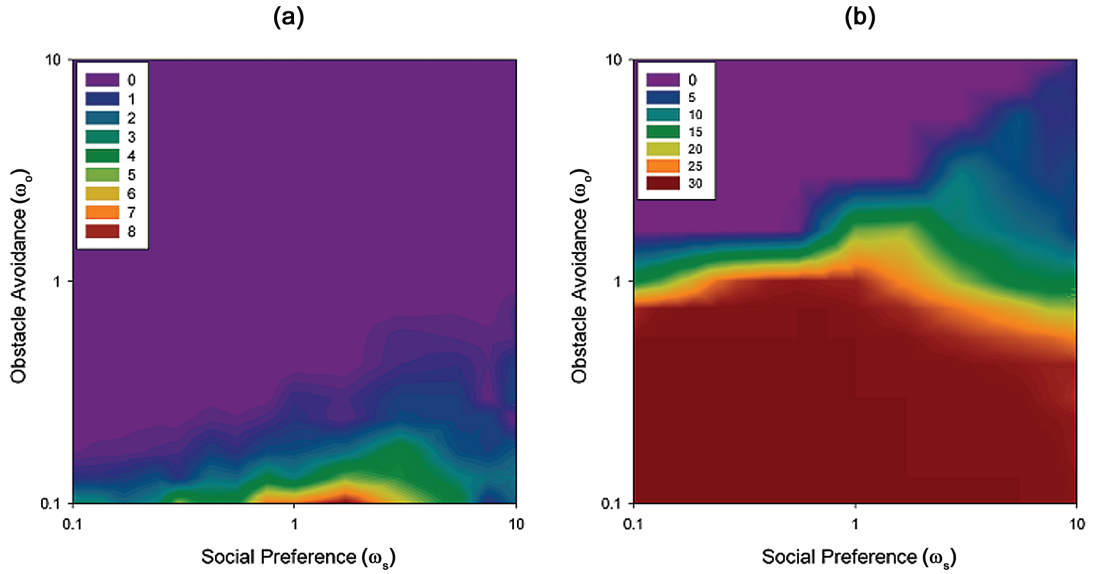
Figure 2.6: Heat Maps generated using: (a) Model I; (b) Model II; plotting the number of collisions against different levels of social and obstacle avoidance preference for a group of size 30 individuals. In all simulations the target preference (w_t) is fixed at $w_t = 1$.

in collision risk when the level of obstacle avoidance is fixed. The result is clearly non-linear (in contrast to Figure 2.4), showing that as group size increases there is an increased per-capita risk of collision. The effect is caused by social interactions, and its strength increases as the strength of these interactions increases. The second row of Figure 2.5 shows that the collision risk scales approximately linearly with the strength of obstacle avoidance. This is reasonable, since social interaction strength is fixed for this second row of results, and confirms that it is the combination of social interactions and group size which drives the non-linear response in collision risk.

Figure 2.6 plots the number of collisions across more comprehensive combinations of social and obstacle avoidance preference. Although the models give quantitatively different results (as would be expected, since the model details differ and in Model I much "larger" social vectors are being assimilated when the group size is large), there is clear qualitative correspondence.

2.6   Discussion

We have made an exploratory simulation study of the collision risk associated with a group of birds, nominally assumed to be geese, with a single obstacle representing a wind turbine. We have made a number of simplifying assumptions in this work, many of which can be challenged. We therefore make no claims about the specific details of the risks we have derived as a function of group size, but rather observe that even in this simplified case there is significant deviation from the simplifying assumptions made in the Band model (Band et al., 2005) which is the most widely used tool in wind farm planning and development. Where such models are used to inform policy their limitations should be carefully considered.

To summarise our results, we show that social interactions can have a large effect on collision risk (Figure 2.5), and that this risk is strongly dependent on group size, in contrast to the asocial case (Figure 2.4). Our conclusions are insensitive to the details of the model implementation since the data represented in the first and second columns of Figure 2.5 behave similarly. Note that the weightings between social and obstacle avoidance vectors change numerically between models to allow a meaningful comparison to be made.

An interesting observation is that for low relative levels of obstacle avoidance small increases in social interaction lead to a higher number of collisions, but that increasing the social interaction eventually leads to a drop in collision risk. This is explained heuristically by a decrease in the overall progress of the group directly towards its target and an increase in information flow from individuals encountering the obstacle, making the group more manoeuvrable when faced with an obstacle. It may be that for our chosen application such large levels of social interaction are unrealistic, resulting in flocks which move artificially slowly around obstacles. For zero social preference the "group" is perfect at avoiding the obstacle and always reaches the target. The question is then whether this is a group or not? This is a common problem in group movement, and we refer the reader to recent work by Bode et al. which proposes an algorithmic method to distinguish asocial from social

movement (Bode et al., 2012b). Our results reveal an important balance between social preference and obstacle avoidance suggesting that in situations where limited information is available about the best way to avoid an obstacle it is more beneficial to be on your own, or part of a strongly social group, than one which is weakly social. This is most likely due to indecision within the group and can be likened to the idea of the "many wrongs principle" (Codling et al., 2007). The transfer of information through the group is critical as it allows those with less knowledge of the way around an obstacle to be guided by those with more knowledge.

There are a number of lessons to be learned from this study. Most important is the observation that there is a lack of empirical evidence to justify the adoption of any particular scheme to model the interaction between moving individuals and obstacles. The manner in which this is integrated in the wider scheme of group interactions needs to be handled with great care; the precise details of this have profound implications for information transfer within the group about impending decisions.

Even in this simple study it is clear that there are significant non-linear effects associated with group size, and that this may have a wide impact on wind farm placement. Given the projections for wind farm construction, both in the UK and globally, it is crucial that more detailed models are created to assess risk to birds moving in groups. As previously discussed, the primary criticism of existing collision risk models is the dependence of the "avoidance factor" on accurate empirical data. Often, due to the location of wind farms, it is not viable to collect such data. Typically values of 95–99% avoidance are assumed. It is important to stress that we do not anticipate that the methodology described in this study can be a replacement for models such as the Band model, but instead could supplement it, especially in generating robust avoidance rates for prototypic wind farm configurations in the absence of *a priori* empirical data. Recent empirical studies confirm collision risk with wind turbines is low (Pearce-Higgins et al., 2012). In general, our results mimic this observation with the average avoidance rate for a group of 30 individuals (in Model I) falling at 98% across all combinations of weightings.

A strength of our approach is to represent obstacles as a collection of points. This is a natural extension of the individual-based interaction rules in models of this type. The technique is readily extensible to varied density and time-dependence of points within an obstacle to simulate areas that require a more a extreme avoidance reaction or moving parts, respectively. This will be the subject of future investigations.

Future versions of our modelling will use established mechanisms for asynchronous updates (Bode et al., 2011a) together with more complex social behaviours (Ballerini et al., 2008a; Bode et al., 2011b) and realistic physics both of birds (Hemelrijk and Hildenbrandt, 2011; Hildenbrandt et al., 2010; Reynolds, 1987) and the turbines (Band et al., 2005). Better representation of the turbines will be necessary in order to effectively scale studies of this type from single turbines to the large arrays of, for example, 100 turbines at Thanet, Kent and 60 turbines at Robin Rigg, Solway Firth (UK Renewables, 2012). Recent work by Masden et al. illustrates potential ways forward in this area (Masden et al., 2012). It is anticipated that the changes in group structure induced by obstacle avoidance will affect the collision risk with subsequent obstacles, putting further distance between the predictions of social models and those where each individual is considered in isolation.

This study forms a fundamental first step towards modelling avoidance rates without the need for extensive site-specific empirical data. We have shown that when social interactions are explicitly considered the relationship between group size and collision risk can be non-linear, contrary to the assumptions used in existing probabilistic models. This finding could have a large impact on predictions of avian collisions with wind farms; it is crucial that further investigation is undertaken.

2.7   Acknowledgments

2.8 Summary

This chapter describes a method for incorporating obstacle avoidance into a typical, synchronously updating, model for simulating collective motion which will act as a benchmark for future model development. Through the course of this work, and subsequent discussion, some interesting questions have been raised regarding the best ways to represent interactions with obstacles, for example, whether responses should be determined at a point level (Model I) where all avoidance strategies are considered or alternatively at an obstacle level (Model II) where only the ideal avoidance strategy is followed in combination with other stimulus. Such modelling questions are addressed in later chapters. The investigation also exposes a gap in knowledge regarding specific parameter choices, both physical and behavioural. In order to provide accurate and reliable insights into real-world applications this is vital and it highlights the requirement for further empirical work, particularly focusing on the interactions of groups with obstacles.

Chapter 3

Assessing the feasibility of using stereoscopic vision to parameterise and validate theoretical models

3.1 Introduction

The model presented in Chapter 2 has nominally been developed to simulate the movements of geese. It provides a theoretical platform in which to investigate the interaction of flocks with obstacles. In addition to the proposed mechanisms for simulating avoidance several key parameter values, particularly those relating to categorising behavioural responses, have been adopted from existing modelling studies and lack empirical basis. In order to generate accurate real work assessments it is important to ground this type of theoretical speculation with empirical observation (Cavagna et al., 2008).

Several existing studies have empirically investigated the interaction of bird flocks with wind turbines (Desholm et al., 2006; Plonczkier and Simms, 2012). These studies have primarily used radar based techniques in order to track the movement of flocks at a wind farm level. Observations have shown that there are significant differences in the way species respond to wind farms with some choosing to risk collisions by flying between turbines and others avoiding the wind farm entirely (Masden et al., 2012). Whilst these results are useful, the resolution of radar only allows flocks to be described at a global level with summary statistics such as average trajectory, extent, shape and in some cases a relative density distribution. In order to observe the underlying mechanisms which produce avoidance behaviours it is necessary to capture movements at an individual-level. Recent advances in GPS technology provide a potential solution to this problem and its use has been demonstrated in an investigation of hierarchical dynamics of pigeons (Nagy et al., 2013). However, the success of GPS for monitoring group dynamics is currently dependent upon the ability to ensure all group members are tagged and can therefore be tracked. In the case of wild geese this level of control is unlikely to be possible and hence GPS alone may not be a suitable approach.

Optical camera based techniques are by far the most accessible and popular approach used in the empirical study of collective motion providing a reliable medium in which all individuals within a group can be observed. Initially, such techniques

were pioneered to analyse collective motion, primarily of fish, in closed lab-based environments (Cullen et al., 1965; Aoki, 1980; Partridge et al., 1980). For the first time researchers were able to quantify behaviours relating to group dynamics such as the relative speed and separation of individuals. However, the observation of birds poses a different challenge as closed situations can be difficult to engineer and it is therefore only practical to conduct experiments in open environments.

The earliest attempts to quantitatively investigate the structure of bird flocks used snapshot images from a single camera to estimate the density of individuals (Van Tets, 1966). More recently the emergence of stereoscopic camera technology has allowed the three-dimensional position of individuals to be reconstructed revealing not only the structure of flocks (Major and Dill, 1978; Budgey, 1998) but also providing the information required to assess the mechanisms of collective motion. The latter was the result of a landmark study which was able to record the movements of thousands of starlings concluding that on average each individual only interacts with a fixed number of neighbours (Ballerini et al., 2008b). Whilst this remarkable result marks a significant advancement in the empirical investigation of collective motion, capturing the movement of individuals at this level of precision for an extended period remains problematic (Hayakawa, 2010). This is one of the fundamental issues faced by stereoscopic research where the limitations of commercial camera technology often forces a trade-off between using high resolution still images at a low frame rate or lower resolution video but with a substantially higher sustainable frame rate (Cavagna et al., 2008). Previous empirical studies (Budgey, 1998; Hayakawa, 2010) which have specifically investigated the structure of goose flocks have used video in order to ensure that sufficient information can be gathered whilst flocks remain within the view of both cameras.

These studies have demonstrated that despite a relatively low image resolution, compared with Ballerini et al. (2008b), three-dimensional positions can be reconstructed with a reasonable degree of accuracy. This is due in part to the fact that, unlike starling, flocks of geese contain comparatively fewer individuals and

with a greater separation between individuals accommodating a lower stereoscopic sensitivity. Budgey (1998) note that nearest neighbour distance shows a strong correlation with wingspan with larger species maintaining a greater distance from their respective neighbours. This relationship was applied in Chapter 2 to scale the radii corresponding to the zones of interaction used in theoretical studies in an effort to provide a more realistic estimates for geese.

In this chapter we describe the development of a portable stereoscopic based system to investigate the interaction of flocks of geese with an obstacle. We discuss methods for calibrating this system and assess the feasibility of using either high resolution still images or lower resolution but higher frame rate video in terms of relative measurement error verses observation time. The aim of this exercise is to reconstruct three-dimensional trajectories of flocks as they interact with the obstacle in an effort to further our understanding of the mechanisms which facilitate successful avoidance manoeuvres and identify situations which may limit this ability contributing to collisions. For example, exploring the distance to an obstacle and the relative position of individuals within the flock where avoidance manoeuvres are initiated and assessing the impact of avoidance on flock structure. The results of this study will provide an empirical basis upon which model validation can be performed. Analysis of the data should also provide sufficient evidence to allow key species specific parameters, such as the radii characterising the zones of interaction, to be determined which it is argued are necessary for models to produce reliable quantitative predictions.

3.2 Methods

3.2.1 Study site

A study site was selected at the Millennium Bridge in York with UK grid reference SE 60215009 (shown in Figure 3.1). Regular flights of geese had been observed at this location in the hours around sunrise throughout the summer period. These daily
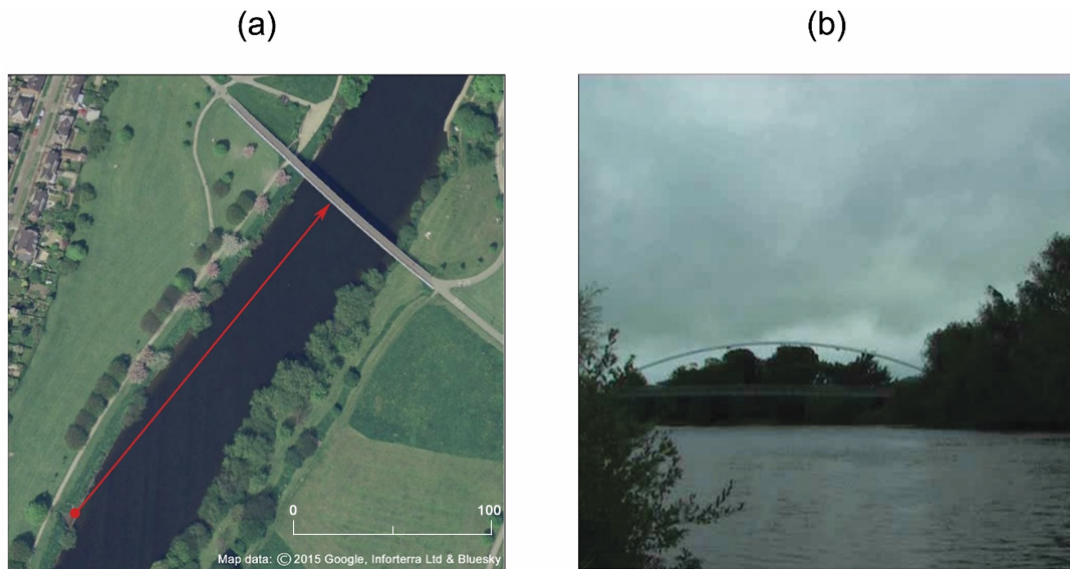
Figure 3.1: Details of the proposed study site at York Millennium Bridge. The images show: (a) an aerial view of the proposed study site with the red dot denoting the position of the stereoscopic apparatus which is located approximately 200 metres from the bridge; (b) a view of the bridge from the setup location. Flocks of geese have been observed migrating towards daily feeding sites around sunrise using the river to navigate. These flocks approach the bridge from the same side as the stereoscopic setup displaying a behavioural response to avoid collisions. By reconstructing the trajectories of individuals we aim to gather evidence relating to the mechanisms of avoidance and through analysis identify key parameter values.

movements from roosting sites on the outskirts of the city to feeding sites in the city centre parks typically followed the River Ouse with flocks required to deviate from this preferred route in order to avoid the bridge. Whilst the bridge is a static obstacle and could perhaps be considered a different proposition to a wind turbine it does exhibit some similar properties, in particular that some sections appear more transparent and hence permeable than others, rendering it a suitable proxy.

The stereoscopic apparatus was positioned approximately 200 metres downstream from the bridge to allow a sufficient distance to capture group movement both pre- and post- interaction with the bridge. Initial observation was conducted without cameras in September 2010 and repeated deployment of stereoscopic apparatus was

conducted for 2 hours around sunrise during the months of July to September in 2011 and 2012.

3.2.2   Stereoscopic vision

The fundamental idea of stereoscopy is that, by taking images of the same object from two different positions in space, we generate enough information to reconstruct its three-dimensional coordinates, provided that relative position of the two cameras is known (Cavagna et al., 2008). This basic concept is illustrated in Figure 3.2 together with the principle equation of stereovision. In this simple example two identical cameras with focal length f are separated by a given distance d along a mutual axis containing both image plane, known as the baseline. By comparing the shift, or disparity s, between the position of an object on each image plane the simple geometric property of similar triangles can be used to compute relative distance z. In practice, however, examples of stereometry are rarely so simple and over the past decade there has been a rapid development of multiple view geometry to provide a more general modelling framework (Hartley and Zisserman, 2003).

These models consider a camera in its simplest terms to be defined as a projective mapping between points in the three-dimensional world and a two-dimensional image. Typically this process is modelled using a central projection in which a ray is drawn from a point in three-dimensional space through another point fixed in space, known as the centre of projection. If we define a given plane in space as the image plane then where this ray intersects the plane represents the image of the point. This mapping is an example of a projective transformation and can be represented mathematically as follows,

$$\sigma m = A[R|t]X \qquad (3.1)$$

where A describes the transformation between the camera axis and the image plane in terms of the intrinsic camera properties, i.e. focal length f_x and f_y, skew γ (the angle between axis on the image plane) and the principle point (u_0, v_0) (the centre

$$s = u_L - u_R = \frac{fd}{z}$$
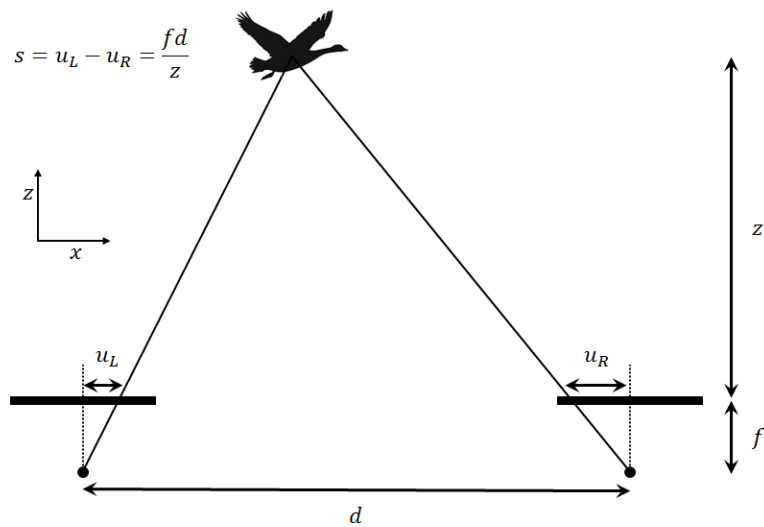
Figure 3.2: An illustration of the principle of stereoscopic vision. This shows the simplest stereoscopic setup with two perfectly aligned identical cameras separated by a fixed distance d along the x axis, termed the baseline. The baseline separation causes a target subject to appear at different positions on each of the image planes, u_L and u_R on the left and right cameras respectively. The difference, or disparity s, between these positions can be combined with the known focal length (in pixels) f and the length of baseline to calculate the distance to a target z by applying the simple geometric property of similar triangles. This fundamental concept underlying stereoscopic vision is expressed in the displayed equation.

of the image plane); $[R|t]$ describes the transformation between the camera axis and the real world in terms of the extrinsic camera properties, i.e. the absolute position and rotation of the camera relative to real world coordinate system. Here, m denotes the projected position of an object on the image plane and X the position in the real world. In order to rationalise differences in the concept of infinity, the observation that parallel lines in the real world intersect at a finite point on the image plane, both m and X are defined in a homogenous coordinate system. It is important to note that this basic camera model only defines the mapping of points up to a scale factor σ, therefore, in order to determine the exact position of a point in three-dimensional space it is necessary to triangulate using rays from multiple view. In practice the rays defined by multiple camera models often do not intersect precisely and so an approximation is required. A numeric approximation, known as the mid-point method is commonly used which estimates the most likely point of intersection to be the mid-point of the shortest line connecting each ray (Hartley and Zisserman, 2003).

When defining stereoscopic systems comprising of two cameras it is usual to define the real world axis to coincide with one of the camera axis thus reducing one of the camera models to the trivial case where R is the identity matrix and t is a zero vector. The other model is then defined in terms of relative position and orientation rather that absolute values which provides a more appropriate comparison for calibrating experimental setups.

3.2.3 Stereoscopic apparatus

The stereoscopic setup comprised of two Canon EOS 500D cameras fitted with standard Canon EF-s 18-55 millimetre lenses. The specification of these cameras advertise a continuous shooting mode supporting bursts of 3.4 images per second at a resolution of 4752 by 3168 pixels for 170 images and a high definition video mode recording at 50 frames per second with a resolution of 1920 by 1080. Each camera was fixed to a custom built clamp which was used to mount them on a rigid beam constructed from

a steel cross-section. The separation between the cameras was adjustable with precise markers 2 metres apart to accurately position the cameras. The beam was supported on a steel tripod with a pivot to allow the system to be rotated easily in order to adjust the direction of view. The cameras were connected via a remote switch to enable synchronised release in either continuous shooting or video modes.

In all experiments the focal length was fixed to the minimum limit of 18 millimetres to provide the widest field of view. This was chosen to maximise the time flocks remained in view which was necessary to ensure interactions both pre- and post-avoidance could be captured. Given this setup the intrinsic camera parameters can nominally be determined using the manufacturers specification of sensor size, stated as 22.3 by 14.9 millimetres, to compute the relative metric dimensions of a pixel. According to this conversion for still images with resolution 4752 by 3168 the focal length measured in the x axis f_x and the y axis f_y of the image plane would be 3836 and 3827 pixels respectively. If we assume the principle point lies at the precise centre of the image plane then it can be defined with pixel coordinates (2376,1584). In order to determine the same parameters for video these values can simply be multiplied by a scale factor according to relative difference in pixel resolution for each axis. This factors can be calculated as 2.475 and 2.933 in the x and y axis respectively.

3.2.4 Calibration and measurement error

As mentioned previously the basic theory of stereometry relies on two identically calibrated and perfectly aligned cameras. In practice this can be difficult and expensive to achieve as it would require purpose built optical equipment. Almost all studies rely on commercially available non-metric cameras which are not calibrated to a high degree. As such many of the camera parameters can vary significantly from those specified by the manufacturer. If not properly accounted for, this discrepancy can have an enormous impact on accuracy of measurements (Cavagna et al., 2008).

Whilst ideally cameras should be subjected to a professional calibration identifying intrinsic parameters, including levels of lens distortion, precisely this process can

be expensive and is beyond the limited resources of this investigation. Instead, we perform calibration and stereoscopic reconstruction using a freely-available computational tool developed in Matlab$^{\circledR}$ by Bouguet (2014), predominantly based on the approach outlined in Zhang (2000).

In order to estimate the intrinsic parameters and additional components of radial and tangential distortion for each camera we conducted experiments taking images of a two-dimensional checkerboard pattern with 3 by 3 centimetre squares (Figure 3.3(a)) from a series of different positions. By relating the position of known point locations on this grid to the relative position on the camera plane through a process of corner extraction (Figure 3.3(b)) a homography matrix describing the transformation from one plane to the other can be estimated. An initial guess for this matrix is computed by rearranging the camera model, which can be simplified as the real world coordinates for X_z are equal to zero, so that the required elements of homography matrix are contained in a single vector (v) such that $Lv = 0$. The solution to this problem is well known, using a single value decomposition (SVD) to determine the eigenvector of L corresponding to the smallest eigenvalue. Using this initial estimate a non-linear minimisation is conducted using the Levenberg-Marquardt algorithm. To ensure sufficient information is available to determine all parameters each homography requires a minimum of 4 pairs of points; the checkerboard provides 48 pairs using the corners corresponding to the interior 7 by 5 grid squares.

In total we took 25 images from different angles within a spherical pattern (Figure 3.3(c)); a minimum of 3 is required to provide information in three-dimensions. By combining the homography matrices generated for each camera angle a closed form solution can applied to provide an initial estimate of all intrinsic parameters (Zhang, 2000). These parameter values, including those describing lens distortion, can then be refined using the same optimisation approach described previously. To ensure reliable estimates this calibration process was repeated 10 times for each camera with the average of these adopted as the parameterisation for the respective models. The results of this calibration are detailed in Table 3.1 alongside corresponding estimates
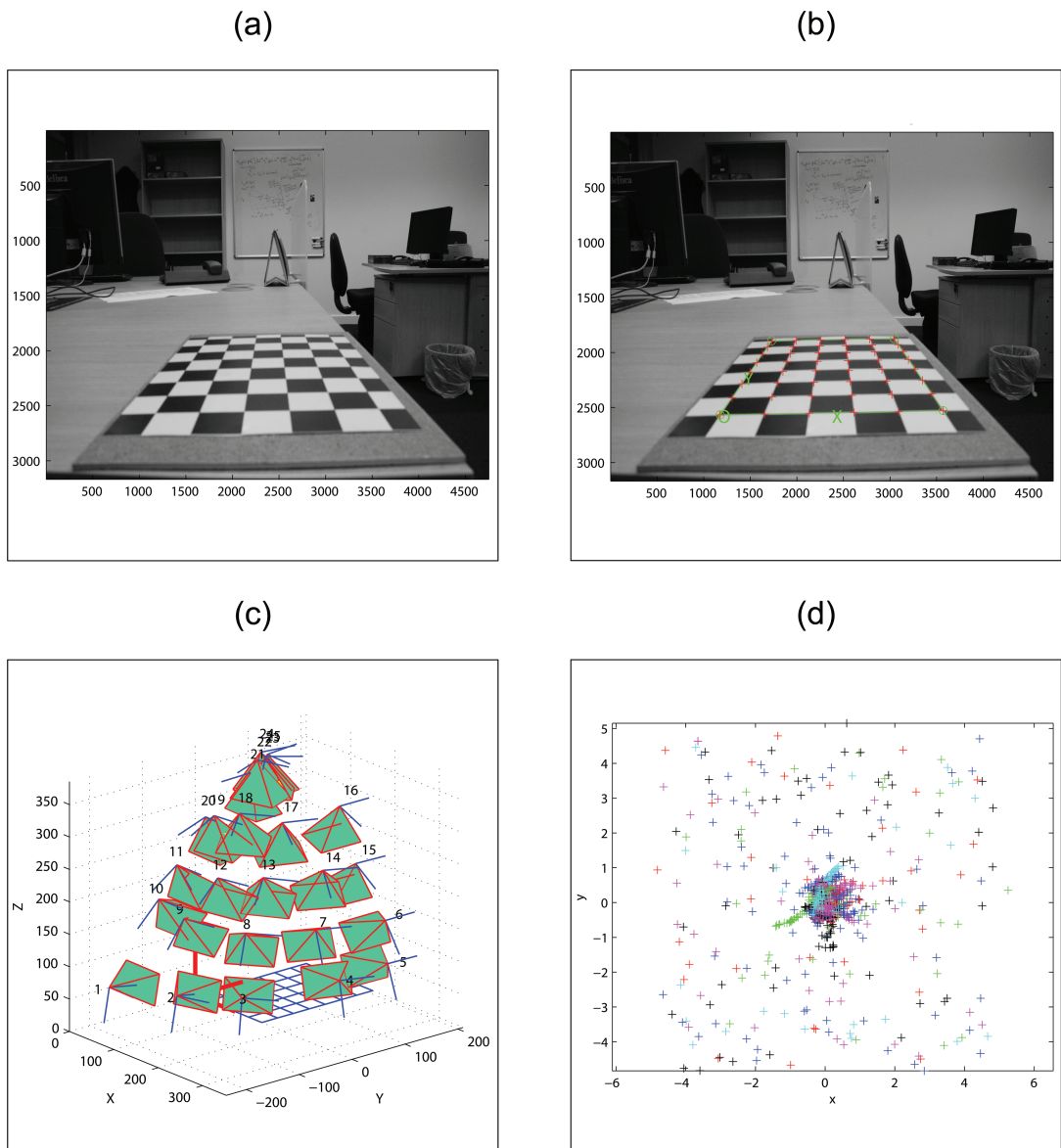
Figure 3.3: The results of calibration experiments to determine intrinsic camera parameters. The images show: (a) the calibration plane with standard checkerboard pattern providing a set of known relative positions; (b) corner extraction, the process of identifying the position of known locations on the image plane; (c) the pattern of 25 different camera angles used to build up a three-dimensional representation of the calibration pattern; (d) the distribution of pixel error produced by the estimated camera model.

Table 3.1: A summary of the intrinsic camera parameters determined by the calibration. Estimates are provided for both still images with resolution of 4752 by 3168 pixels and video resolution of 1920 by 1080. Parameters f_x and f_y denote the focal length measured in pixels according to the pixel dimensions in x and y respectively; u_0 and v_0 denote the position of the principle point on the image plane; γ denotes the skew between axis on the image plane, this was negligible and thus assumed to be zero throughout the calibration; k_i denote the components of distortion with first and second elements representing radial distortion and the third and fourth tangential, as was the case for skew the additional fifth element of distortion remained effectively zero and consequently was not considered.

	Stills (4752x3168)		Video (1920x1080)	
Parameters	Left Camera	Right Camera	Left Camera	Right Camera
f_x	3916 ± 7	1582 ± 3	3940 ± 10	1592 ± 4
f_y	3913 ± 7	1334 ± 2	3941 ± 9	1344 ± 3
u_0	2327 ± 11	940 ± 5	2334 ± 6	943 ± 3
v_0	1724 ± 13	588 ± 4	1772 ± 12	604 ± 4
γ	0	0	0	0
k_1	-0.185 ± 0.008	-0.186 ± 0.009	-0.185 ± 0.008	-0.186 ± 0.009
k_2	0.158 ± 0.026	0.179 ± 0.032	0.158 ± 0.026	0.179 ± 0.032
k_3	0.009 ± 0.001	0.011 ± 0.001	0.009 ± 0.001	0.011 ± 0.001
k_4	0.001 ± 0.001	-0.001 ± 0.0004	0.001 ± 0.001	-0.001 ± 0.0004
k_5	0	0	0	0

for video resolution images. These suggest that the camera parameters do in fact differ from those specified by the manufacturer.

It can be seen in Figure 3.3(d) that the pixel error produced by this calibration is clustered radially around zero with average error of approximately 1.25 pixels in each dimension. Whilst this may seem large the sensitivity of any stereoscopic system is limited to 1 pixel below which changes in position cannot be measured (Cavagna et al., 2008). An error of 1.25 pixels is comparable to this limit suggesting that the estimates provided in this calibration are reasonably accurate.

Using these intrinsic parameters we can now determine the extrinsic parameters for the stereoscopic setup. We conducted experiments using the outline of a badminton court to position identical objects at known locations (Figure 3.4(a)). As before, by relating the position of these images to those on the image plane this time using the known intrinsic parameters we were able to infer the position of each camera in the real world. By applying the inverse transformation for the left camera to both camera models we obtain the relative transformation between the cameras. We repeated this 3 times disassembling the apparatus between each experiment in order to capture any differences which may occur due to inaccuracies in the setup procedure. These results were averaged concluding that the vector separating the camera positions was $(-1.98 \pm 0.005, -0.002 \pm 0.002, 0.072 \pm 0.01)$ metres and the relative rotation defined by the angles of roll, pitch and yaw was $(0.025 \pm 0.0003, -0.0001 \pm 0.0007, 0.003 \pm 0.002)$ radians. The small standard deviation observed in each parameter value indicates that the setup procedure could be reproduced with relative consistency.

To test the accuracy of the stereoscopic setup we conducted another experiment again placing objects at different positions and relative heights on the badminton court (Figure 3.4(a)). The measurement errors observed in this experiment are plotted in Figure 3.5(b) and summarised in Table 3.2. Using the relationships outlined in Cavagna et al. (2008) we estimate the error which would be observed using the same cameras in video mode. Here, the absolute error is independent of resolution, instead relying on the relative alignment of the cameras, and therefore remains unchanged.

71
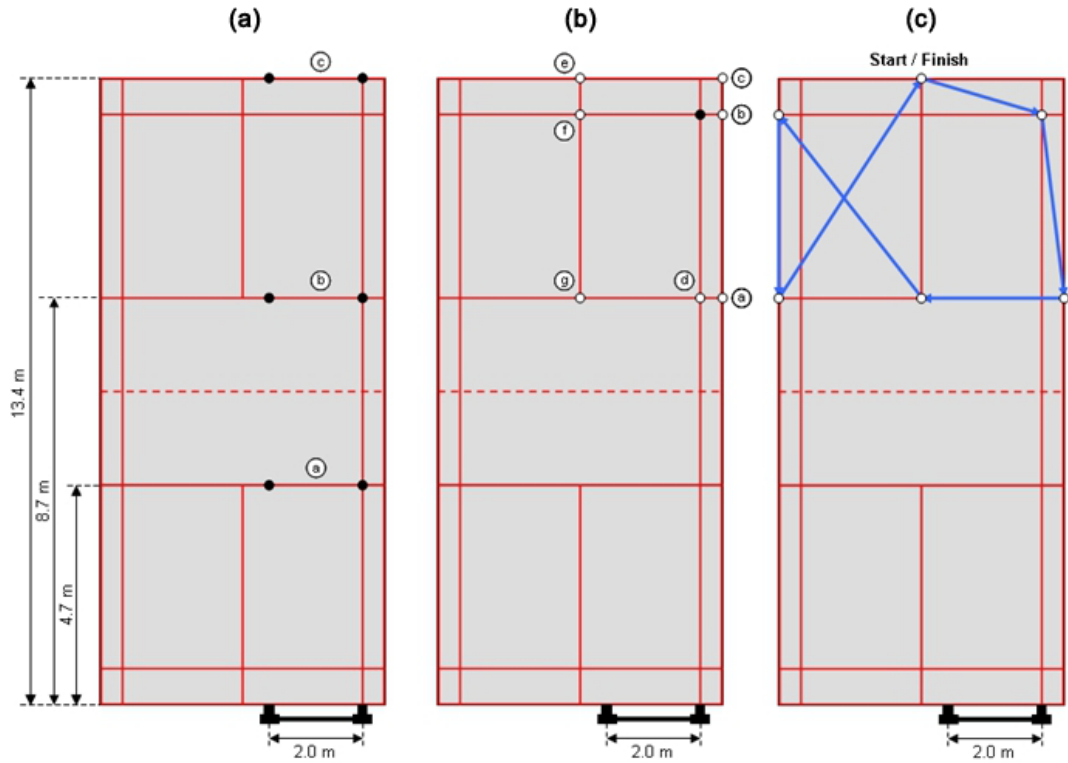
Figure 3.4: An illustration of calibration experiments to determine the extrinsic parameterisation of the stereoscopic setup and test the method of reconstruction. These experiments are conducted on a standard badminton court where the outline can be used to identify the relative position of objects. The arrangement in: (a) marks the placement of calibration objects arranged at known positions on a plane (at a height of 5 cm above the court) which are used to estimate the relative separation and alignment of the cameras mounted on the stereoscopic rig, the extrinsic parameters; (b) marks the placement of calibration objects arranged at known positions which are used to assess the accuracy of the stereoscopic apparatus (white circles indicate an object at a height of 5 cm above the court with the black circle denoting an object at 65 cm); (c) marks the path followed by a subject carrying a calibration objects which is used to test the accuracy of trajectory reconstruction. In all experiments the position and orientation of the stereoscopic camera setup remains unchanged.
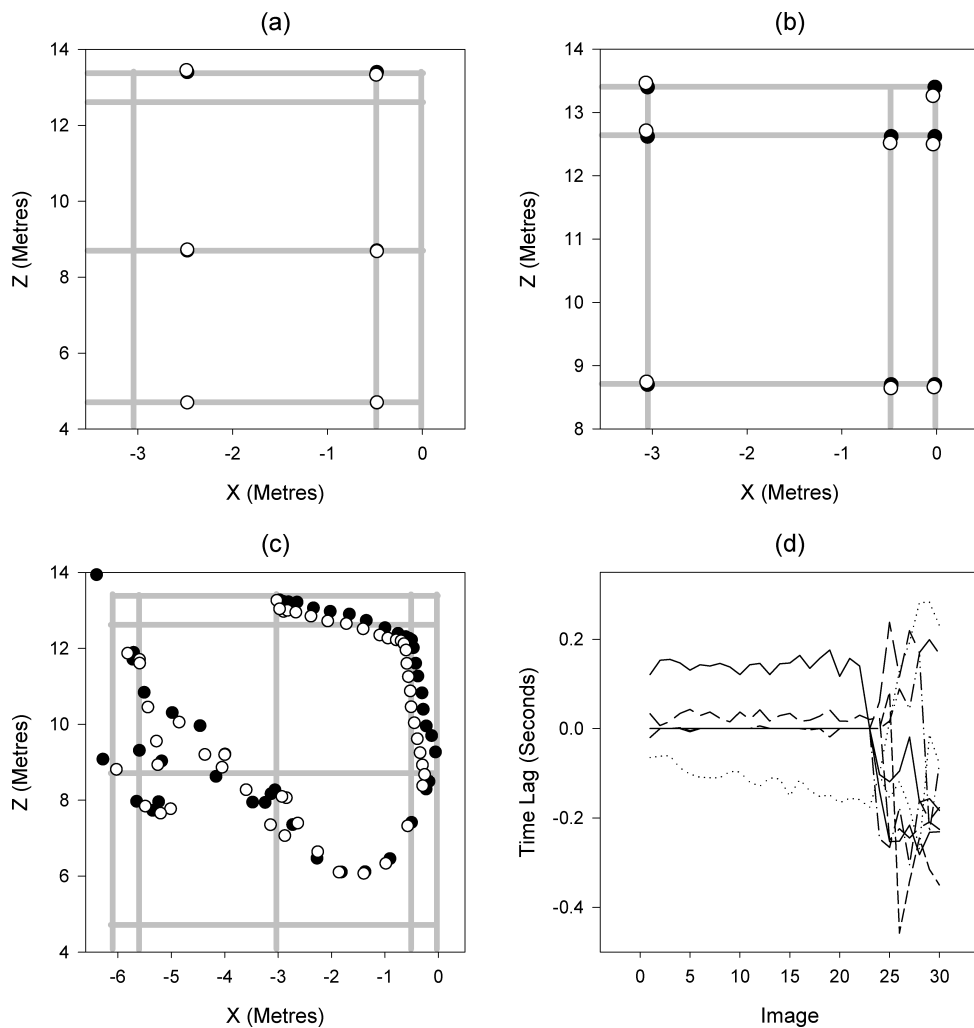
Figure 3.5: Results of the stereoscopic calibration and testing. (a) and (b) plot the reconstructed position (white markers) of calibration objects (black markers) placed at know positions on a badminton court which were used to parameterise and independently test the stereoscopic system (note some calibration objects are covered by the reconstruction and hence are not visible); (c) plots two reconstructed trajectories of a subject moving along a fixed preplanned route around the badminton court; (d) plots the time lag between corresponding images taken by each of the cameras in the stereoscopic setup on continuous shooting mode indexed by the image number. For the static objects shown in (a) and (b) the accuracy of estimated positions is good. Whilst initially this is also the case for a moving object, over time accuracy is seriously reduced due to desynchronisation between the cameras which is shown to occurs after approximately 20 images.

Table 3.2: A summary of the absolute and relative measurement errors determined from calibration experiments taking still images of objects at a distance of 10 metres. Using the relationships outlined by Cavagna et al. (2008) these results are scaled to estimate the measurement error which would be observed at various distances using the image resolution of both stills and video.

z	Stills (4752x3168)						Video (1920x1080)					
	Δx	Δy	Δz	δx	δy	δz	Δx	Δy	Δz	δx	δy	δz
10	0.02	0.01	0.06	0.01	0.01	0.03	0.02	0.01	0.06	0.02	0.02	0.08
50	0.32	0.19	1.17	0.13	0.12	0.53	0.32	0.19	1.17	0.36	0.32	1.43
100	1.26	0.76	4.69	0.53	0.47	2.12	1.26	0.76	4.69	1.43	1.27	5.73
200	5.06	3.04	18.8	2.11	1.88	8.48	5.06	3.04	18.8	5.72	5.08	22.9

Whilst these errors may seem acceptable at an average distance of 10 metres it must be noted that relative error increases by a factor equal to squared distance. The table also details an estimate of both absolute and relative error at various target distance up to 200 metres, the distance required at our chosen study site.

Finally, we performed an experiment designed to test the ability of the system to reconstruct the trajectory of moving object. Here, a subject followed a specific path around the badminton court shown in Figure 3.4(c) carrying an object to provide a consistent feature to identify in each image. The results of this experiment, displayed in Figure 3.5(c), show that initially the calibrated setup performs well matching the trajectory taken by the subject, however, over time both the accuracy and the frequency of points is reduced. This occurs as a result of a desynchronisation between the cameras. Further tests which used the camera setup to capture images of a digital timer found that this desynchronisation occurs after approximately 20 images corresponding to a time of 6 seconds (Figure 3.5(d)). This is a disappointing result and given the requirements of the investigation mean that video provides the only viable option. However, the relative errors associated with this means that accurate assessment of parameters especially at 200 metres may be unreliable.

3.3 Results

Despite regular deployment of the stereoscopic setup at our chosen site where interactions had previously been observed we recorded no useable data. This highlights the limitations of this approach in that observation is not continuous and relies heavily on site selection. However, during the course of this work some data was collected at an alternative site on the University of York campus. Whilst there is only a small quantity of data and this does not incorporate any interaction with obstacles, an analysis of flock structure and dynamics are presented here in order to demonstrate the type of summary statistics which may be extracted from the reconstruction and how these may be interpreted to infer particular parameter values in our models, specifically those relating to social interactions. Since the data is limited the values obtained from the reconstruction do not always fall within the expected ranges; this is discussed and alternative values from existing literature are suggested.

3.3.1 Reconstruction data and analysis

Following the failure to observe flocks at our primary study site the stereoscopic apparatus was deployed at secondary site on the University of York campus, with UK grid reference SE 63855052, where frequent flights could be observed. The detail of this site are shown in Figure 3.6. At this site we were able to capture footage of a single flock of 6 geese using the video based stereoscopic setup described previously. From this video footage synchronised images were extracted at a rate of 20 frames per second yielding 23 distinct time steps for which reconstructive analysis could be conducted. Owing to the limited amount of data the position of each individual on the image plane was extracted manually. In future work should larger amounts of data be captured an automated approach could be implemented using a suitable open source motion tracking software, such as SwisTrack (Correll et al., 2006), which has been used in other similar experiments (Bode et al., 2010a).

Using these point locations on the image together with the known parameters of the stereoscopic apparatus we reconstructed three-dimensional trajectories for each
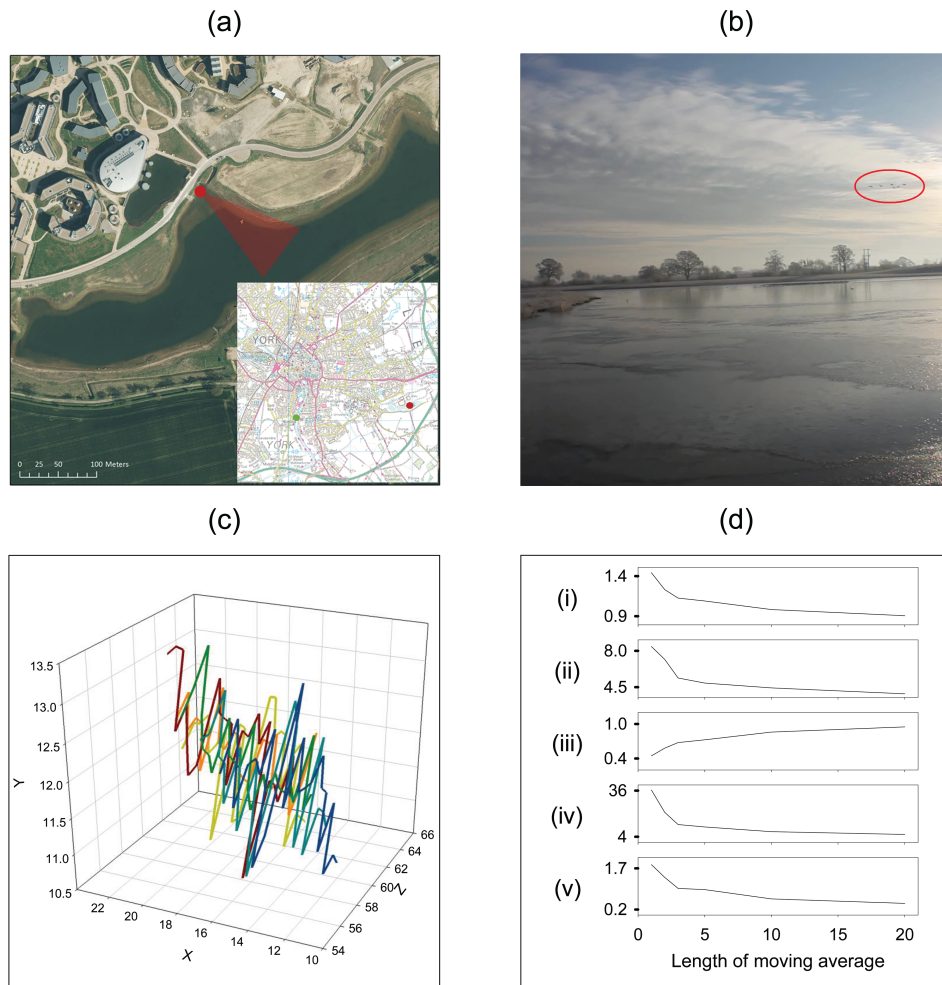
Figure 3.6: Details of a secondary study site with plots of reconstructed trajectories and analysis. (a) provides an aerial view of the study site outlining the position and orientation of the stereoscopic apparatus (red dot and cone respectively) with an inlay showing the location on a map of the surrounding area (green and red dots mark primary and secondary sites respectively); (b) is an image taken using the stereoscopic apparatus showing a flock of 6 geese (circled in red) which were observed at the study site; (c) plots the reconstructed three-dimensional trajectories for this flock; (d) plots the relationship between various summary metrics extracted from the reconstruction as a function of moving average length. The metrics shown are: (i) nearest neighbour distance; (ii) furthest neighbour distance; (iii) polarity; (iv) speed; and (v) turning rate. The reconstruction shows erratic movements likely due to system errors. By applying a moving average to smooth trajectories metrics appear to converge towards a stable value.

individual. These reconstructed trajectories are plotted in Figure 3.6(c). It is clear by comparing the trajectories in this figure with the video footage that the accuracy of the reconstruction is limited and consequently a direct analysis of these trajectories would be unreliable. In order to address this issue we propose a similar approach to that used in Budgey (1998), applying a moving average to smooth each trajectory. This method of noise reduction is valid assuming that the system error is evenly distributed with mean equal to zero. We computed several metrics to assess the structure and motion of the flock using various lengths of moving average to demonstrate that given a suitable smoothing coefficient each statistic converges towards a stable value. Figure 3.6(d) suggests that for all metrics to converge sufficiently a moving average across 10 images should be applied.

3.3.2 Analytical metrics and model parameterisation

The following discussion presents the estimates of computed metrics, namely neighbour distance, flight speed, flock polarity and average turning rate from the data described in Section 3.3.1. For each their reliability is assessed in the context of similar published studies and our own visual observation. Where estimates from previous studies are unavailable, as is the case for turning rate, comparison is provided using a theoretical approach based on well defined equations of flight (Pennycuick, 2008).

Using specific metrics, primarily neighbour distances, we outline the considerations which could be applied to parameterise the simulation model detailed in Chapter 4. The limited data collected as part of this study alone would be insufficient to make any statistically significant conclusions. To supplement this discussion additional analysis is presented using data obtained from a previous stereoscopic study (Budgey, 1998). The raw data supplied by Budgey (Pers. comm.) describes the reconstructed positions of 17 different flocks of various sizes at a single snapshot in time. This information can therefore only be used to inform flock structure and cannot provide information flight speed, flock polarity and average turning rate. Whilst the data

presents three-dimensional information it shows, consistent with observation, that geese tend to fly at similar flight heights with only minimal deviation (less than a metre). As such, the distances measured between neighbours can plausibly be applied to parametrise a two-dimensional model. In the absence of supporting trajectory data, the metric describing turning rate is difficult to validate empirically. Instead, as mentioned previously a theoretical argument is presented to provide comparison for our observations and suggest a suitable parameterisation for the maximum turning rate of geese.

Neighbour distance

Neighbour distances are computed as the relative distance between each individual at a specific snapshot in time. These distances are commonly used to describe and assess the spatial structure of groups. Figure 3.7 presents the data supplied by R. Budgey (Pers. comm.) detailed above to explore the structure of goose flocks and assess any relationship with flock size. Based on these distributions of nearest neighbour and neighbour distance an argument is outlined below as to how the radii characterising the zones of social interaction (repulsion, orientation and attraction) could be determined. The distances which define these interaction zones are a key component in models of collective motion and have been shown to significantly alter the characteristics of group motion (Couzin et al., 2002).

The nearest neighbour distance for each individual is one of most common metrics computed in studies of collective motion. The results from our reconstruction suggest that for the observed flock of 6 individuals the average nearest neighbour distance across all snapshots along the trajectory converges towards a distance of approximately 1 metre. Whilst this distance is plausible it is noticeably smaller than the range of distances observed in Figure 3.7(a)(iii). This perhaps shows that the dataset obtained from our stereoscopic set up is unsuitable to derive flock parameters from due to the lack of data and large errors in measurement of relative distance. At a distance of 50 metres, as is the case for the flock reconstructed here, the relative
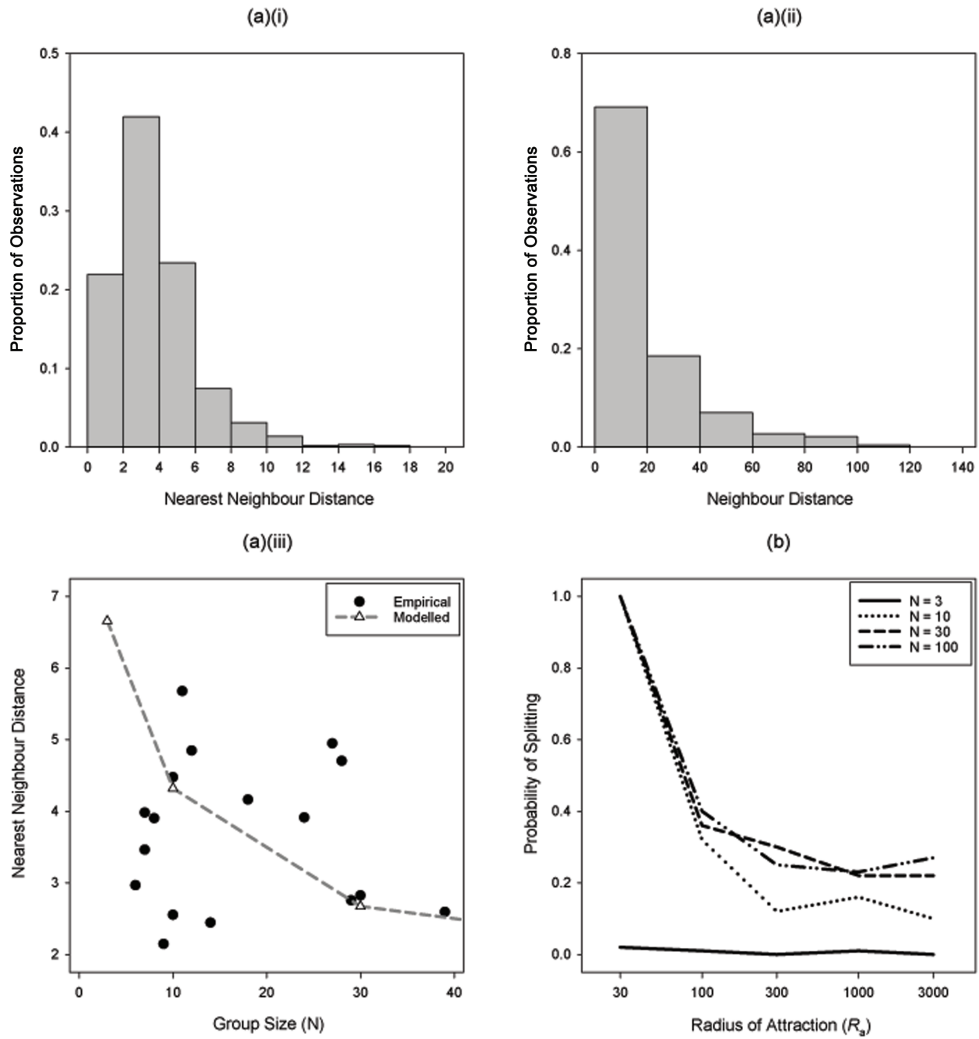
Figure 3.7: Plots present an analysis of the flock reconstruction supplemented with additional data supplied by Budgey (1998) to estimate the radii characterising zones of social interaction. (a) Summarises this data by plotting: (i) a histogram of nearest neighbour distances (NND); (ii) a histogram of neighbour distances (ND); (iii) average NND as a function of group size for both empirical and modelled data. (b) Plots the probability of splitting for simulated social groups ($w_s = 1$) of varied size (N) using the model outlined in Chapter 4 as a function of the radius of attraction (R_a). Empirical observation indicates fewer neighbours than anticipated in the range 0–2 metres with all nearest neighbours appear within 18 metres. NND is weakly correlated with N as opposed to modelled data which exhibits a strong negative correlation. In simulations, R_a must remain above 100 metres (approximately the maximum ND observed empirically) to maintain cohesive groups.

error between individuals 1 metre apart is estimated as 1.43 metres meaning that the average nearest neighbour distance could in fact be 2.43 metres. This value is instead much closer to the distances seen in Figure 3.7(a)(iii). Based on the distribution of nearest neighbour distance derived from Budgey (Pers. comm.) the radii of repulsion and alignment can be inferred according to the following argument.

Taking into account only attractive interactions, individuals would cluster together around the centre of the flock, the distribution of nearest neighbour distances would show most occurrences for the closest nearest neighbour distances (0–2 metres), decreasing with distance. Figure 3.7(a)(i) shows a distribution that approaches this but with significantly fewer individuals in the first bin (0–2 metres) than would be anticipated by this explanation. This indicates the zone of repulsion and is consistent with the average wingspan of the geese studied, reported as 1.5 metres (Ogilvie, 2011).

In addition, it is observed that all individuals have a nearest neighbour within a distance of 20 metres. This indicates that at distances that are larger than this, individuals will move to reduce the separation, giving a value for the closest distance at which attraction begins to occur. Between the zones of repulsion and attraction lies the alignment zone in which birds align with each other in order to maintain a separation. The data therefore indicates that this zone should span distances between 2 and 20 metres.

The distribution of neighbour distances can also be useful with the furthest neighbour distance representing the maximum flock width. Figure 3.7(a)(ii) plots this distribution from Budgey (Pers. comm.). It shows that the majority of neighbours lie within 0–20 metres supporting the conclusion from Figure 3.7(a)(i) that at distances larger than this attraction is likely to occur. It can also be seen that the furthest neighbour distance, and therefore the maximum width of the observed flocks, is 140 metres. As the flock observed in our study contained relatively few individuals it is perhaps unsurprising that the flock width calculated is well within this limit at around 4.5 metres. In comparison with flocks of similar size, as previously observed for nearest neighbour distance, the width recorded from Budgey (Pers. comm.) is

nearly double at 8 metres. Again, this difference is likely due to the high measurement errors estimated for the stereoscopic system.

It may be possible that the maximum flock width could indicate the radius of attraction for social groups. However, it is noted in Reynolds (1987) that, unlike other animals such as fish, birds have long-range visual capabilities and that this allows widely separated flocks to join together. Therefore, it is likely that the radius of attraction in fact extends beyond the maximum flock width. For the models outlined in this thesis the zone of attraction represents the limit of sensory perception. This zone also applies to interactions with obstacles. Studies at wind farm sites have recorded that geese display avoidance behaviour up to 1000 metres from turbines (Hötker et al., 2006). Consequently, in models containing obstacle interactions it is suggested that this distance should be used instead to define the zone of attraction.

Flight speed

Flight speed can be extracted from our reconstruction by calculating the distance between sequential positions on an individuals trajectory and dividing by the length of the time step, in this case 0.05 seconds. The average flight speed recorded for the flock across the period of observation was 7 m/s which is comparable to the observations expressed in Ogilvie (2011) for flights at low altitude which is used in the model described in Chapter 2. However, a higher speed of around 15 m/s has been recorded for geese during migrations, which is more relevant to the scenario simulated using the models in this thesis.

Flock polarity

The internal alignment, or polarity p, of the observed flock is determined using the heading vector $\underline{v}_i$, the vector connecting sequential positions on the smoothed flight trajectory, of each individual. It is computed as follows,

$$p = \frac{1}{N} \left| \sum_{i=1}^{N} \frac{\underline{v}_i}{|\underline{v}_i|} \right| \tag{3.2}$$

where N is the flock size (Couzin et al., 2002). This produces a value between 0 and 1 with higher values indicating a greater degree of alignment. Figure 3.6(d) shows that initially for a moving average of 1 (corresponding to the raw data) the flock appears poorly aligned with a polarity of 0.45 but as the length of moving average is increased polarity also increases converging towards a value of 0.95 for a moving average of 20. This value suggests a high degree of polarity which is consistent with the casual observation of geese.

Turning rate

An estimate of the average turning rate can be determined by calculating the angle between sequential heading vectors extracted from our reconstruction data. For a moving average of 20 this calculation produced an average turning rate measured across all time steps of approximately 0.42 radians, or 22 degrees, per 0.05 seconds. This would suggest that if an individual were to turn in a consistent direction the potential turning rate would be 440 degrees per second, i.e. an individual could turn more than a full circle within a second; this result seems unreasonable. The maximum observed turning rate according to our reconstructed trajectories was even larger at approximately 1000 degrees per second, nearly 3 full turns. This again illustrates the issues around calculating parameters from such a limited and imprecise dataset.

Using known physical parameters a more reasonable turning rate can be calculated from established equations of flight (Pennycuick, 2008). In the models used in this thesis the maximum turning rate (θ) is considered to apply to changes in heading rather than position. By considering a banked turn, in which an individuals movement follows an arced path, the maximum angle between sequential heading vectors is equal to the angle defining the arc length connecting the corresponding sequential positions; equivalent to the speed of travel v_0. To account for the two-dimensional environment in which individuals move such banked turns should be considered to occur horizontally, so that the vertical component of lift balances gravitational forces. Whilst the speed of movement is known in order to calculate the arc angle the

radius defining the turning circle, or tightness of turn, is also required. Considering a horizontal turn as described above Pennycuick (2008) derives the equation to determine minimum turning radius corresponding to the maximum turning angle as follows,

$$r_{lim} = \frac{2m}{C_L \rho S} \qquad (3.3)$$

where C_L denotes the maximum coefficient of lift, S is the wing area, m is mass and ρ is air density. Using specific values for geese provided by Pennycuick (2008) where C_L, S, m and ρ are given as 1.6, 0.331 m^2, 3.77 kg and 1.23 kgm^{-3} the minimum radius of a horizontal banked turn can be estimated as 11.57 metres. Therefore according to the basic equation defining an arc, $\theta = v_0/r_{lim}$, and assuming a speed of 15 m/s as outlined above the maximum turning rate is 1.29 radians, approximately 80 degrees, per second.

3.3.3 Model comparison

Using the parameters for speed, radius of interaction and turning rate suggested in the previous section, simulations were conducted according to the modelling approach outlined in Chapter 4 to compare the spatial distribution of groups with empirical data.

The plot in Figure 3.7(a)(iii) shows the variation of average nearest neighbour distance in relation to group size. It can be observed that the modelled data appears over a similar range to that of empirical data confirming that the parametrisation produces a representative group structure. However, simulated groups display a strong relationship between nearest neighbour distance and group size which is not present in the empirical data. The decreases in nearest neighbour distance, observed in the modelled data, is a result of increased desire for group centring. As more individuals are added, naturally the group must expand to maintain minimum nearest neighbour distances. However, this expansion is resisted by individuals towards the outer edge of the group who attempt to improve their position by moving towards the

group centre. These behaviours counteract each other increasing the density of the group, reflected by the decrease in nearest neighbour distance. This is a commonly observed difference between modelled and empirical data as discussed by Hemelrijk and Hildenbrandt (2012). For geese in particular this result could be due to the omission of factors, such as the energetic benefit of maintaining flight in the "upwash" of leading birds (Bajec and Heppner, 2009), which may contribute to the relative spacing of birds.

In addition to comparing the spacing between individuals the plot in Figure 3.7(b) tests the width of groups produced by the model. Rather than measuring this directly the parametrised model is used to explore the effect of varying the radius of attraction (R_a). In the absence of a common navigational direction Reynolds (1987) notes that in groups containing individuals whose sensory capability prevents at least some knowledge of all neighbours (e.g. fish) localised centres of mass could form, leading to group splitting. Therefore, the width of groups can be inferred by determining the attraction radius required to maintain stable cohesive groups. It can be observed (figure 3.7(b)) that when the radius of attraction is greater than 100 metres all groups maintain cohesion. Below this distance larger groups exhibit significantly reduced cohesion, indicating that group width is approximately 100 metres. This value is comparable to the maximum width of flocks estimated from the empirical data.

Whilst it is not shown here it should also be noted that simulated groups exhibit high polarisation which is characteristic of the flocks observed empirically. As mentioned previously the distances used to define the radii of interaction can have a significant effect on the pattern of movement produced within models. The fact that the parameterisation used here produces movements similar to those observed in the field is further evidence to suggest that the identified values are reasonable.

3.4 Discussion

In this chapter we have described the development of a portable stereoscopic camera system which could be used to investigate the interaction of geese with obstacles, such

as wind turbines. We outline methods to calibrate this system and perform tests to assess its limitations. Using data gathered in the field we reconstruct trajectories for a flock of geese and demonstrate how appropriate model parameters could be extracted given data of suitable context, quality and quantity. By comparing the behaviour of simulated groups according to this parameterisation with empirical observations we assess the realism of the model and suggest mechanisms which could explain differences in group structure. The results of this comparison show that whilst some properties are reproduced by the model, such as flock width, others are less well defined. For example, the nearest neighbour distance in simulated groups is strongly correlated with group size but a similar pattern is not clearly evident in empirical data. It is argued that this may be due to the omission of mechanisms related to aerodynamics efficiency. Whilst this may limit the realism of the model it should not impact the qualitative assessment of obstacle avoidance.

Our assessment of the stereoscopic system shows that whilst the resolution of still images allows more precise reconstruction the cameras used in this study were only able to maintain synchronisation at a suitable frame rate for a short period, approximately 6 seconds. Based on our observations of geese this would be insufficient to capture the full interaction of flocks with an obstacle allowing an assessment of behaviour both pre- and post- avoidance. Consequently, we conclude that at present video provides the most viable option for this type of study. However, the limited resolution of video impacts the accuracy of the system. At a distance of 200 metres, that required to observed flocks at our chosen site, both the absolute and relative positional errors are approximately 20 metres, i.e. 10%. Whilst this error is large we have demonstrated, for observations recorded at a distance of 50 metres, that a moving average can be implemented to reduce noise allowing metrics describing group structure and movement to be computed with a reasonable degree of accuracy; comparing favourably with similar values found in existing literature. This approach may not be suitable for assessing group interactions with an obstacle. Unlike the relatively stable flocks captured here, flocks performing avoidance manoeuvres may be

subject to significant disruption the observation of which would be limited by applying a moving average. It is therefore necessary to consider methods for improving the accuracy of the stereoscopic system.

The relationships outlined in Cavagna et al. (2008) suggest that errors in absolute position are a result of misalignment between the cameras and that these could be improved by accurate measurement of alignment in the field each time the system is deployed rather than applying a general calibration result inferred from reconstruction data as is the case here. Relative error is instead dependent upon the baseline length, the relative separation of the cameras, and the image resolution with increases in each reducing error. In order to maintain the mobility of the system it would be impractical to consider increasing the length of the baseline meaning that the only way to reduce relative errors would be to increase image resolution. Recent advances in commercial video technology may provide a solution to this problem. The wide spread release of 4k video has begun to bridge the gap between the resolution of still images and video providing high speed image capture at a standard resolution of 3840 by 2160. This signals a shift in the use of camera technology away from traditional point and click image capture towards more continuous approaches where stills are instead extracted in post processing. Further advances are anticipated in the near future with an 8k video standard in development which would provide a resolution of 7680 by 4320. At this resolution the relative error in our system would be reduced significantly to approximately 2.5%.

The integration of an accompanying GPS based system could also improve the experimental design. As already stated this method alone is unsuitable to use in uncontrolled experiment as it cannot be guaranteed that all members of a flock are tagged. However, GPS data from a sample of individuals within a flock could be used to ground the stereoscopic reconstruction data providing the necessary information to perform validation and reference the absolute position of the flock relative to the real world. The latter would be particularly beneficial for assessing avoidance manoeuvres where absolute position relative to an obstacle is required and can be challenging to

infer from stereoscopic data.

The lack of data captured at our primary study site highlights the variable nature of observing animals in an open environment. It is perhaps reasonable to suggest that the fieldwork proposed in this chapter could be considered overly ambitious for an initial investigation given the limitations of the technology and resources available. An alternative approach may be to conduct exploratory experiments in a more controlled lab-based environment using fish where repeated obstacle interactions could be manufactured and observed at a closer distance which is not subject to the same levels of measurement error. Though behaviour may vary across taxa this would at least provide a basic understanding of the mechanisms relating to avoidance and in the absence of other such studies could serve as a benchmark for future investigations.

Chapter 4

Obstacle avoidance in social groups: new insights from asynchronous models

4.1   Preface

As stated previously in the Thesis Declaration this chapter has been published in a peer-review journal. It is presented as it appears in print with the following revisions:

1. Minor grammatical and referencing errors have been corrected to improve clarity.

2. Referencing to relevant discussion elsewhere in the thesis has been incorporated.

3. Text has been added to provide clarification on the meaning of transparency of obstacles in relation to vertex density.

4. Comment has been added regarding the choice of minimum spacing between obstacle vertices.

5. Equation 4.1, detailing the calculation of selection probability for each update partners, and accompanying text has been revised to clarify the distinction between selection weight and probability.

6. Explanation of the generation of random turbulence has been modified to reflect the definition of a Von Mises distribution i.e. with a κ-parameter rather than a standard deviation as used in an equivalent Wrapped Normal distribution.

7. The definition of simulation metrics has been revised and added to in order to provide additional clarity.

8. Comment has been added to clarify the method used to simulate heterogeneity in the preference weightings of individuals for social and obstacle avoidance behaviours.

9. Definition of turbulence (w_e) added to Table 4.1.

10. Comment has been added to provide additional discussion of the observations relating to network structure and group cohesion in relation to the previous findings of Bode et al. (2012c).

11. Discussion of Figure 4.6 relating to navigation of groups in turbulent environments has been revised to emphasis the argument that the observations at first glance may appear to contradict Codling et al. (2007) but do in fact support these conclusions with increased avoidance of more social groups driven by a failure to navigate in the target direction rather than a deliberate avoidance strategy.

12. Note added to clarify the meaning of "no collision risk" in the discussion of variations in environmental turbulence.

Significant additions to the text are presented in *italics* delineated by square brackets.

4.2 Abstract

For moving animals, the successful avoidance of hazardous obstacles is an important capability. Despite this, few models of collective motion have addressed the relationship between behavioural and social features and obstacle avoidance. We develop an asynchronous individual-based model for social movement which allows social structure within groups to be included. We assess the dynamics of group navigation and resulting collision risk in the context of information transfer through the system. In agreement with previous work, we find that group size has a non-linear effect on collision risk. We implement examples of possible network structures to explore the impact social preferences have on collision risk. We show that any social heterogeneity induces greater obstacle avoidance with further improvements corresponding to groups containing fewer influential individuals. The model provides a platform for both further theoretical investigation and practical application. In particular, we argue that the role of social structures within bird flocks may have an important role to play in assessing the risk of collisions with wind turbines but that new methods of data analysis are needed to identify these social structures.

4.3 Introduction

Collective motion can be observed in a wide variety of biological systems, inspiring scientists to investigate the mechanics behind such apparently complex behaviour (Aoki, 1982; Major and Dill, 1978; Heppner, 1997; Czirók and Vicsek, 2001). Many of these studies have developed individual-based models to assess the effect of behavioural and environmental factors (Couzin et al., 2002, 2005; Codling et al., 2007; Bode et al., 2011a; Croft et al., 2013). These models simulate motion through local interactions by applying rules based on proximity with individuals exhibiting three core behaviours: repulsion (avoiding collision with other individuals); orientation (aligning with nearby

individuals); and attraction (movement towards distant individuals) (Reynolds, 1987; Couzin et al., 2002). Additional rules can be incorporated to represent environmental factors, for example, navigation towards a target or response to predators (Inada and Kawachi, 2002; Couzin et al., 2005; Codling et al., 2007; Bode et al., 2011a).

Typically, such individual-based models do not constrain the number of interactions that contribute to the motion of an individual. These are known as "metric" models, as they sum the interactions with all cues within a given distance of a focal individual (Couzin et al., 2005; Codling et al., 2007; Croft et al., 2013). However, empirical evidence suggests that social interactions may in fact be topological, with each individual responding only to a fixed number of other individuals (Ballerini et al., 2008a). Studies which develop an asynchronous updating method have demonstrated that this topological property for interactions emerges spontaneously (Bode et al., 2011a). Significant features of this modelling approach include varied speed distributions and emergent stochastic noise in the decision making process, both of which contribute to a greater degree of biological realism.

The importance of this updating scheme becomes apparent when individuals interact with other environmental factors and averaging becomes inappropriate. Of particular interest is when these environmental factors are of significant societal or conservational relevance. For example, a growing demand for renewable energy has led to a significant increase in the number of wind farm developments (UK Renewables, 2013). Wind farms are often sited in areas which intersect existing flight paths of migratory bird species, thereby forming a potential barrier to movement (Masden et al., 2009). It is important that we understand the impact such developments could have on the level of avian mortality as a direct result of collisions in order to protect the population of at risk species (Drewitt and Langston, 2008). There is considerable variability in the collision risk for avian species from wind turbines, not least due to variable sampling techniques and carcass loss from scavengers, estimates for per turbine collision rates per annum span 4 orders of magnitude (Drewitt and Langston, 2008). However, few studies in the field of collective motion have investigated the

interactions of bird flocks with wind turbines or other obstacles (Banks, 1979; Martin, 2011), primarily because of ambiguity in the methodology for incorporating obstacles (and their avoidance) within existing models.

The previous work, presented in Chapter 2, investigating the interaction of groups with a single obstacle shows that group size has a non-linear relationship with collision risk, and that whilst initially social interactions cause a higher per capita risk of collision this is reduced with further increases (Croft et al., 2013). This has implications for the modelling of real-world applications, especially for avian collisions where current probabilistic models (Band et al., 2005) have no explicit dependence on group size and cannot incorporate changes in behaviour driven by social dynamics (Chamberlain et al., 2006).

Recent studies using an asynchronous update scheme have outlined a robust framework to investigate the effect of complex behaviours such as the influence of social networks (Bode et al., 2012a). This has important applications in simulating real-world animal movement where empirical evidence suggests that both ability and influence are unlikely to be distributed evenly (Lamprecht, 1992; Kurvers et al., 2009; Nagy et al., 2013). The results show that when compared to previous studies, which focus on the effects of varied ability (Couzin et al., 2005; Leonard et al., 2012; Richardson et al., 2014), underlying networks representing simple examples of leadership can have a significant impact on group dynamics and navigational performance. Whilst leadership provides one example of a social network structure, other characteristics such as clustering, as a result of strong interactions between members of family groups, could also be present and have the potential to produce distinct group behaviours (Krause et al., 2014). This highlights the importance of identifying plausible network structures in order to produce realistic simulations of animal movements. In the case of geese such network structures are not well established; and in pigeons it has been shown that in-flight hierarchies cannot be inferred reliably from ground-based networks (Nagy et al., 2013). Network structures in other systems are better developed, for example in humans (Moussad et al., 2010),

in other social animals (Pinter-Wollman et al., 2014) and in other application areas (Kumar et al., 2010; Watts, 2004).

Here, we describe an individual-based model with an asynchronous updating algorithm to investigate group interactions with obstacles. Using this model we explore the response of individuals to changes in group size. We determine the effect this may have on collision risk; initially with a single obstacles, and then with an array of obstacles representing a typical wind farm. We parametrise and then continue to simulate group interactions with an obstacle array, investigating the impact underlying social networks have on collision risk by comparing four example networks (homogeneous, random, clustered and leadership; to be defined in Section 4.4) each representing a distinct structural characteristic. We discuss how different environmental factors may contribute to collision risk, paying particular attention to the role of weather conditions, such as environmental turbulence and visibility. These factors have proved difficult to assess empirically as many studies rely upon a degree of visual observation to determine behaviour (Desholm et al., 2006; Drewitt and Langston, 2008; Plonczkier and Simms, 2012). Finally, we investigate the trade-off between avoidance and migratory pressures such as energetic efficiency (Pennycuick, 2008) by introducing a fixed straight route which group members attempt to follow, thereby minimising energy expenditure. Such behaviour imposes a previously ignored cost to obstacle avoidance which may have an important impact on predicted collision risk.

4.4 Methods

4.4.1 Modelling framework

The model is adapted from the stochastic implementation outlined in Bode et al. (2012a) (further justification for this choice with respect to obstacle avoidance is included in Chapter 5).

Groups consist of a set of $\{1, \ldots, N\}$ individuals each represented by a position

$\underline{x}_i$ and a unitary heading vector $\underline{\hat{v}}_i$ in continuous two dimensional space. Inspired by computational techniques for object reconstruction, obstacles are represented by a finite set of $\{1, \ldots, M\}$ vertices and connecting edges (Hartley and Zisserman, 2003). Each obstacle vertex is represented by a position $\underline{p}_i$ and an outwardly facing normal vector $\underline{\hat{n}}_i$. By describing obstacles in this way we provide a flexible approach for approximating any shape, size or orientation without the need for complex differential geometry. The degree of error in this method can be controlled by varying the number of vertices which comprise each obstacle (see Section 5.3.4 for further details). This allows us to distinguish between obstacles of equal size which induce different avoidance potentials, for example as a result of varying levels of transparency, without altering the way individuals respond to singular vertices. In this study we minimise the error in behavioural response by adopting a standard spacing of 1 spatial unit between vertices; provided the minimum distance used to categorise behavioural response is greater than this value, individuals will detect the obstacles and react appropriately. [*Further investigation presented in Section 5.3.4 show that whilst a spacing of 1 is consistent with the representation used in Chapter 2, in fact the minimum standard spacing used here could be larger, approximately 7, due to an increased radius of repulsion for obstacle interactions.*] Motivated by our wind turbine application, obstacles are considered to be transparent to the extent that they do not occlude vision.

In common with established models (Reynolds, 1987; Couzin et al., 2002, 2005), an individual determines a direction of motion by responding to selected navigational cues within a given sensory zone, including migration towards a particular target (Codling et al., 2007). This sensory zone is defined by a circle of radius R_a centred on the individual, with an omitted blind angle β to the rear (Heppner et al., 1985). However, unlike these models, individuals are updated asynchronously according to the following algorithm:

1. Choose individual i at random.

2. Choose an "update partner" j (which may be another individual, an obstacle

vertex, or the target direction) with probability P_{ij} at random from all stimuli within sensory zone (see below). If there is no stimulus then continue on current heading.

3. Determine $\hat{\underline{v}}_i$ in response to chosen partner j.

4. Update $\underline{x}_i$ and $\hat{\underline{v}}_i$.

We ensure that each individual updates on average once per time interval Δt by performing N realisations of the steps 1–4 (Bode et al., 2010a). Simulation outputs are recorded every $\tau = \lambda \Delta t$ seconds, where λ (≥ 1) defines the average number of updates performed by each individual. When $\lambda > 1$ the resulting behaviour between consecutive model outputs is the sum over a number of updates (Bode et al., 2012a). The choice of λ is discussed in Table 4.1.

The probability of an individual selecting a particular update partner is initially weighted based on the type of interaction. Interaction weighting are defined as social (w_s), obstacle (w_o) and target (w_t). Each of these weightings is modified according to a spatial relationship providing distinction between partners of the same type. Social and obstacle interactions are each scaled by a factor equal to the inverse of relative distance ($d_{ij} = |\underline{x}_j - \underline{x}_i|$); capturing the averaged effect of visual occlusion. In addition, obstacle vertices which appear outside of the frontal region defined by a sector of angle α and radius greater than $R_r{}^o$ are considered to have a weighting of zero.

In order to emulate the effect of social networks within the group we construct an underlying fixed matrix with elements e_{ij} (≥ 0). This matrix remains unchanged through the simulation and contains information on the long-term social preference and bonds between group members. The factor $\epsilon_{i,j}$ further scales the probability of an individual i selecting a particular neighbour j. The details and implications of this methodology are discussed in detail elsewhere (Bode et al., 2011b,c).

Finally, the weighting for target navigation comprises two parts, a constant directional part (w_{t0}), and a variable part (w_{t1}) which is determined by a function of

the angle between the individuals current heading and its ideal target direction (ϕ). As an individual orientates away from its ideal target heading this angle becomes greater, increasing the target selection weighting. This simulates a desire for group members to follow a particular route with strong route fidelity, a well established trait of migratory birds (e.g. Biro et al., 2007). In summary, for an individual i in a group with individuals $n = \{1, \ldots, N\}$ augmented with the obstacle vertices $m = \{1, \ldots, M\}$ and the target, then update partner $j \in \{N + M + 1\}$ is chosen with weighting w_{ij} such that:

$$
w_{ij} = \begin{cases} w_s e_{ij}/d_{ij} & j \leq N \\ w_o d_{ij} & N < j \leq N + M \\ w_{t0} + w_{t1}(1 - \cos(\phi)) & j = N + M + 1 \end{cases} \tag{4.1}
$$

and hence the probability of selection (P_{ij}) can be calculated as w_{ij} divided by the sum of all weightings.

It is important to note that this differs from previous implementations of this model (Bode et al., 2012a) which use a constant probability for the target; here the target is merged into the pool of update partners that can occur at each micro-step, and as a result the target preference is dependent upon the weight of other stimuli.

Once a partner has been selected, the updating individual must determine how to respond according to the type of update partner. If a neighbour is selected, then the focal individual's sensory zone is divided into hierarchical interaction zones of radius $R_r{}^s$, $R_o{}^s$ and R_a which dictate whether repulsion, orientation or attraction manoeuvres are performed respectively. Here, attraction manoeuvres are applied with a velocity of $2v_0$, representing the increased thrust required by an individual to reduce their distance to neighbours, maintaining group cohesion. Similarly, if an obstacle vertex is selected a repulsive manoeuvre is applied within a zone of radius $R_r{}^o$. For any vertices which appear at a distance greater than $R_r{}^o$ we apply a pre-emptive avoidance strategy equivalent to social alignment which aims to limit more extreme repulsive action. Previously, it has been proposed that individuals should

attempt to align themselves with the surface of an obstacle at the point of interaction (Croft et al., 2013). For birds, which have been shown to have largely monocular vision (Martin, 2011), this type of information requires a degree of depth perception that is likely to be beyond their sensory capability. Instead, in this model we suggest a simpler response where individuals turn away from obstacle vertices to maintain a minimum angle of α between their heading and the trajectory intersecting the vertex. The cumulative effect of this response results in an individual attempting to avoid an obstacle on a trajectory which requires the least deviation from its current heading.

If target navigation is selected then an individual aims for a point that is a fixed distance (d_t) from its current projected position along the group target trajectory, inspired by route fidelity found in other species. This target trajectory is defined by the straight line starting at the initial group centre of mass and continuing indefinitely in the direction specified by a fixed target vector $(\hat{v}_t)$. This implements instantaneously perfect navigation on a linear route. Other studies have considered error in navigation (Codling et al., 2007), but when this variation is introduced into the model presented here it is dominated by the inherent noise in the underlying algorithm (Bode et al., 2010b). For the application to collision avoidance, navigation error is therefore of less importance then some of the other features varied in our analysis.

To represent the finite ability of an individual to execute a turn in the direction of its preferred heading, we implement a maximum turning rate of θ. In simulations which apply a movement error to represent environmental turbulence we rotate the calculated heading vector, following the application of a turning limit, by an angle randomly drawn from a Von Mises distribution with mean of zero and kappa w_e^{-1} such that small values of w_e correspond to low levels of error. Intersections with obstacles are recorded when the trajectory of an individual intersects either an obstacle vertex or connecting edge. In this implementation of the model we consider the probability of these intersections resulting in a fatal collision to be zero. Consequently, intersecting individuals are not removed from simulations. The implications of this choice on obstacle avoidance is addressed in Section 5.3.3.

We compute various metrics to summarise the data from our simulations. **Target navigation ability** is defined as the fraction of the trajectory that all birds spend travelling in the target direction. This is computed as the dot product of the mean group direction (the vector from the initial mean group position to the current mean group position) with the target direction, scaled by the mean distance travelled. [*Consequently, this metric not only describes how accurately a group has navigated in the target direction but also how direct the trajectory.*] The **probability of splitting** is computed by calculating the fraction of simulations which contain more than one group at the end of the simulation. [*The simulation time was tested and set so that groups had sufficient time to reach a new stable state following obstacle interactions, see Section 5.2 for details.*] We include both spontaneous splitting and interaction with the obstacle to enable a measure of relative disruption to be computed. The number of groups is calculated using an equivalence class relation with the equivalence based on the radius of alignment. The probability of avoidance is computed by averaging the number of individuals that intersect a single wind turbine (micro) or array of wind turbines (macro) across all independent simulations of a given scenario. The latter measure should be assumed in all cases unless otherwise stated.

4.4.2 Parametrisation

Parameters are chosen to nominally represent flocks of pink-footed geese (*Anser brachyrhynchus*) interacting with an array of wind turbines. Where possible parameter values have been taken from empirical data. Time and space steps, and model parameters, are related to their real world units and values in Table 4.1. Following (Siemens AG, 2014) the width of obstacles used in simulations is fixed at 100 metres, which represents a typical offshore wind turbine.

In simulations where we investigate the effect of heterogeneity in the abilities of group members, the values of obstacle avoidance and target preference are varied. For each individual the respective parameter values stated in Table 4.1 are scaled by a factor randomly selected from a Normal distribution with mean equal to 1

and standard deviation w_h, which provides a quantification for heterogeneity. [*To ensure that parameter values remain appropriate, i.e. non-negative, the distribution is truncated at either end between 0 and 2 with factors generated outside of this range resampled until a suitable value is achieved. Given the levels of w_h used in simulations it should be noted that whilst possible resampling of factors is unlikely to be required.*]

Table 4.1: List of parameters used in model simulations. Values stated are for a typical group interacting with a square array of 25 obstacles. Where appropriate, physical parameters have been set based on values from existing empirical studies.

Symbol	Value	Description and Unit (where appropriate)
N	30	Number of individuals within the group (Croft et al., 2013).
τ	1	Time interval for each individual to perform, on average, λ updates (in seconds) (Bode et al., 2011a, 2012a).
Δt	0.01	Time interval for each individual to perform, on average, a single update step (in seconds) (Bode et al., 2011a, 2012a).
λ	100	Update frequency represents the average number of updates an individual performs per second (Bode et al., 2011a, 2012a; Healy et al., 2013).
v_0	15	Average cruise speed in metres per second (Pennycuick, 2008).
α	45	Angle of pre-emptive obstacle avoidance needed to observe a minimum distance of $R_r{}^o$ from vertexes.
β	60	Angle of rear blind region of an individual (in degrees) (Heppner et al., 1985).
θ	80	Maximum horizontal turning rate (degrees per second) (Pennycuick, 2008).
$R_r{}^s$	2	Radius of social repulsion, in metres, representing the average size of an individual, in this case the wingspan (Pennycuick, 2008).

Table 4.1: List of parameters used in model simulations (continued from the previous page).

Symbol	Value	Description and Unit (where appropriate)
$R_r{}^o$	150	Radius of obstacle repulsion, in metres, average minimum distance maintained by individuals from obstacles, in this case geese from wind turbines (Desholm et al., 2006).
$R_o{}^s$	20	Radius of social alignment, in metres, maximum nearest neighbour distance within groups, in this case flocks of geese (Budgey, 1998).
R_a	1000	Radius of attraction, in metres, representing the maximum perception distance of an individual, in this case the maximum distance from wind farms which geese show avoidance action (Hötker et al., 2006).
w_s	1	Social preference weighting, the priority an individual shows towards selecting a neighbour for an "update partner".
w_o	1	Obstacle avoidance weighting, the priority an individual shows towards selecting an obstacle vertex for an "update partner".
w_t	0.1	Target preference weighting, the priority an individual shows towards selecting the target for an "update partner".
w_{t0}	0.1	Baseline target preference weighting, the minimum weighting which guarantees successful navigation towards a designated target.
w_{t1}	0	Variable target preference weighting, the coefficient which scales the maximum target preference weighting.
w_n	0.1	Network weighting, the magnitude of increments applied to interaction matrix elements used in random network generation.

Table 4.1: List of parameters used in model simulations (continued from the previous page).

Symbol	Value	Description and Unit (where appropriate)
w_h	0	Heterogeneity, the standard deviation of the normal distribution used to vary avoidance and target preferences between individuals.
w_e	1e-15	Error weighting, the magnitude of movement error used to simulate environmental turbulence.
d_t	30000	Target heading distance, defines the distance along group target trajectory which an individual navigates towards. This is chosen to minimise the lateral effect on group structure.

In order to simulate underlying social networks we define interaction matrices with elements e_{ij} denoting the strength of the social connection individual i has towards neighbour j. For a **unitary homogeneous network** we consider connections between neighbours to have a weight equal to 1 ($e_{ij} = 1$). Connections between the same individual are disallowed ($e_{ii} = 0$). **Random networks** are generated relative to this unitary matrix so as to maintain a balance between the average weight of all detected social interactions relative to obstacle and target interactions. Initially, we assume that all individuals are at least weakly connected with weight w_n. Connections are selected at random and incremented by w_n until the sum of all elements is equal to that of the homogeneous case.

For **clustered and leadership networks** the connections which can be incremented are limited to a specific subgroup. In the case of a leadership network l individuals are randomly identified as leaders. The only matrix elements which can be incremented are those which describe the connections from a remaining group member to any of these leaders. In the case of clustered networks, group members are assigned a number between 1 and c representing a fixed number of subgroups.

The only matrix elements which can be incremented are those which describe the connections between group members with matching cluster index. Unless otherwise stated simulations use a unitary homogeneous network.

4.4.3 Simulations

Simulations consist of two phases: an initial warm up, followed by a phase of interaction with obstacles. Each phase is performed for a period of 1000 time steps in an unbounded environment. The warm up phase allows groups to form a representative configuration in the absence of obstacles. Here, we define a representative configuration to mean that all individuals belong to an equivalence class where neighbours are declared equivalent if they are within a distance equal to the radius of alignment ($R_o{}^s$). Thereby, each individual must as a minimum be in a position to align with at least one neighbour. It should be noted that individuals can become permanently separated from the main group. In such cases where a representative configuration is not formed the warm up phase is repeated.

The group is then reset with its centre placed on a selected origin and rotated so that the average heading is equal to the specified target direction. In simulations with a single obstacle we use a fixed origin which is located 5000 metres from the obstacle centre in the target direction. Otherwise, groups interact with an array containing 25 obstacles uniformly arranged on a square grid at 500 metre intervals, the representative spacing of wind turbines (Masden et al., 2012).

To focus on behavioural effects and minimise the effect of starting conditions we perform the following randomisation scheme on the initial positions. The origin is randomly selected on a line segment with midpoint 6000 metres from the array centre (approximately 5000 metres from the nearest obstacle) in the target direction and extending perpendicular to this vector. The group centre may be placed either side of the segment midpoint at a distance corresponding to the cross-sectional width of the obstacle array excluding a 50 metre buffer zone at both ends. This guarantees that, if there is no avoidance behaviour, individuals will intersect the area bounding

103

the array. By varying the origin of groups we sample all potential interactions with the array. To minimise the number of direct routes through the array we offset the angle of approach, between the target direction and the orientation of columns in the array, by 12 degrees, at which the probability of an individual avoiding all obstacles without evasion is negligible.

Once the simulation warm up phase is complete, the phase of obstacle interaction is initiated, during which individual level trajectory data is recorded at discrete time intervals (τ). For each set of parameters we perform 100 iterations and using this trajectory data calculate the statistics characterising group dynamics and collision risk.

4.5 Results

Prior to introducing any obstacles, the first step is to establish what baseline target preference is necessary for the model to reproduce the observed biological phenomenon of coherent group navigation along a nominated trajectory. Figure 4.1 summarises this process: Panel (a) confirms that the minimum target preference required, relative to a social weighting of unity, is approximately 10^{-2}; Panel (b) shows that group cohesion is initially improved by a common navigational direction but that there exists a maximum baseline target preference of approximately 10^{-1}, above which relative social preference is insufficient to maintain group cohesion. Combining these results we identify this maximum threshold as an appropriate value for baseline target preference across all group sizes. In addition to the results shown in Figure 4.1 we observe that mean nearest neighbour distance decreases as a function of group size, consistent with Hemelrijk and Hildenbrandt (2012).

We can now begin to explore the effect of avoidance preference in relation to collision risk (Figure 4.2). In common with a simpler fixed time step model (Croft et al., 2013), we find that avoidance is dependent upon group size, with smaller groups displaying an increased ability to avoid both single obstacles and arrays across all parameter values. Furthermore, it can be seen in Figure 4.7 that this relationship

104
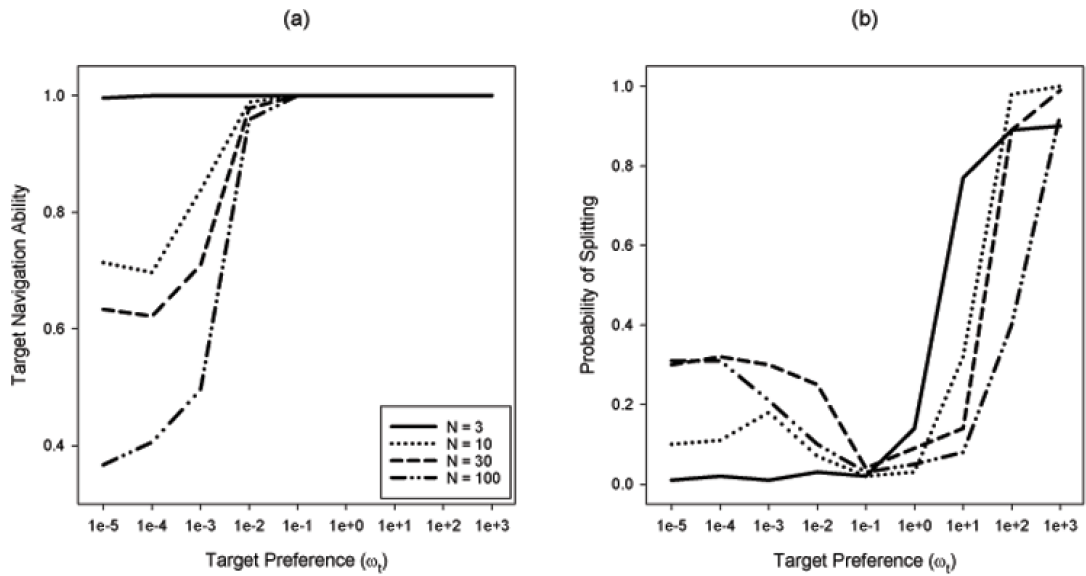
Figure 4.1: Parametrising target preference for coherent directed groups. For social groups $(w_s = 1)$ of varying size (N) in an obstacle-free environment, we plot: (a) average proportion of distance travelled parallel with target trajectory; (b) probability of a group splitting; (recorded after 1000 time steps) as a function of baseline target preference (w_{t0}). We observe that beyond a critical value $(0 < w_t \leq 0.1)$, dependent on N, navigation occurs directly along the target trajectory. This common direction appears to improve group cohesion reducing the probability of splitting but as w_{t0} increases further social preference is overwhelmed resulting in an increased proportion of groups splitting.
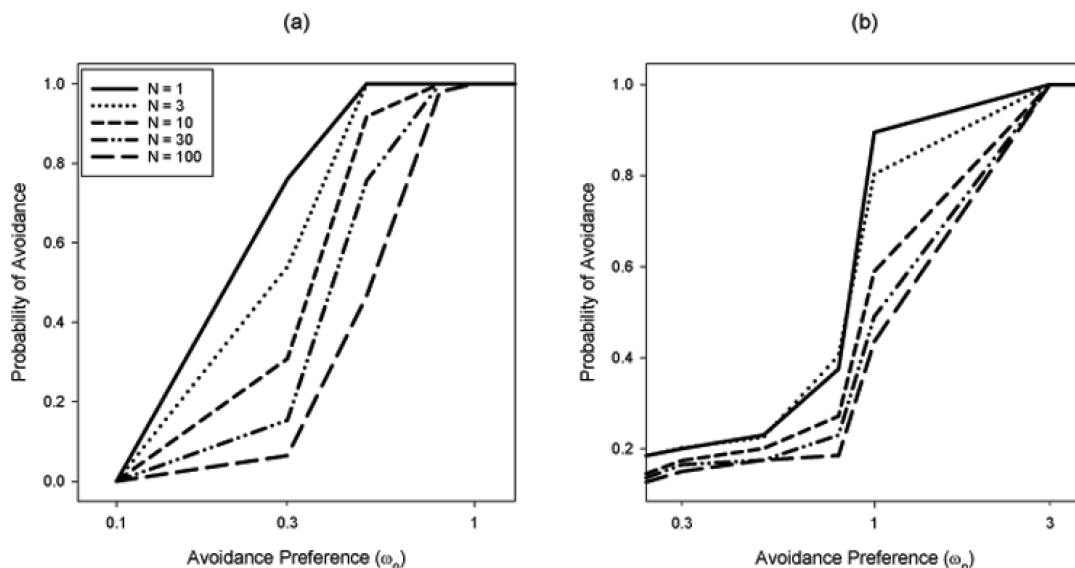
Figure 4.2: Avoidance of an obstacle does not guarantee avoidance of an array. For social groups ($w_s = 1$) of varying size (N) and baseline target preference ($w_{t0} = 0.1$) we plot the probability of avoiding the region bounding an array containing: (a) a single obstacle; (b) 25 obstacles uniformly arranged on a square grid at 500 metre intervals; (recorded after 1000 time steps) as a function of avoidance preference (w_o). For each, group target trajectory intersects the array at an angle which minimises the probability of avoiding all obstacle given no avoidance behaviour. As expected the probability of avoidance increases with w_o. However, this relationship is not linear but instead shows a sharp step at a critical value of preference particularly evident in (b). In common with previous studies (Croft et al., 2013) there appears a dependence upon N, with smaller groups displaying a higher propensity for avoidance. We note that the probability of avoiding all obstacles (micro) in case (b) (not shown) is qualitatively similar to (a) with transitions appearing at marginally lower values of preference. Consequently, groups demonstrate total avoidance of all obstacles in (b) prior to any avoidance of the array as a whole.

can be non-linear. In the context of avian interactions with wind turbines we aim to identify a suitable parameter value for avoidance preference by comparing the data in Figure 4.2(b) to estimated wind farm avoidance rates for migrating geese. This plot shows a sharp improvement in avoidance around a value of 1 with an average probability of avoidance across all group sizes reaching approximately 60%. This lies well within the range of estimates for wind farm avoidance observed by empirical studies which record values between 50 and 70% (Cook et al., 2012). Empirical studies also observe that of the remaining individuals which enter the wind farm area more than 99% successfully avoid all wind turbine structures resulting in an overall avoidance rate of approximately 99.8% (Pendlebury, 2006; Plonczkier and Simms, 2012). However, it should be noted that there are some studies which record 100% avoidance (Desholm et al., 2006) – for our chosen value of $w_o = 1$ individuals entering the array are able to successfully avoid all obstacles.

Using the parameter values identified above for all subsequent simulations we explore the effect that heterogeneity within a group has on collision risk. In particular, we exploit the potential of an asynchronous update scheme to implement varying types of underlying social networks which may influence group decisions.

Figure 4.3 shows that different network structures have distinct effects on both the probability of avoiding an obstacle array and the resulting group structure. We see that groups which navigate according to a homogeneous network show the least ability to avoid obstacles, but demonstrate little disruption to group structure (measured by the probability of the group splitting). Comparing subsequent groups to this benchmark we notice that any degree of heterogeneity within a network produces a higher probability of avoidance, but that in both leadership and clustered networks this can be at a cost to group cohesion. This is most notably the case for leadership groups, which demonstrate a high probability of avoidance but also a high probability of splitting. For these groups we see that avoidance is related to the number of leaders, with fewer influential individuals providing the highest levels of avoidance. The number of leaders does not affect splitting, which remains high. Clustered groups
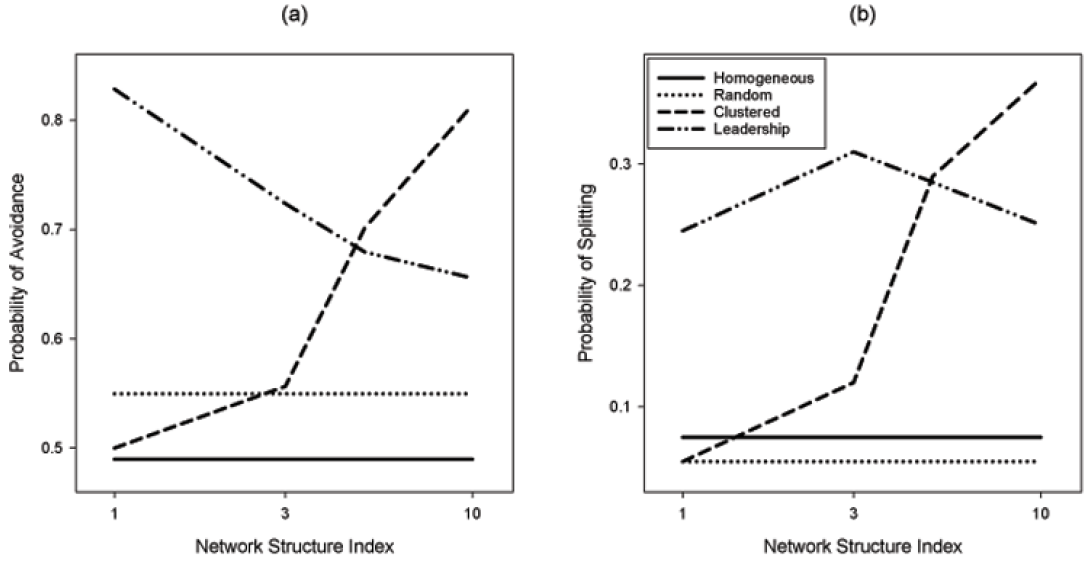
Figure 4.3: Heterogeneous social structure promotes obstacle avoidance. For social groups ($w_s = 1$) of 30 individuals with baseline target preference ($w_{t0} = 0.1$) and avoidance preference ($w_o = 1$) intersecting an array containing 25 obstacles uniformly arranged on a square grid at 500 metre intervals, we plot: (a) probability of avoiding a region bounding the array; (b) probability of a the group splitting; (recorded after 1000 time steps) for various examples of underlying social network (homogeneous, random, clustered and leadership), as a function of network structure index indicating the precise number of clusters or leaders in respective network types (homogeneous and random networks are invariant). We observe that homogeneous groups display the least avoidance ability, generally followed by random networks. Clustered networks produce increasing avoidance and splitting with the number of clusters. Groups which employ a single leader exhibit the highest levels of avoidance but as the number of leaders increases avoidance is reduced.

appear to follow a pattern similar to that seen for group size. Here, as the degree of clustering is increased, thus reducing the number of individuals per cluster, we observe an increase in avoidance. This is matched by an increase in the probability of splitting suggesting that clusters may begin to act independently as their size is reduced. [*It should be noted that in fact, consistent with the previous findings of Bode et al. (2012c), groups which interact according to a random social network exhibit a greater degree of cohesion. This may not follow for leadership or clustered groups despite their respective heterogeneity due to the implementation of network creation. In both cases networks are generated as extreme examples to emphasis the effect of the different characteristics with only a fixed weak connection maintained towards non-preferentially influential neighbours, i.e. group members that are neither a leader nor part of the same cluster. It is therefore unsurprising that groups with these types of underlying network are prone to a greater degree of splitting compared with a more egalitarian network structures. In future investigations intermediate structures could be produced by allowing the strength of any connection within the network to be randomly increased according to a weighted selection process based on likely preference (similar to that used in the model algorithm to select an update partner). This should produce a higher degree of connectivity across the group and therefore reduce the probability of splitting.*]

For all networks the probability of avoidance shows a bimodal distribution in that, for a given simulation, either all group members traverse the array, or all successfully avoid the array. This is of particular significance when considered with Figure 4.4 which maps the trajectories of groups responding to the array. Despite varying probabilities of avoidance we see only marginal differences between movement patterns. This suggests that avoidance is limited by the ability of a group to initiate an avoidance response rather than an ability to perform the action. The horizontal trajectories seen for leadership networks (panel (d)) are likely due to a loss of contact with the lead individual during separation. A lower preference for other group members increases the probability of separations becoming permanent resulting in

109
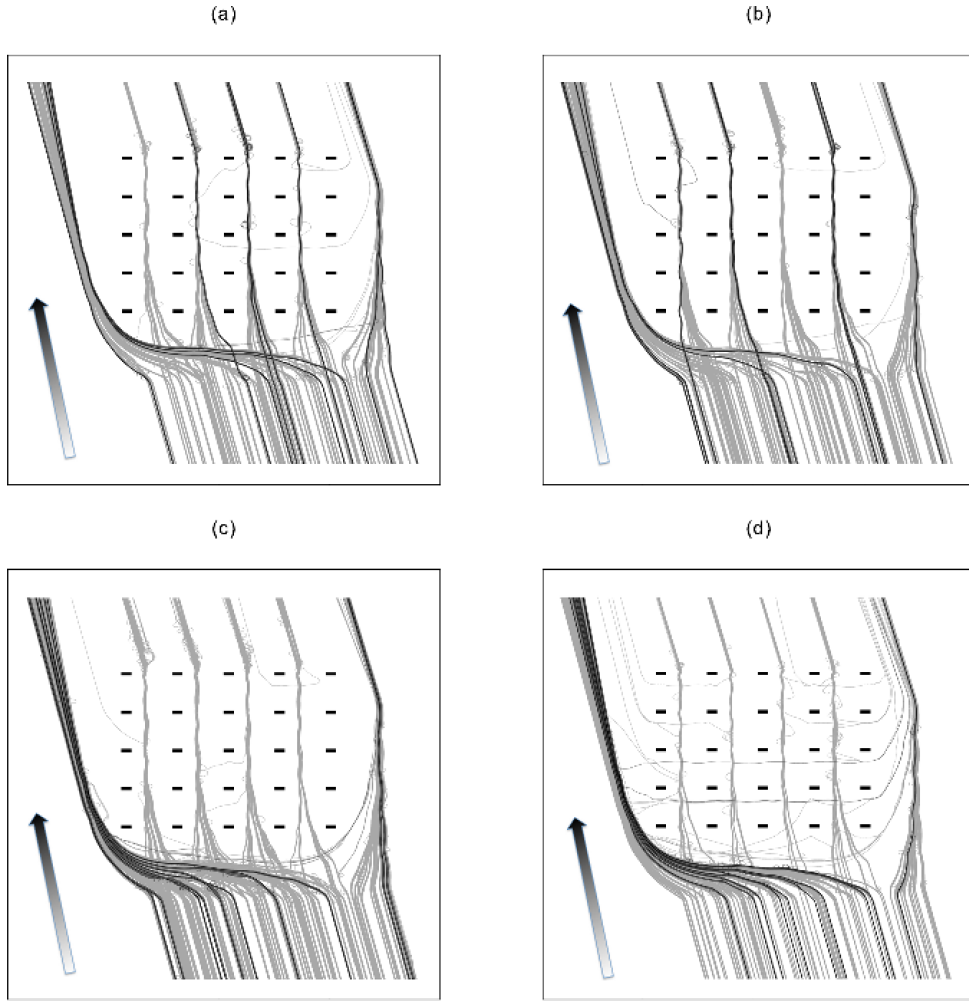
Figure 4.4: Similar movement patterns for distinct network structures. Mapped trajectories for groups with baseline target ($w_{t0} = 0.1$) and avoidance preference ($w_o = 1$) intersecting an array which contains 25 obstacles uniformly arranged on a square grid at 500 metre intervals and: (a) homogeneous; (b) random; (c) clustered; (d) leadership; underlying network structures. Each plot displays trajectories for 100 groups (light grey) of 30 individuals. 10 groups are highlighted (dark grey) with a focal individual (black). In (d) this focal individual represents the group leader. These plots can be compared to empirical data presented in Masden et al. (2012). We observe similar patterns of movement for all networks with only marginal differences in coherence ((b) shows less splitting) and cohesion ((c) shows high and (d) low density reflecting neighbour distances). See also supplementary movies S1a–S1d, corresponding to the panels in this figure.

this self-navigation through the array.

Motivated by previous studies (Couzin et al., 2005; Leonard et al., 2012), we then introduce groups which contain individuals with heterogeneous abilities, in this case the preference for avoidance and target navigation, i.e. $(w_o)_i = w_o * N(1, w_h)$ and similarly for the target weighting for each individual i. The results shown in Figure 4.5 demonstrate that as the magnitude of heterogeneity is increased groups experience an increased disruption to group cohesion and reduced probability of avoidance. This suggests that the relative variation of avoidance and target preferences alters the balance towards target navigation. In general, we see that groups which rely on fewer individuals for navigational decisions are more affected by this variation.

In order to assess whether the collisions observed by empirical studies could be explained by an increased risk as a result of environmental conditions, we vary the magnitude of movement error and the radius of attraction, the limit of an individuals sensory zone, to simulate turbulence and visibility respectively. Figure 4.6 shows that in both cases as parameters are varied to simulate poorer environmental conditions groups which rely on a particular individual for navigation are significantly influenced, transitioning from showing the most avoidance to the least. In the case of turbulence, if we assume that accurate target navigation and avoidance ability are related, then this result appears to contradict Codling et al. (2007) as asocial groups are shown to navigate less effectively in variable environments than their social counterparts. However, the trajectories mapped in panel (b)(i) (when compared with Figure 4.4(a)) support the idea that at least for social groups, target navigation is significantly affected by turbulence. In highly turbulent environments groups are less likely to follow the target trajectory intersecting the array, and this appears to drive the improvement in their ability to avoid obstacles. For those groups which are able to maintain accurate target navigation, such as those which rely on a particular individual, we have clear evidence that avoidance behaviour is susceptible to poor conditions. Our simulations suggest that in all groups environmental conditions affect avoidance behaviour, but the response is dependent on the social structure.
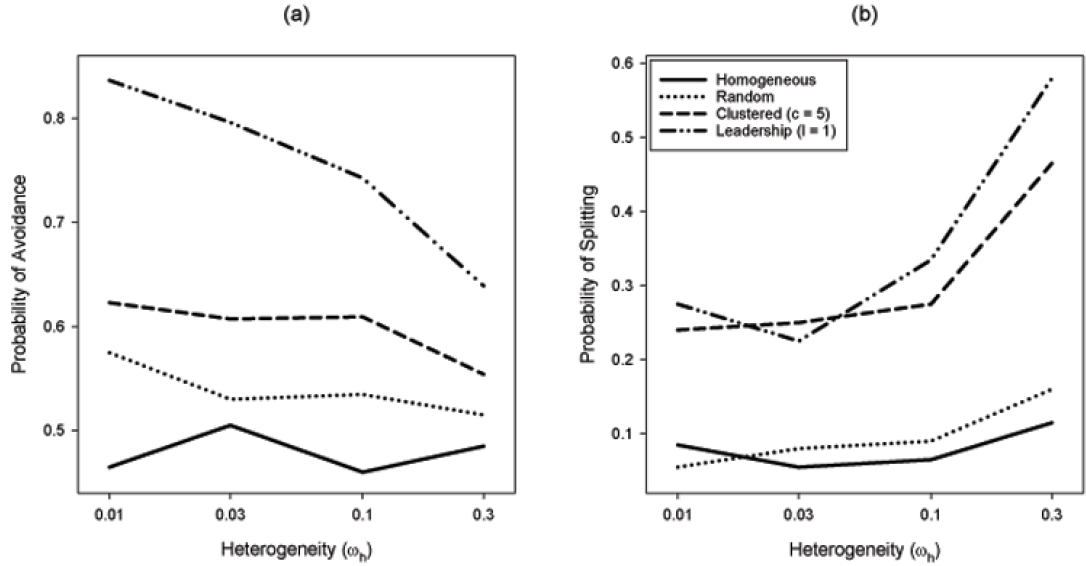
Figure 4.5: Variable ability reduces avoidance and group cohesion. For social groups ($w_s = 1$) of 30 individuals with baseline target preference ($w_{t0} = 0.1$) and avoidance preference ($w_o = 1$) intersecting an array containing 25 obstacles uniformly arranged on a square grid at 500 metre intervals, we plot: (a) probability of avoiding a region bounding the array; (b) probability of a the group splitting; (recorded after 1000 time steps) for various examples of underlying social network (homogeneous, random, 5 clusters and a single leader), as a function of heterogeneity w_h (magnitude of variation in avoidance and baseline target preferences). We observe that groups with a single leader are the most affected by changing heterogeneity showing a decrease in avoidance and increase in splitting as abilities become more variable. Clustered networks also induce this pattern although it is less pronounced. Groups with homogeneous and random networks appear largely unaffected by changes in heterogeneity showing only at small increases in splitting at high levels.
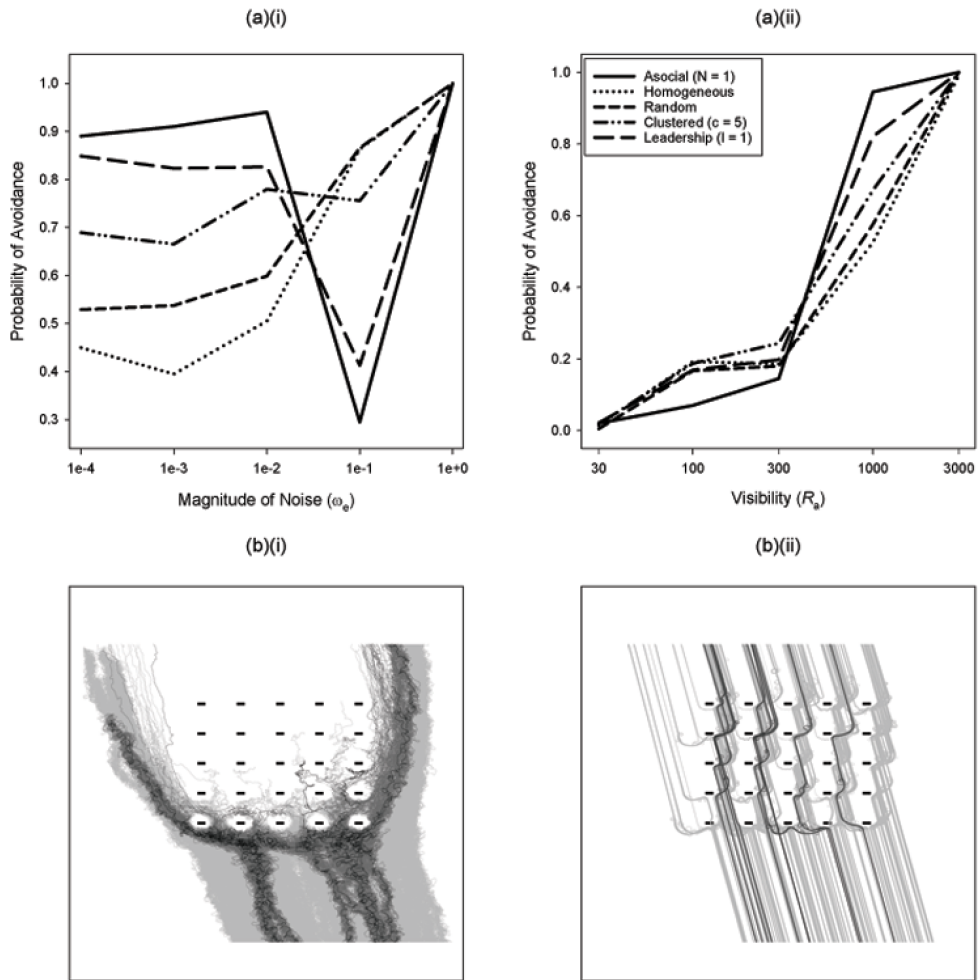
Figure 4.6: Leaderless groups appear less susceptible to environmental factors. For social groups ($w_s = 1$) with baseline target preference ($w_{t0} = 0.1$) and avoidance preference ($w_o = 1$) intersecting an array containing 25 obstacles uniformly arranged on a square grid at 500 metre intervals, we plot: (a) probability of avoiding a region bounding the array (recorded after 1000 time steps) as a function of: (i) turbulence (w_e); (ii) visibility (R_a); for various social structures; (b) trajectories for 100 groups of 30 individuals (light grey) with underlying homogeneous network in an environment where: (i) $w_e = 0.1$ (increased from 0); (ii) $R_a = 100$ (decreased from 1000). 10 groups are highlighted (dark grey) with a focal individual (black). Groups with a leader initially display the most avoidance but as conditions worsen they transition to showing the least. Mapped trajectories show that when visibility is reduced collisions can occur.

The increased dependence on local decisions makes it less likely that the groups will enter the array but the effect of this is to cause greater disruption to the group which may have significant effects on other fitness costs not captured here.

Despite the erratic movements of groups in turbulent environments (panel (b)(i)), individuals retain the ability to avoid obstacles and we observe no collision risk ("micro" probability of avoidance is zero) for any level of turbulence. This is not the case in environments which simulate low visibility. We find that, as visibility is reduced, groups show much later and more extreme avoidance responses resulting in the stepped movement patterns in panel (b)(ii). Here, we see that for some groups the loss of pre-emptive avoidance means they are no longer able to react in time to prevent intersections with obstacles.

Finally, we investigate the effect of introducing a variable target preference simulating the desire of groups to follow a direct migratory route with high fidelity. This is implemented by an allowing an increase in selection of an individual when the local angular deviation from the route increases. For comparison we parametrise the component of variable target preference (w_{t1}) such that with an inflated avoidance preference of $w_o = 3$ the avoidance rate for a group of 30 individuals is equivalent to the typical case. It should be noted that the use of a variable target preference with this parametrisation does not alter the results seen for groups in obstacle-free or single obstacle environments. The plot in Figure 4.7(a) shows that this need for route fidelity significantly alters the relationship between avoidance and group size, reversing the trend from non-linearly decreasing with group size to show a marginal increase. The change in avoidance is most noticeable for smaller groups which show a reduction in avoidance whereas the values for larger groups remain relatively unchanged. In comparison with groups which apply no cost to avoidance, the mapped trajectories shown in panel (b) show that, despite evidence indicating an earlier initiation of avoidance, the response is limited by the increased route fidelity. Consequently, groups are much less likely to avoid the array when required to travel across the corridors between columns of obstacles.
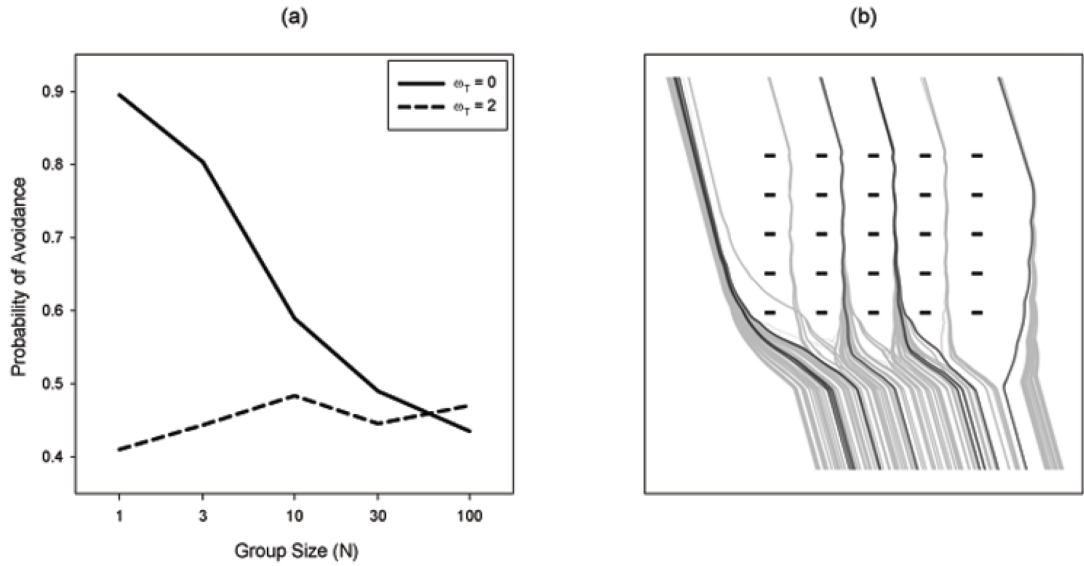
Figure 4.7: Route fidelity outweighs collision risk for small groups. For social groups ($w_s = 1$) with baseline target preference ($w_{t0} = 0.1$) intersecting an array containing 25 obstacles uniformly arranged on a square grid at 500 metre intervals, we plot: (a) probability of avoiding a region bounding the array (recorded after 1000 time steps) for different sets of avoidance and variable target preference ($w_o = 1$, $w_{t1} = 0$ and $w_o = 3$, $w_{t1} = 2$), as a function of group size (N); (b) trajectories for 100 groups of 30 individuals (light grey) with avoidance ($w_o = 3$) and variable target preference ($w_{t1} = 2$). Groups with no consideration for route fidelity show a non-linear relationship where avoidance decreases with group size. When an cost to avoidance, due to a lack of fidelity, is introduced the relationship with group size is reversed. Mapped trajectories show few avoidance manoeuvres which cross multiple corridors between columns. Groups are most likely to traverse the array along the nearest corridor in the target direction. Exceptions occur when this is an outer corridor with groups instead choosing to navigate outside the array.

4.6   Discussion

We have outlined a method by which obstacle interactions can be incorporated into an asynchronous individual-based model without compromising biological realism. The novel mechanism by which our model balances social and navigational forces creates a trade-off between group interactions and responses to environmental cues. Social interactions are dependent not only on social preference but also relative distance, meaning that groups with decreased nearest neighbour distance will exhibit more social tendencies. When individuals interact socially they pass on indirect information about environmental cues. This information is necessarily "noisy", but averaging across multiple neighbours can filter noise (Codling et al., 2007; Codling and Bode, 2014). A complementary study (Chepizhko et al., 2013) shows that the noise experienced by individuals can have an important role on group dynamics in the presence of obstacles – where this noise is small, the group may be too inflexible to adjust to the presence of obstacles and maintain cohesion.

For environmental cues, such as target navigation, where the directional information is similar for all group members, averaging provides a robust method by which individuals can combine knowledge to formulate a cohesive group response. However, when individuals are subject to conflicting information averaging can result in an inappropriate group decision, as can be the case for obstacle avoidance where response is highly dependent upon spatial position. This is of particular relevance where the ideal avoidance strategy is unclear, for example when an obstacle is spaced equally either side of the group centre. In such situations the movements of an informed individual or cluster can sufficiently influence group decisions to initiate a successful avoidance response (Couzin et al., 2005) and break the decision deadlock (Seeley et al., 2012). This is consistent with our results for varied group sizes which show an increase in avoidance for groups comprising fewer individuals. Here, average information is obtained across a smaller sample thus allowing for a greater bias from particular individuals, with leaders emerging more frequently. When information cannot be resolved to achieve a unified group decision this results in the formation

of localised subgroups which overwhelm the social bonds holding the group together and separate away in a different direction.

Our results show that underlying social networks produce significant differences to both group structure and navigational response. When compared with the leaderless homogeneous case described above, we find that for any underlying networks where preference is shown towards interactions with particular individuals, groups demonstrate a higher probability of avoidance. This is consistent with the similar improvements shown elsewhere (Bode et al., 2012c). This behaviour results from an increased bias within the group decision making process. Consistent with existing studies we observe that groups with fewer influential individuals provide the most effective response to contradictory environmental information (Leonard et al., 2012). In contrast with this type of leadership, examples which simulate clustering show the emergence of smaller independent groups showing less cohesion but maintaining an ability to initiate avoidance actions without clearly defined leaders.

Whilst a reliance upon fewer individuals for navigation can be beneficial it is also less robust to sensory variability (Codling et al., 2007). When variation is applied to both target and avoidance preferences the ability of such individuals to lead a group may not justify the influence which neighbours show towards them resulting in impaired navigational responses. Conversely, we find that when movement error is applied to simulate turbulence, groups which navigate either asocially or with a single leader maintain coherent target navigation even in highly disruptive environments. Unlike in Codling et al. (2007) where this result represents a positive outcome, in our model avoidance ability is not maintained at a relative level and whilst other groups avoid the array as a result of inaccurate navigation those which maintain target navigation consequently intersect the array more frequently. However, it is clear that even at high turbulence individuals maintain a safe distance from obstacles which suggests in our chosen parameter range that the risk of collision is effectively zero. This is not the case when the sensory range of individuals is reduced, mimicking conditions of poor visibility 4.6. Collisions are observed when the sensory range falls

below the radius of obstacle repulsion thus reducing the distance in which individuals have to respond to initiate an avoidance manoeuvre.

Throughout this study we have assumed that collision rates are the result of deficiencies in sensory ability. We challenge this assumption by suggesting that all groups may in fact posses an ability to avoid obstacles but instead choose to enter arrays because of strong route fidelity related to migratory efficiency. By introducing a variable element to target preference which produces an increasing desire to select target navigation as individuals deviate further away from the optimal target trajectory, we show that groups containing fewer individuals are much more likely to voluntarily enter the array. This has potentially important consequences for groups that are weakened, for example by lack of food, and may make different times of the year more important for collision vulnerability.

The ultimate goal of this modelling study is to quantify the risk of avian collisions with wind turbines. We recognise that at present the model outlined here is limited to specific scenarios in which individuals show no vertical avoidance. In reality, large-scale studies suggest that in good conditions birds, such as geese, favour vertical avoidance. Our modelling methods are amenable to generalisation to three-dimensions (Plonczkier and Simms, 2012) where data are available. However, through simulations with an array containing multiple obstacles we demonstrate that the cumulative avoidance response to those obstacles is sufficient to produce movement patterns which can be compared to those recorded by empirical studies. We show that by selecting reasonable parameter values we can reproduce estimated avoidance rates. Furthermore, we use the model to explore conditions which are difficult to assess empirically. These results reinforce the suggestion that birds are most at risk of collision when conditions reduce detection distance, for example during nocturnal navigation.

The effect of social networks has not previously been modelled in the context of obstacle avoidance. We have shown in this study that social interactions can affect the ability of a group to perform suitable avoidance responses and it would therefore be

ecologically informative to include realistic social networks when assessing risk. The structure of networks has been shown to have considerable impact on group behaviour, in ecological examples (Couzin et al., 2005; Bode et al., 2011c) as well as in other biological settings (Newman, 2003). Compared with our simple examples, goose social networks have been shown to be more complex and highly variable (Lamprecht, 1992; Kurvers et al., 2009). The relationship between in-flight communication networks and important social structures, such as foraging groups or family grouping, has been shown to have complex correlations which make it difficult to interpolate between them (Nagy et al., 2013). Therefore, caution must be exercised in making social inferences from in-flight interactions and consequences. Our results indicate that movement patterns, similar to those obtained by current radar studies which assess collision risk, cannot be used to infer the structure of social networks. This observation highlights the need for greater focus on the motion of individuals in the context of obstacle avoidance. To address these deficiencies new experimental approaches are necessary so that individual-based social network models can be verified and utilised to their full potential to predict avoidance rates *in silico*. With these advances it may be possible to inform decisions regarding the impact on birds prior to the construction of wind farms.

4.7 Acknowledgments

4.8 Supplementary material

Supplementary films 1–4, which accompany Figure 4.4 panels (a)–(d) respectively, are provided on compact disk with the submission of this thesis.

119

4.9 Summary

The model outlined in this chapter builds on that described previously, incorporating more considerations for bird specific limitations and parameterisation. It is argued that the adoption of an asynchronous update scheme enhances the biological realism of the resulting motion, matching the observations of recent landmark empirical studies (Ballerini et al., 2008b). The use of this approach also overcomes some of the difficulties specific to obstacle avoidance which were highlighted in Chapter 2, particularly allowing multiple avoidance strategies to be represented without conflict necessarily resulting in inaction and potentially collision. Instead, a more natural decision making process is simulated based on a priority response (similar to that described by Reynolds (1987)) in which errors of judgment can occur but are probabilistically most likely when navigational information is noisy.

Importantly, the resulting simulations demonstrate that avoidance of an array can be achieved through the cumulative response to distinct obstacles represented by a "cloud" of individual vertices, and that the probability of such an avoidance in the model is quantitatively comparable to those observed in radar studies of geese (Plonczkier and Simms, 2012). This represents a significant step towards providing a platform capable of assessing the design of wind farms pre-construction to minimise the risk of avian collision risk.

Chapter 5

Investigating the effect of obstacle layout and representation on collision risk with wind turbines

5.1 Introduction

The work presented in previous chapters has addressed factors affecting avoidance by exploring various social and behavioural mechanisms within a group as well as environmental considerations such as poor weather conditions. Of these, results indicate that visibility is the most likely cause of collision suggesting a possible mitigation strategy to reduce bird strikes with wind turbines post-construction may be to limit operation during periods where visibility is low. Whilst this approach is straightforward to implement it is not an ideal solution for energy production. An alternative would be to consider mitigation options pre-construction.

A recent publication by Masden et al. (2012) has conjectured that the configuration of wind turbines within an array can have a significant impact on avoidance rates. Using a mechanistic modelling approach this investigation considers the effect of layout in terms of permeability, how likely birds are to enter the array thereby risking collisions; and straightness, how far birds must travel in order to avoid the array which is related to energy expenditure. The optimal layout should seek to minimise both of these measures. However, it is argued that the importance of each is dependent on the typical behaviour of specific species, for example when species are prone to collisions a layout which encourages avoidance of the entire wind farm is more favourable over optimising energy expenditure. For migratory species such as geese, which migrate over long distances, energetic considerations are perhaps more important (Pennycuick, 2008) and so layouts which improve the straightness of trajectories and prevent wind farms acting as a barrier to movement (Masden et al., 2009) would be beneficial. The findings suggest that permeability can be controlled by adjusting the spacing between columns (defined by linear alignment in the general direction of approach) and the number of rows; with closer spacing and more rows inducing a reduction. It is also shown that of several potential configuration patterns, including uniform and random arrangements as well as a clustered layout which provides a clear path through the wind farm whilst discouraging movement between close turbines, that a diagonal arrangement orientated in the general direction of approach produces the

least straight trajectories, though this appears to be related to higher avoidance rates.

The approach outlined by Masden et al. (2012) is informative, providing a method by which avoidance rates can be assessed. However, as is the case in all existing avian collision risk models (CRMs) (Band, 2000; Band et al., 2005), it does not consider social interactions between individuals. The trajectories produced represent the average group position, similar to those recorded by radar studies, rather than that of single individuals. Consequently, it is not possible to accurately assess strike rates with regard to distinct wind turbines. This is a specific feature of the models developed throughout this thesis which demonstrate an ability to explore the interaction of individuals with obstacles and identify any collisions that may occur. Other factors such as disruption to group structure which may impact energetic efficiency can also be assessed.

The model described in Chapter 4 provides an alternative method developing an individual-based approach for simulating collective motion and obstacle avoidance according to an asynchronous updating routine introduced by Bode et al. (2011b). It has been demonstrated that this approach produces more biologically realistic movements and decision making, reproducing variable speed distributions (Aoki, 1982) and emergent properties, such as the observation that individuals on average interact with a limited number of near neighbours (Ballerini et al., 2008b). The asynchronous approach also solves several of the issues relating to interactions with obstacles highlighted by our initial modelling study, presented in Chapter 2. In particular it allows all possible avoidance strategies to be represented with a relative probability of selection. In doing so a natural decision error emerges and contrary to a synchronous approach the result of equal but conflicting strategies is not inaction. Instead as only a single partner is chosen per update, a clear navigational decision is guaranteed. Depending on whether the correct decision has been made, at the next update step, it will either be reinforced or overruled, and the movement reversed. By combining responses in this way priority is given to the most urgent actions up to a set movement limit, as per the optimal method suggested by Reynolds (1987). The

resultant direction over the time-step then reflects an effective and consistent response to the situation rather than averaging conflicting responses which may prove to be ineffective, i.e. an optimal avoidance response might be to head directly north or east but a combined response averaging the two heading north east results in collision.

This chapter investigates some of the factors considered in Masden et al. (2012) to examine the impact of wind farm design on collision risk in light of the additional capabilities of the developed model. By comparing outcomes we aim to provide a validation for the behaviours which emerge. We also investigate the impact of obstacle representation in the model, namely the strike rate given the intersection of an individuals trajectory with an obstacle and the granularity, or spacing between obstacle vertices, has the potential to introduce errors in detection and consequently alter behavioural response. In future studies these variables could be used to distinguish between obstacles, or parts of an obstacles, with different properties without altering the core behavioural mechanisms for avoidance. For example, a moving wind turbine blade offers a degree of transparency, compared to the solid tower, meaning individuals may be less likely to show avoidance and unlike collisions with the tower, birds may pass through the blades unharmed. To justify this approach it is important that we understand its limitations and demonstrate that the parameter choice produces results as anticipated.

5.2 Modelling framework

The model and general parameterisation is identical to that outlined in Section 4.4. Here, we provide additional discussion of key modelling concepts and developments with particular regard to simulating "bird-like" subjects. We also present evidence to justify the choice of specific parameter values listed in Table 4.1 as well as further explanation of the simulation framework, primarily relating to the formation of representative groups which is required to ensure consistent initial conditions for all simulations.
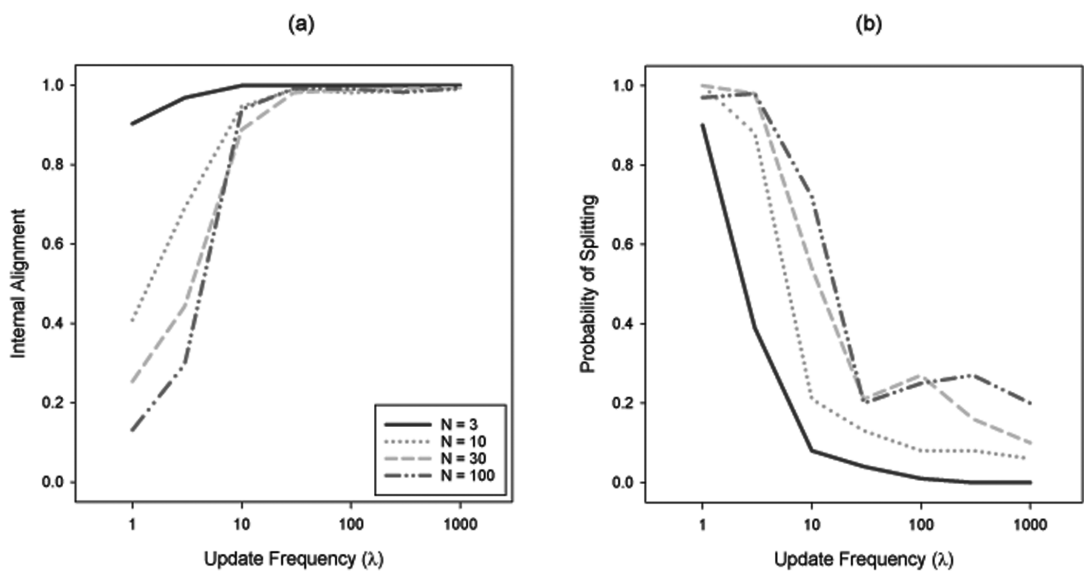
5.2.1 Update frequency

The initial work by Bode et al. (2010a) has shown that the choice of update frequency can greatly affect group behaviour. It is therefore important that an appropriate value is selected. For group motion to be maintained individuals must interact with at least two distinct neighbours (Huth and Wissel, 1992). In order to ensure that this is represented by the random sampling approach outlined in this model it is necessary for the update frequency to remain above a minimum level. The specific parametrisation and considerations for target navigation can affect this minimum. In order to assess this for the specific model used here groups of varying size are simulated according to different update frequencies. The plots in Figure 5.1 show that with no consideration for target navigation the minimum value required to achieve cohesive group motion is approximately 30 updates per time step. However, since all simulations require the inclusion of target navigation, to guarantee interactions with obstacles it is practical to use a higher update frequency. A value of 100 updates per time step was selected as a sufficiently high frequency to ensure cohesive group movement is maintained. Whilst previous studies have not inferred any direct links between update frequency and physical or neurological information, a recent study has linked the reaction speed of animals to their critical flicker frequency (CFF) (Healy et al., 2013). Interestingly, for birds this is typically 100 hertz. Given that our time step is 1 second this is equivalent to our selected update frequency. In future studies this equivalence may provide a suitable basis for parameter identification.

5.2.2 Target navigation

In order to assess the risk obstacles pose to groups it is necessary to introduce target navigation ensuring any avoidance is as a result of behaviour rather than random movement. To integrate with the algorithm for group movements any implementation of this behaviour requires two components: a directional response; and a selection weighting.

A suitable choice for directional response is dependent upon the situation which

Figure 5.1: Collective motion requires a minimum update frequency. For social groups ($\omega_s = 1$) of varied size (N) plots show: (a) internal alignment; (b) probability of splitting; as a function of update frequency (λ). The results indicate that in order to guarantee robust collective motion in groups of any size each individuals must perform a minimum of 30 updates (on average) per time step.

simulations are designed to investigate. For example, studies which represent movements between specific locations, such as roosting and feeding sites, use a fixed point to determine directional response (Codling et al., 2007), whereas, for longer-distance migrations this point is undefined, often being considered to exist at infinity with individuals instead orientating towards a fixed target heading (Croft et al., 2013). For the specific scenario of migratory birds interacting with a single wind turbine, the work in Chapter 2 chose to implement the latter. This is in part to avoid the inherent lateral variation associated with fixed point interactions, which has the potential to significantly alter group structure and avoidance behaviour depending on relative proximity. However, when interacting with an array of wind turbines (wind farm) additional considerations must be taken into account. In particular, for migratory birds the pressures of maintaining perpetual flight over large distances presents an energetic challenge (Pennycuick, 2008). Consequently, it is likely that energetic efficiency will have a role in decisions regarding avoidance, with groups demonstrating a form of route fidelity to minimise the distance travelled (Drewitt and Langston, 2008).

Simulating this behaviour poses a conflict because it requires an element of spatial variation not present with a fixed target heading. To solve this problem the notion of a target point must be reconsidered; rather than a fixed point an individual aims for a moving point which remains at a fixed distance (d_t) from its current projected position along a defined target trajectory. This type of route fidelity has been observed in empirical studies investigating long-distance navigation in birds, for example the homing behaviour of pigeons (Biro et al., 2007). For simplicity the target trajectory is defined as a straight line containing the initial group position (centre of mass) and extending infinitely in a specified direction. This is illustrated in Figure 5.2(a) and represents the most energy efficient route from the starting point to an eventual destination. Unlike in the case of a fixed target point, at any position a given distance from the target trajectory the lateral component of directional response remains constant with magnitude proportional to the distance of deviation relative
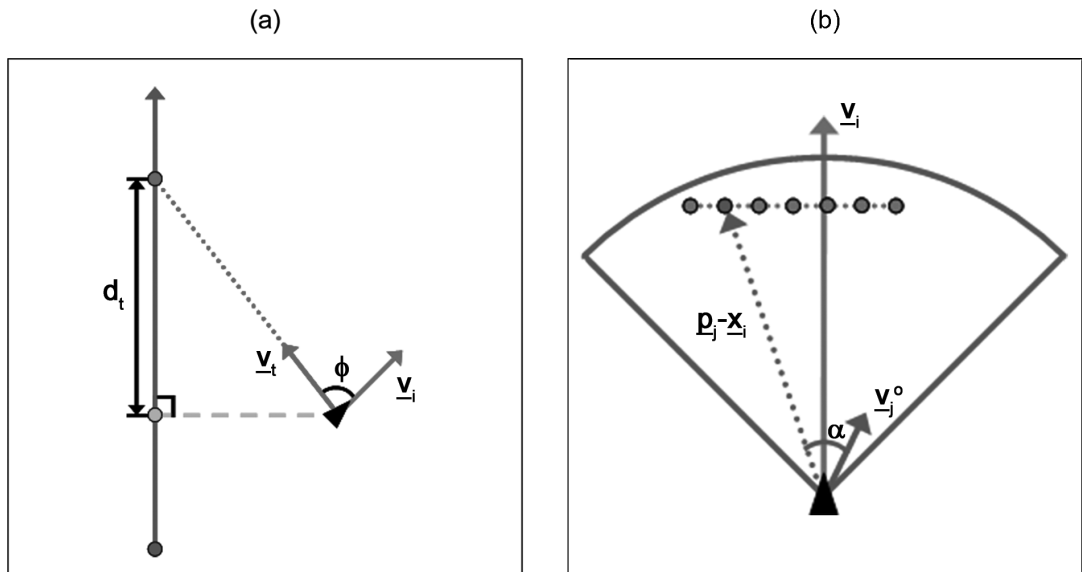
Figure 5.2: Illustration shows: (a) the target navigational response for an individual (black triangle) with given target trajectory (vertical arrow). The dashed line maps the projected position of the individual onto the target trajectory. The dotted line plots the target navigational response of the individual aiming for a point a given distance (d_t) along the target trajectory ahead of the projected current position. The marked angle (ϕ) between the individual's current heading ($\underline{v}$)and the target navigational response ($\underline{v}_t$) influences the strength of preference for selection; (b) the response of an individual (black triangle) to a single obstacle vertex located within the zone of pre-emptive avoidance. The marked angle (α) between the dotted line ($\underline{p}_j - \underline{x}_i$) and the response vector ($\underline{v}_j^o$) is the same as that used to describe the zone of interaction (defined as a sector centred on the individuals current position with angular range ($-\alpha,\alpha$) about the current heading ($\underline{v}$)).
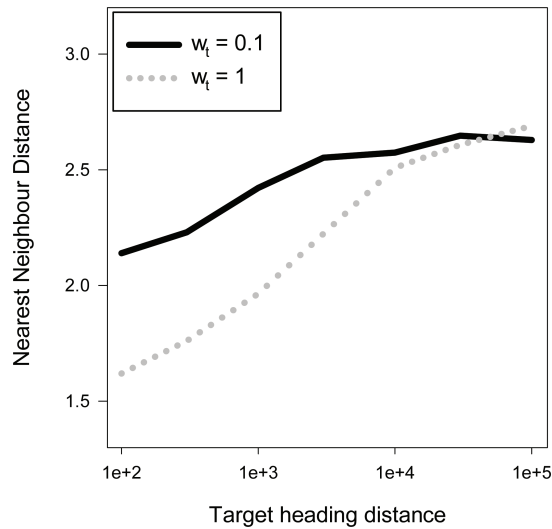
Figure 5.3: Target heading distance can effect the structure of groups. For social groups ($\omega_s = 1$) of 30 individuals the plot shows average nearest neighbour distance (NND) as a function of target heading distance d_t for a range of target weightings w_t (consistent with those which may be experience should energetic efficiency be applied). The results demonstrate that as d_t is reduced, increasing the lateral component of motion toward the target, groups become more compact. To prevent this effect a minimum target heading distance of 30000 metres must be observed.

to d_t. This means that the effect of this lateral component can be reliably controlled by a suitable choice of d_t. Figure 5.3 shows that as d_t distance is reduced, increasing the lateral component of directional response, so is nearest neighbour distance. The rate at which this change occurs is dependent on the relative preference for target navigation w_t. This can be explained by imagining a group travelling with centre of mass positioned directly on the defined target trajectory. As target distance is reduced the inward component of the resulting directional vector for each individual not on this trajectory increases. Eventually, this inward component increases to such an extent that the inherent resistance of the group to compress is overwhelmed and it begins to collapse onto a line, the target trajectory. In order to limit such effects we chose to implement a large target heading distance, 30000 metres, beyond which nearest neighbour distance becomes relatively stable for all values of w_t.

In Bode et al. (2012a) selection weighting represented a fixed probability such that individuals chose either to perform target navigation or to respond to an "update partner" within their sensory zone. Whilst this approach allows for a direct control of selection probability, the inference is that even in the event of a near collision an individual remains equally likely to navigate towards the target. For social navigation where groups form relatively stable configurations these events are infrequent and so this modelling choice is relatively unimportant. However, in simulations including obstacles, avoidance is designed to directly contradict target navigation, presenting a clear trade-off. To reflect this, target navigation is instead included in the pool of potential update partners, thus scaling the weighting of selection relative to the priority and number of other interactions. The balance between group and target navigation is controlled by multiplying the relative weightings for each type by a given factor representing preference. A recent study by Codling and Bode (2014) has shown that the weight of target navigation is related to navigational performance with only a small relative weighting required to maintain optimal performance regardless of any navigational error. This is analogous to the result shown in Figure 4.1 which similarly suggest that a minimum target weighting is required to produce optimal navigational performance but that further increases do not improve performance.

The weight an individual assigns to target navigation (w_t) is considered to reflect a desire to follow the target trajectory or optimal navigational strategy, thereby reducing energy expenditure. To simulate this w_t is allowed to increase as an individual deviates away from the ideal target trajectory. The magnitude of this increase is determined according to the angle between an individuals heading and the calculated target direction (ϕ), shown in Figure 5.2(a), as follows,

$$w_t = (w_{t0} + w_{t1}(1 - cos(\phi))) \tag{5.1}$$

where w_{t0} and w_{t1} denote the minimum baseline and the magnitude of variation respectively.

As noted previously navigational uncertainty as implemented in Codling et al.

130

(2007) is not considered to ensure that interactions with the obstacles occur predictably and that any avoidance is as a result of behaviour rather than imperfect navigation along the target trajectory. Consistent with the findings of Codling and Bode (2014) given the relatively small weighting required to produce optimal performance target navigation is rarely chosen directly and so any error relating to this vector would be negligible in comparison to that emerging from the stochastic model algorithm.

5.2.3 Obstacle avoidance

In accordance with the approach outlined in Chapter 2, obstacles are represented by a finite set of vertices each with a vector to describe the surface, in this case an outwardly facing normal. However, in contrast, rather than apply a circle of fixed radius to determine collisions, the set of vertices is ordered such that the vector between sequential vertices defines a connecting edge. This implementation allows intersections between obstacles and individuals to be identified precisely. Significantly, this development means that the distance between vertices can be varied without impacting the ability to detect intersections (and hence collisions), which was not previously the case. Visual occlusion can also be applied simply by tracing the line of sight to each neighbour and vertex. The increased accuracy that this provides has a computational cost. To improve efficiency each obstacle is defined with a bounding box which is initially used to test for intersections. If an intersection with this bounding box is detected then a more detailed search is conducted. This reduces the number of unnecessary calculations thus limiting the impact on runtime of simulations. Similarly, a bounding box can also be defined to represent the region containing an array of obstacles thus allowing the number of individuals which enter the array to be recorded. To maintain a comparison with the obstacles used previously a standard granularity of 1 vertex per spatial unit is adopted.

As is the case for group navigation, appropriate directional response to obstacle vertices is categorised based on relative proximity. Similarly, it is assumed that

individuals respond to close obstacles by applying a repulsive behaviour thereby maintaining a minimum distance. In addition to this behaviour, geese also have been shown to demonstrate some long-distance avoidance (Plonczkier and Simms, 2012). This can be challenging to represent in simulations as the visual perception of birds can be difficult to encapsulate in models.

Studies have determined that, despite a wide field of view, birds have very limited stereovision (Heppner et al., 1985; Martin, 2011). In light of this research the relative depth perception required to align with the surface of an obstacle, as is suggested in Chapter 2, would be beyond the capabilities of most birds (including geese). Instead, it is perhaps more likely that birds simply turn away from obstacles until avoidance has been guaranteed. This response can be simulated by introducing a minimum angle by which individuals attempt to maintain between their current heading and the direct heading towards each obstacle vertex (is illustrated in Figure 5.2(b)). Any vertices which lie outside of the region defined by this angle are ignored. As a minimum the avoidance angle should be chosen so that, in general, individuals pass an obstacle without the need for more extreme repulsive action. The angle required to achieve this varies depending on proximity. However, the monocular vision of birds means that this distance and therefore the specific angle by which to turn cannot be assessed. To ensure that the angle is always sufficient, obstacles must be assumed to lie on the limit of repulsion requiring an angle of 45 degrees. The maximum angle which should be applied is 90 degrees, at which an individual no longer exhibits any forward motion towards a vertex.

Each obstacle vertex is considered similar to that of a conspecific. Consequently, all vertices within the sensory zone are added to the pool of potential update partners with a weighting proportional to the inverse distance from the updating individual. As was introduced for integrating target navigation in Section 5.2.2, each weighting is further scaled by a given value related to the preference for interactions of this type. By allowing individuals the choice to respond to obstacle vertices in this way (similar to Model I in Chapter 2), rather than combining responses prior to

selection forming a single response vector at the obstacle level (as is the case in Model II in Chapter 2), all possible avoidance strategies can be represented. This is particularly important in situations where a clear avoidance strategy is not present; for instance when an individual is heading along a trajectory intersecting an obstacle close to its centre. Here, unlike in the case of conspecifics where a single response can be defined, multiple equally valid responses could be followed in order to perform successful avoidance. This situation may lead to a degree of indecision which would be removed if avoidance were calculated at the obstacle level. Instead, the accumulation of responses to obstacle vertices selected according to the model algorithm enables an avoidance strategy to emerge through sustained selection of similar responses, with each new response gradually reinforcing the direction of movement, while retaining the possibility for an individual to change their mind. The latter would be more likely when presented with equal strategies with an even selection of conflicting responses leading to inaction.

5.2.4   Initial conditions

Initial conditions are important for interactions with obstacles. The simulations performed in Chapter 4 consider groups following a migratory route which is interjected by obstacles. In order to ensure that any variations in group structure are a result of obstacle interactions (avoidance behaviour) each group must begin with a stable representative configuration.

In Chapter 2, groups were initially placed randomly within a circle of fixed radius. They were then updated within this circle until either all individuals aligned with at least one neighbour or a maximum time limit of 100 time steps was exceeded. If an individual left the circle radius it was reflected back to prevent splitting (as defined in Chapter 4). However, in comparison with groups which are randomly placed in a circle, the aforementioned approach shows little difference. Once groups were released they began to organise, settling into a new stable formation before any obstacle interactions. To avoid these possible ambiguities in this study a more robust

method is described below. Firstly, it is necessary to define a representative group configuration. In accordance with the empirical data in Figure 3.7, each individual is required to have at least one neighbour within 20 metres, previously identified as the radius of alignment. Therefore, for a group to be considered representative, all individuals must belong to an equivalence class where neighbours are declared equivalent if they are within this distance.

Prior to warm-up individuals are placed sequentially into an obstacle-free environment as follows. In turn each individual chooses a neighbour from those already placed in the environment (if none have been placed then the individual is placed at the origin). This individual is then placed randomly so as to align with the chosen neighbour (i.e. the relative distance between them corresponds to the distances defining the zone of alignment). The process is repeated until all individuals have been placed in the environment. To promote a high degree of alignment, as is observed in flocks of geese, all individuals are initially orientated parallel to a defined target trajectory. This method ensures that the initial configuration immediately satisfies our criteria for a representative group and that this group structure is relatively stable with all group members spaced at a comfortable distance from each other and aligned in the same direction. Consequently, we would not anticipate a dramatic change in the summary statistics following release, but some restructuring is to be expected due to the stochastic variation included in the model. Once all individuals have been placed and orientated the group is allowed to move, for a fixed number of time steps, according to the algorithm outlined in Section 4.4.1. It should be noted that target preference is applied during this warm-up phase. This common direction increases group cohesion (measured using the probability of splitting as defined in Section 4.4.1, with low probability of splitting indicating high group cohesion) and in an unbounded environment reduces the probability of individuals becoming permanently separated from groups.

Figure 5.4 shows that to ensure groups of all sizes have the opportunity to organise themselves into a stable configuration the warm-up must last at least 400 time steps
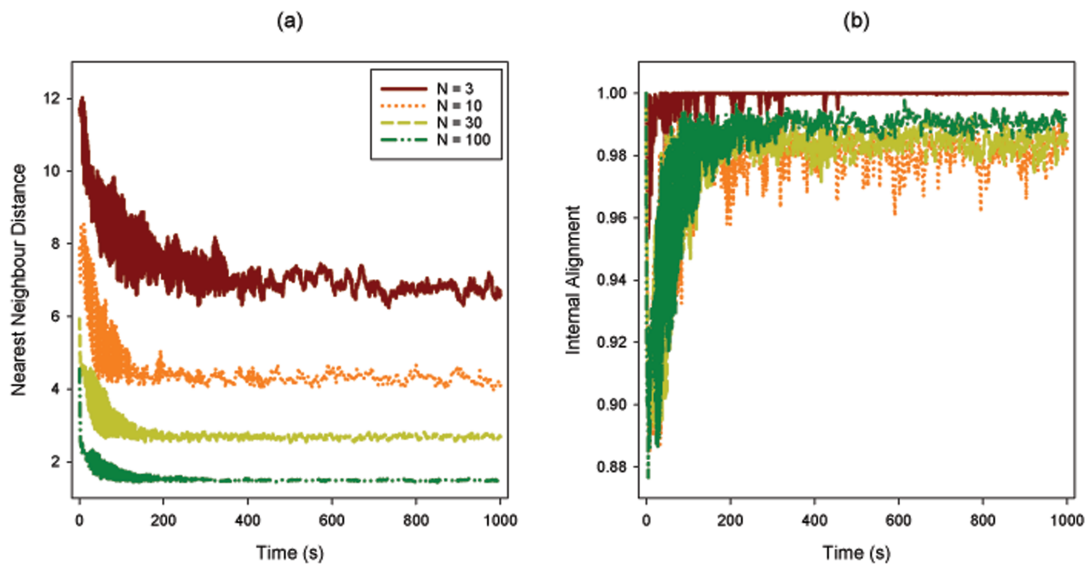
Figure 5.4: In an unbounded environment group configuration reach a stable steady state. Plots show: (a) average nearest neighbour distance; (b) internal alignment; for groups of varying size (N), as a function of simulation time. Groups are randomly placed and allowed to warm-up in an unbounded obstacle-free environment. The results indicate that groups of all sizes reach a stable group configuration after approximately 400 time steps. The time for a group to stabilise is related inversely to the number of individuals (larger groups stabilise faster).

(seconds). At the end of the warm-up groups are tested to ensure a representative configuration has been achieved. The process is repeated until this condition is met.

5.2.5 Simulation time

To ensure that the long-term disruption of avoidance can be assessed, simulations must allow groups to stabilise following an interaction. Figure 5.5 shows simulations conducted using both a single obstacle and an array. It can be seen from these that the internal alignment of groups is disrupted during avoidance, but quickly stabilises. For both a single obstacle and an array this re-stabilisation occurs within approximately 150 and 500 time steps respectively. Since initial interaction occurs around 250 time steps allowing a simulation time of 1000 time steps ensures that any effects seen can be compared with simulations conducted in obstacle-free environments (equivalent to representative groups prior to obstacle interactions) to determine the impact of avoidance on group structure.

It is interesting to note that in simulations with an array of obstacles groups containing 10 individuals show the highest levels of disruption, taking the longest to re-stabilise following the initial avoidance manoeuvre. It has been shown previously (Figure 3.7(a)(iii): modelling results) that group size is related to nearest neighbour distance with larger groups displaying more compact formations. As interactions within this model are weighted based on distance such differences may also effect the relative sociality of groups. Given this inference the result is explainable in the context outlined in Chapter 2 and the findings of Chepizhko et al. (2013) both of which suggest that there is an intermediate level of social navigation at which groups are unable to effectively resolve conflicting information.

5.3 Simulations

Unless otherwise stated simulations are performed according to the procedure outlined in Chapter 4 using a homogeneous group of 30 individuals with a standard preference
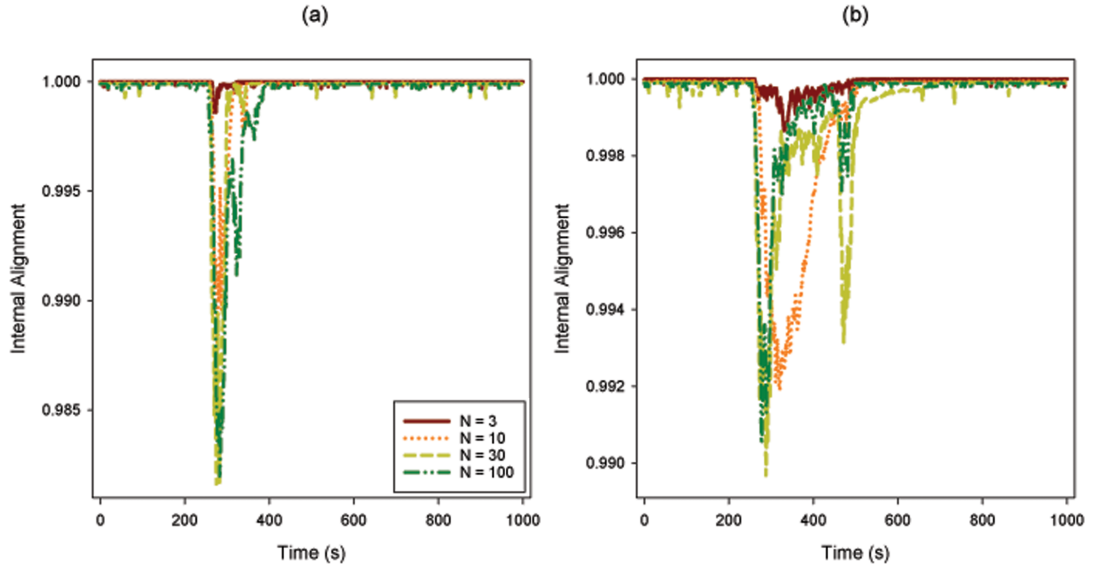
Figure 5.5: Groups rapidly re-stabilise following disruption as a result of interactions with obstacles. For social groups ($w_s = 1$) of varying size (N) with baseline target preference ($w_{t0} = 0.1$) intersecting an array containing: (a) a single obstacle ($w_o = 0.3$); (b) 25 obstacles uniformly arranged on a square grid at 500 metre intervals ($w_o = 1$); plots show internal alignment as a function of simulation time. In both cases initial disruption occurs after approximately 250 time steps (smaller groups appear to reacting later). The magnitude (and consequently the period) of this disruption is dependent on N (larger groups appear more disrupted). Following disruption internal alignment quickly returns to the prior stable value. In (b) larger groups show a secondary peak of disruption (after 400 time steps). This could be a consequence of the transition from obstacle avoidance back to target navigation. In all cases groups reach a stable state well within the maximum simulation time.

weighting of $w_s = 1$ and $w_t = 0.1$ for social and target navigation respectively. Obstacle avoidance weighting is fixed at $w_o = 0.3$ in simulations with a single obstacle and $w_o = 1$ in simulations with an array in order to ensure that variations in avoidance and collision risk can be observed. Initially, groups are randomly placed in an obstacle-free environment and allowed to move according to the warm up routine described in Section 5.2.4. Groups are then replaced in an environment containing the obstacle array with average group heading orientated along a fixed target trajectory intersecting the array and average position randomly selected on a line segment perpendicular to this trajectory with length equivalent to the cross-sectional width of the array. For each scenario 100 independent simulation runs are performed and combined to produce averaged summary metrics describing: disruption to group cohesion (probability of splitting); straightness of navigation (target navigation ability); wind farm permeability (macro avoidance); and strike rate with wind turbines (micro avoidance).

5.3.1 Array layout

To investigate the effect that array layout has on avoidance behaviour we perform simulations varying the spacing between rows, columns and obstacles, and the number of obstacles per row and column. In all cases the position of the array remains unchanged relative to the initial position of the group. As the array layout is different in each scenario it is no longer possible to specify a single angle at which given no avoidance ($w_o = 0$) intersection with an obstacle is guaranteed (as is argued previously in Section 4.4.3). Instead, all groups approach the array head on (corresponding to an approach angle of 0 degrees). At this angle it is trivial to calculate the collision risk for individuals given no avoidance behaviour as the total length of obstacles per row divided by the width of the array. By comparing this rate relative to that displayed by groups a standard metric can be computed to assess the effects across all array layouts. As in previous simulations a minimum bounding region is defined for each array to determine avoidance rates. Whilst the mechanism for defining this
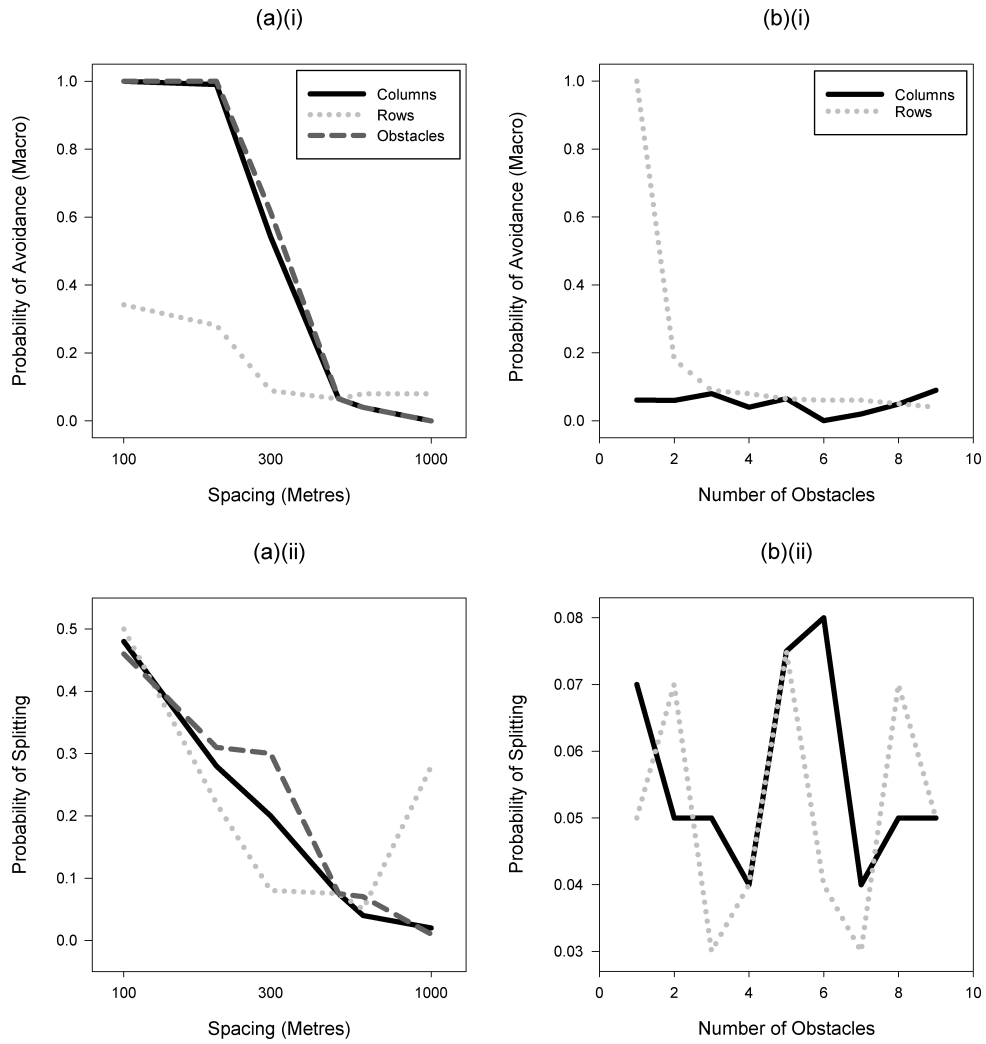
Figure 5.6: The spacing between rows in an array influences avoidance rates. For social groups ($w_s = 1$) of 30 individuals with baseline target preference ($w_{t0} = 0.1$) plots show: (a) the relative spacing between rows, columns and obstacles; (b) the number of obstacle per row and column; in relation to: (i) the probability of avoiding all the region bounding (macro) an array containing 25 obstacles uniformly arranged on a square grid at 500 metre intervals; (ii) probability of a group splitting (recorded after 1000 time steps). The results show that row spacing controls the permeability of an array with closer spacing encouraging groups to avoid the array. However, this avoidance causes greater disruption to group structure indicated by an increased probability of groups splitting. None of the other factors explored showed any significant impact on the rate of avoidance.

region is constant in all simulations it should be noted that the specific dimensions are dependent on those of the array and hence variable.

In agreement with the results presented in Masden et al. (2012) Figure 5.6(a)(i) shows that increasing the spacing between columns increases the permeability of arrays, exhibited as a decrease in the macro avoidance rate. Initially, the spacing between rows shows a similar, albeit less pronounced effect, with the macro avoidance rates decreasing but as spacing is increased above 300 metres no further decreases are observed. This is likely a consequence of the decision to limit the interaction range for obstacle avoidance to 1000 metres (see Section 4.4.2). Whilst more compact arrays appear to limit the number of groups entering an array the results shown in Figure 5.6(a)(ii) suggest that there is a negative impact on group structure. As spacing is decreased the probability of a group permanently splitting as a result of avoidance is increased.

Contrary to Masden et al. (2012) the results in Figure 5.6(b)(i) show no relationship between the number of obstacles per column and the macro avoidance rate. Again, this may be related to the limited interaction range of individuals simulated in this model. As may be expected for an array consisting of a single column (1 obstacle per row) groups show 100% avoidance of the array. However, this is a special case in which entering the array head on would mean intersecting an obstacle. Despite some array layouts encouraging groups to traverse between obstacles no intersections with obstacles were observed in any simulations (i.e. the micro avoidance rate is 100%). In general the size of an array, i.e. the number of obstacles it contains, has a negligible impact on avoidance rates.

5.3.2 Angle of approach

The angle at which a group approaches an obstacle or obstacle array can significantly alter its perceived appearance affecting cross-sectional width, spacing and relative size of obstacles within the array. Figure 5.7 shows the consequences of this change in perception by plotting the relationship between angle of approach and avoidance
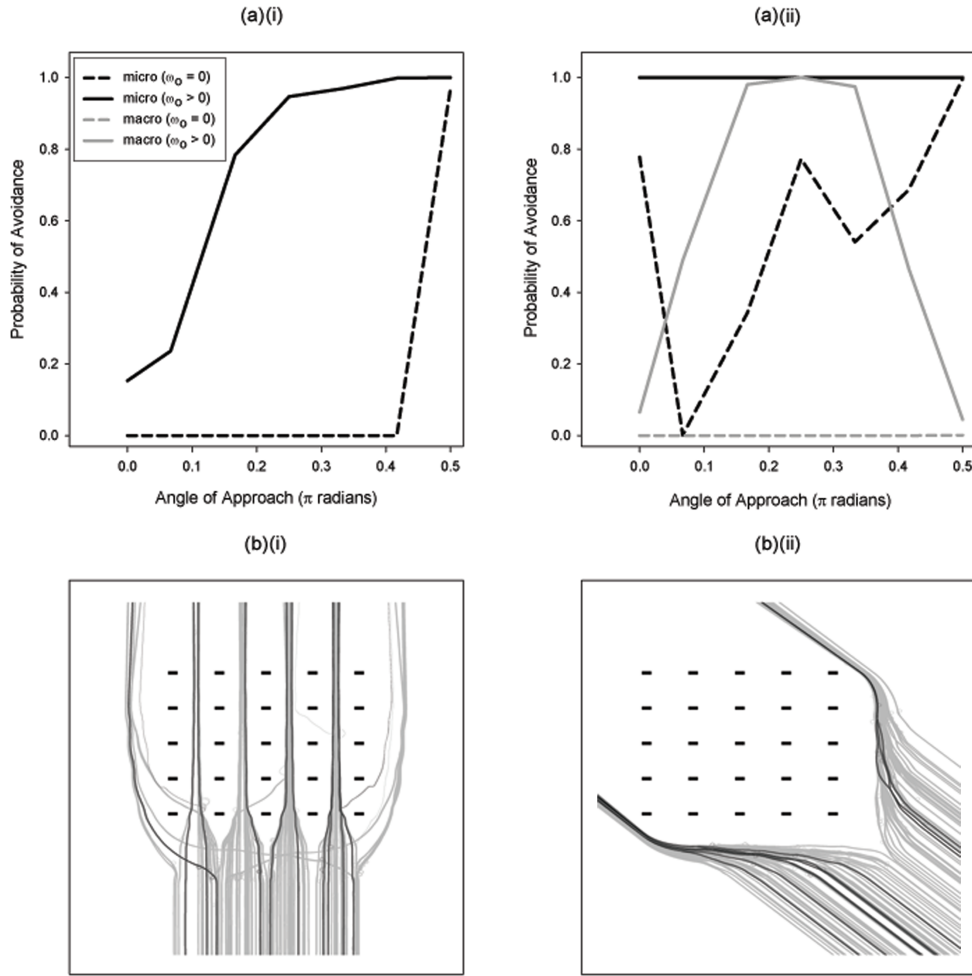
Figure 5.7: The angle of approach significantly impacts avoidance rates. For social groups ($w_s = 1$) of 30 individuals with baseline target preference ($w_{t0} = 0.1$) plots show: (a) probability of avoiding all the obstacles in (micro) and the region bounding (macro) an array containing: (i) a single obstacle; (ii) 25 obstacles uniformly arranged on a square grid at 500 metre intervals; (recorded after 1000 time steps) given zero and non-zero avoidance preference ((i) $w_o = 0.3$; (ii) $w_o = 1$), as a function of the angle which groups approach the array; (b) trajectories for individuals in 100 groups (light grey) approaching an array at an angle of: (i) $0°$; (ii) $45°$. 10 groups are highlighted (dark grey) with a focal individual (black). In (a)(i), avoidance increases with angle as cross sectional width reduces. In (a)(ii), avoidance (micro) given zero preference indicates the proportion of this width occupied by obstacles showing a maximum at $12°$. However, maximum avoidance (macro) is observed at $45°$.

rates for both obstacles (micro) and the array as a whole (macro).

For a single (linear) obstacle it is perhaps unsurprising that the results indicate that as angle of approach increases, thereby reducing cross sectional width, avoidance increases (in this case of a single obstacle micro and macro avoidance are identical).

For an array we record both the probability of avoiding obstacles (micro avoidance) and the array as a whole (macro avoidance). Given zero preference for avoidance behaviour all groups intersect the array. Here, the avoidance of obstacles (micro avoidance) indicates the likelihood of random spatial positioning presenting a direct route through the array. This reflects the proportion of the cross sectional width (of the array) which is occupied by obstacles. For an array, which contains 25 obstacles arranged in a square with uniform spacing of 500 metres, Figure 5.7(b) suggests that an angle of approximately 0.2 radians (12 degrees) minimises the direct routes. The maximum micro avoidance rate is observed when the angle of approach is perpendicular to the array layout where obstacles align resulting in maximum spacing. When avoidance preference is applied no intersections with obstacles are observed (micro avoidance is constant at 100%). However, the probability of avoiding the array as a whole now varies. It may be reasonable to anticipate that the most avoidance will be exhibited at 12 degrees where the fewest clear routes are visible. This appears not to be the case. Instead, 45 degrees is shown to be the ideal angle of approach to maximise the macro avoidance rate.

5.3.3 Strike probability

The improvements in obstacle representation mean that rather than simply detecting collisions it is now possible to identify intersections. In the case of wind turbines an intersection does not necessarily result in a collision. This risk is dependent upon the angle of intersection and mechanical properties relating to the turbine structure, such as blade length. The lack of visual occlusion offered by wind turbines means that individuals which survive an intersection could, through social attraction, encourage others to do the same thereby altering the probability of avoidance. This
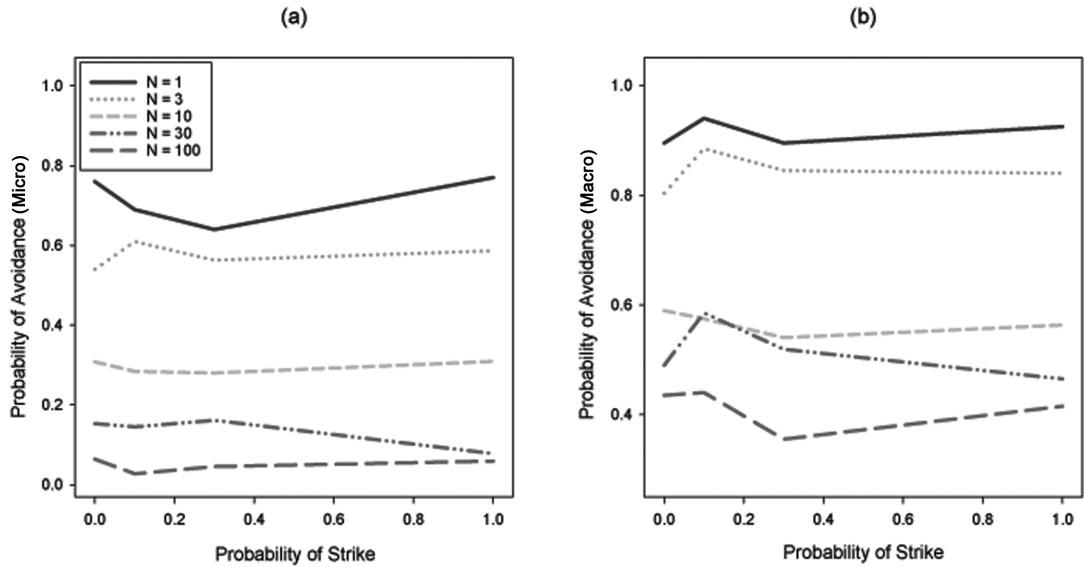
Figure 5.8: Avoidance rates are unaffected by the strike probability associated with obstacle intersections. For social groups ($w_s = 1$) of varying size with baseline target preference ($w_{t0} = 0.1$) plots show: (a) probability of avoiding a single obstacles ($w_o = 0.3$); (b) probability of avoiding the region bounding an array containing 25 obstacles uniformly arranged on a square grid at 500 metre intervals ($w_o = 1$); as a function of the probability of striking obstacles given an intersection. The results show no significant trends relating the avoidance to the probability of striking an obstacle.

can be assessed by applying a simple fixed probability of striking the rotor given an intersection, the strike probability.

The results shown in Figure 5.8 demonstrate that, at least for the obstacle representation used in these simulations, the threat of collision given an intersection has no bearing on avoidance. This is perhaps due to the choice of obstacle granularity which, as a consequence of using relative distance to determine selection weighting, suppresses any chance of interactions between neighbours either side of the obstacle.
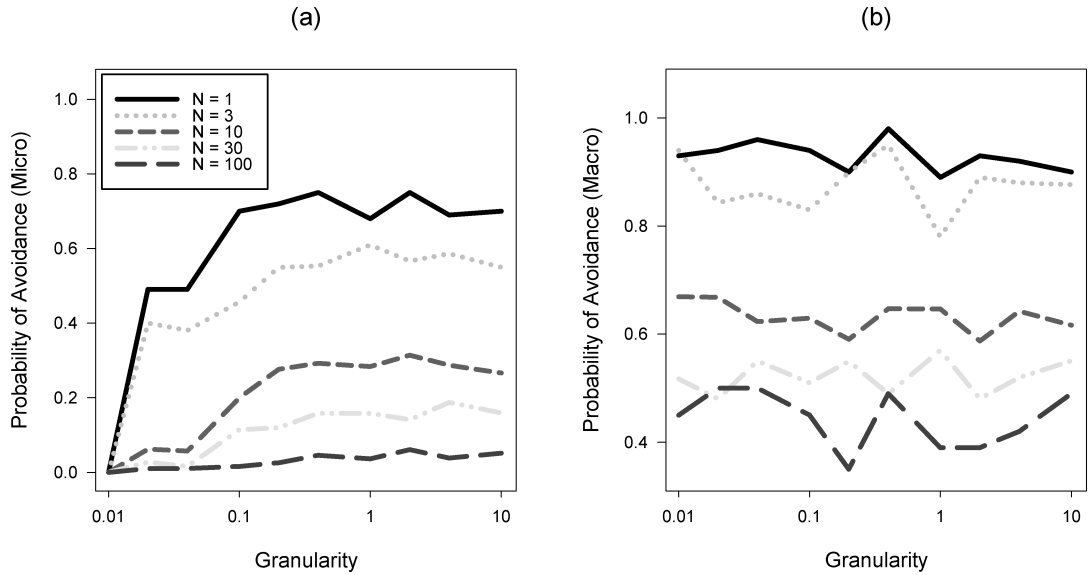
5.3.4 Granularity

In previous simulations we have defined obstacles with a standard density, or granularity g, of 1 vertex per spatial unit. It is argued that this is required in order to ensure

that individuals can accurately identify the correct behavioural response (illustrated in Figure 2.1). However, there is an increasing need to consider more realistic obstacles where perceptual variation, such as the varying degrees of transparency exhibited between a moving wind turbine blade and the supporting tower, may elicit a different avoidance response. One way that this distinction could be simulated without altering the way individuals respond to obstacle vertices would be to vary the granularity of obstacles, or specific sections of the same obstacle.

It is reasonable to assume that if we simply reduced the granularity of an obstacle then avoidance would also be reduced as fewer vertices would mean a smaller overall probability of selecting an avoidance behaviour relative to social and target navigation. However, as already stated granularity may also influence the accuracy with which individuals categorise behavioural response. To explore this effect in isolation we perform simulations using obstacles with varying uniform granularity maintaining the total weight of avoidance for each obstacle. This is done by scaling the weight of avoidance (w_o) relative to that used for the standard representation containing 101 vertices (w_o^*) such that $w_o = w_o^*(101/(100g + 1))$.

Figure 5.9(a) shows that for interactions with a single obstacle, where collisions are possible, that as granularity is reduced there is a critical limit below which detection errors begin to occur reducing avoidance. This result is analogous with observations regarding the spacing between obstacles in an array (Section 5.3.1). The limit of granularity corresponds to an approximate spacing of 7 spatial units which given the parameterisation defined in Table 4.1 is consistent with the argument presented by Figure 2.1. It is suggested in the previous section that the choice of granularity may prevent social interactions across obstacles. However, when granularity was reduced no qualitative differences were observed between the behaviour of asocial $(N = 1)$ and social groups $(N > 1)$.

Figure 5.9(b) shows that at an array level behaviour appears invariant to obstacle representation. This could be as avoidance occurs on a different spatial scale where relatively small changes in granularity have no relative impact on perception.

Figure 5.9: Avoidance rates are reduced when granularity falls below the minimum density required to detect the correct behavioural response. For social groups ($w_s = 1$) of varying size with baseline target preference ($w_{t0} = 0.1$) plots show: (a) probability of avoiding a single obstacles ($w_o = 0.3 * (101/(100g + 1))$); (b) probability of avoiding the region bounding an array containing 25 obstacles uniformly arranged on a square grid at 500 metre intervals ($w_o = 1 * (101/(100g + 1))$); as a function of obstacle granularity (the density of vertices comprising the obstacle). It is important to note that obstacle avoidance weighting is scaled relative to that used in simulation with the standard obstacle representation containing 101 vertices in order to maintain a constant avoidance potential for the obstacle(s) as a whole relative to social and target navigation. In the case of interactions with a single obstacle, where individuals tend to move closer to obstacles, the results show that despite offering the same combined "strength" of avoidance there exists a critical density below which errors in judgment lead to reduced avoidance. In simulations with obstacle arrays the cumulative response to all vertices remains sufficient to maintain accurate avoidance at all levels of granularity.

5.4 Discussion

In general our results compare well with the broad scale conclusions presented in Masden et al. (2012), specifically that avoidance increases when the spacing between columns is reduced. Whilst intuitive, it provides important validation that the model behaves in a reasonable manner. However, the observations regarding numbers of rows is not consistent. We observe no significant relationship between avoidance of the array and the numbers of rows. This could be caused by several modelling choices which combine to limit the impact. Firstly, the decision to investigate flocks approaching the array head on means the linear projection or perceived cross section remains constant, whereas in Masden et al. (2012) trajectories from 10 approach angles are combined each experiencing a different perception which varies dependent on numbers of rows (the more rows, the less apparent space is between obstacles, which we have already seen promotes avoidance).

Perhaps the most interesting result is that the angle of approach can affect avoidance so significantly. Unexpectedly it is not the angle where apparent spacing between columns is minimised (12 degrees) that yields the most avoidance but rather an angle of 45 degrees. This is consistent with a similar simulation in Masden et al. (2012) which demonstrates that arrays arranged in a diagonal produce the least straight trajectories and appears to show that this is due to increased avoidance. This may be explained by considering the perception of the array at this angle. As individuals move towards the array obstacles nearer to the interior will be closer and hence appear larger effecting a greater avoidance response than those at the outer edges which are further away. This biases movement away from the centre of the array, reinforcing movements towards the exterior edges and therefore promoting avoidance. In short, approaching the array at this angle presents clear avoidance strategies facilitating early decision making even in an egalitarian group. Conversely, in the case where no gaps are visible, groups heading towards the interior of the array have no clear avoidance strategy, i.e. the obstacle appears to be infinite in both directions. Here, group decisions are only affected through the emergence of a leader (discussed in

146

Chapter 4) on the periphery who is eventually able to encourage the group in their chosen direction. Otherwise, deadlock results in no decision at all with the group entering the array.

In order to test potential mechanisms through which realistic differences in the properties of obstacles may be simulated while maintaining a consistent approach to determine avoidance responses we explored the effects of parameters relating to obstacle representation, namely the strike probability and granularity. It has been suggested that strike probability may affect avoidance as individuals surviving an intersection could encourage others to follow. However, our results show that this is not the case; there is no relationship between strike probability and avoidance in the current implementation of the model. Whilst it is initially argued that this may be due to the choice of obstacle granularity, and that reducing this value may allow social interactions across obstacles to impact avoidance, further investigation showed no evidence to support this explanation. Instead it is likely that the use of relative distance to scale selection weightings may prohibit the emergence of this behaviour; as an individual moves closer to an obstacle the relative distance to vertices tends towards zero and since no limit has been defined the corresponding weight of avoidance approaches infinity. This may also explain the lack of collisions observed in our simulations. To rectify this a minimum distance could be defined below which the weighting for a particular update partner no longer increases. The impact of granularity on avoidance behaves as anticipated demonstrating that as the spacing between vertices increases there is a limit beyond which individuals can no longer accurately detect changes in appropriate behavioural response. This is important as it confirms that reducing granularity to simulate differences in perception will not only reduce avoidance due to a smaller overall weighting contributing to the decision process but may also introduce an additional detection error compounding the effect. Interestingly, the observed similarity of the effects of spacing between vertices within an obstacle and those of spacing between obstacles in an array suggest that there may be transferable properties visible at different spatial scales which may be used

147

to infer results across situations.

This chapter demonstrates the potential use of the model to assess avian avoidance rates at wind farms. We demonstrate that simulations produce sensible and explainable results which are comparable with those presented in existing work (Masden et al., 2012). Whilst no collisions are observed for any scenario the model does at least provide the functionality to record individual collisions as well as assess any potential disruption to group structure which is not a feature of other collision risk models including that developed by Masden et al. (2012). This is vitally important to fully understand collision risk and adds to the discussion regarding energy expenditure with disruption and splitting of flocks potentially leading to greater energy expenditure, not just as a result of direct avoidance but longer term post avoidance, as smaller groups are aerodynamically less efficient (Kshatriya and Blake, 1992) and potentially susceptible to poorer navigation (Codling et al., 2007).

Chapter 6

Discussion and conclusions

6.1 Discussion

The study of collective motion is a rapidly emerging field of research with diverse applications in biology, physics and computer science. For biological systems in particular collective motion can occur in many different forms (Krause and Ruxton, 2002). This has inspired a wide range of empirical and modelling studies as scientists seek to understand how and why distinctive movement patterns evolve (e.g. Couzin et al., 2002; Wood and Ackland, 2007; Ballerini et al., 2008a; Bode et al., 2012b; Nagy et al., 2013). Prior to the work presented in this thesis no studies had explicitly investigated the impact of social interactions within animal groups on an individual's ability to avoid obstacles. The capability to avoid hazardous obstacles is an important feature of navigation within natural environments and understanding the mechanisms which result in successful avoidance manoeuvres could provide insights into the cause of animal collisions with man-made structures. With the rapid development of the wind power industry in the UK this has become a significant ecological problem which must be addressed (Elphick, 2008). The discussion presented in this chapter aims to assess the impact of this thesis to the fields of collective motion and avian collision risk modelling.

Impact on modelling collective motion

The most significant contribution of this thesis to the modelling of collective motion is the introduction and representation of obstacles. Rather than obstacles comprising of primitive solid shapes each with distinct geometric characteristics and computations as described in Reynolds (1987), obstacles are instead represented as a finite set of points (see Figure 2.1). In this way obstacles of any shape or size can be approximated free from the inherent problems associated with intersections between lines and complex polyhedra. Importantly, each point can be considered and interacted with independently, in an equivalent manner to that defined for social interactions (see Figure 1.1), according to rules based on a generalised geometric computation. This mechanism provides a simple and intuitive approach for incorporating obstacles into

any existing individual based model. An interesting feature of representing obstacles as a set of points is that approximation error, controlled by the spacing between points, can become a model parameter. Varying the density of points can represent differences in obstacle perception and therefore avoidance behaviour. For example, decreasing the density of points results in fewer obstacle interactions being represented and induces a less extreme avoidance response. This could represent a set of obstacles or areas of a single obstacle which are transparent or less easily observed. Where obstacles of the same size may be perceived differently, for example due to differences in colour, variations in the density of points will allow appropriate avoidance responses to be simulated without altering the core behavioural mechanisms for avoidance. The application of this has summarily been explored in Chapter 5 using obstacles with uniform spacing. An interesting observation is a similarity in the effects of spacing between vertices within an obstacle and those of spacing between obstacles in an array. This suggests that there may be transferable properties visible at different spatial scales which may be used in future to infer results across situations.

Prior to the work in this thesis it had been asserted that it was advantageous to navigate as part of a group (Codling et al., 2007; Codling and Bode, 2014). However, the studies in Chapters 2 and 4 have shown that this is not necessarily the case where obstacle avoidance is required. The asynchronous modelling approach outlined in Chapter 4 has provided valuable insights into the mechanisms which influence avoidance behaviours. The algorithmic implementation reduces averaging and allows the flow of information to be traced more clearly through the group. This has led to the concepts discussed in Section 4.6 and the explanation developed here can be applied to reinterpret the results in Chapter 2. Avoidance behaviour is highly dependent on spatial position and the responses of individuals to obstacles can be contradictory. In small groups an averaged decision can be subject to bias from particular individuals. However, for larger groups, the number of individuals that contribute to decisions is unlikely to result in significant bias towards a clear avoidance response. These deadlocks lead to an increased collision risk. Perhaps the

most difficult result to explain is the observation that highly social groups display decreased collision risk compared with moderately social groups despite reduced obstacle awareness. In these groups fewer individuals are informed about the location of obstacles and so the averaged group decision has more potential to be biased resulting in a coherent avoidance manoeuvre; similar ideas are discussed in Leonard et al. (2012).

The application of underlying network structures in Chapter 4 has shown that any social heterogeneity facilitates group decision making and therefore effective avoidance behaviour. Such networks could provide a natural mechanism by which deadlocked decisions may be broken. The results in Figure 4.3 show that groups with fewer influential individuals are more likely to display successful avoidance. However, this comes at the cost of cohesion and groups must balance staying together against the benefits of more effective decision making. This perhaps suggests that social networks in animal groups are most likely to contain multiple influential individuals rather than a single leader.

Impact on avian collision risk modelling

The remote location of wind farms, particularly those situated offshore, presents difficulties in obtaining detailed empirical estimates of collision risk (Langston and Pullan, 2003). Models have become an important tool for predicting collision risk for many species. Whilst these models are generally robust, accurate quantitative assessment has been limited by the availability of avoidance rates which account for the behavioural response of birds towards wind farm structures (Chamberlain et al., 2006). This behavioural response is based on many implicit factors such as the configuration and internal communication of flocks (flock size and social interactions) as well as the spatial configuration of wind farms (Drewitt and Langston, 2008). Estimates for avoidance response have been found to be highly site- and species-specific (Cook et al., 2012). However, the current guidance for impact assessment studies assumes a fixed rate of avoidance for each species (the avoidance rate for

geese is estimated to be approximately 99.8%) based on empirical evidence (Scottish Natural Heritage, 2013). The modelling frameworks described in this thesis provide a platform in which the relationship between avoidance and implicit factors, such as flock size, can be explored and understood.

The key finding of this work is that social interactions within groups induce a significant non-linear relationship between collision risk and group size. The initial investigation in Chapter 2 shows that, for interactions with a single "wind-turbine" like obstacle, in the absence of social interactions (asocial groups) risk is independent of group size. This supports the use of a fixed avoidance rate. However, when social interactions are applied, avoidance displays a clear dependence on group size, with increased risk for individuals belonging to larger groups. Intuitively this result is understandable; increasing the number of individuals creates a more cluttered environment limiting the available space for manoeuvres resulting in a greater risk of collision.

Despite a different algorithmic approach, the study in Chapter 4 confirms this result for a single obstacle and demonstrates that when extended to consider an array containing multiple obstacles an identical dependence between avoidance (of the array) and group size is observed. For geese in particular, which have been shown to interact and navigate socially (Kurvers et al., 2009), this could have significant implications for the way collision risk is estimated. It must be concluded that the assumption that avoidance is independent of situation specific factors, and can be applied as a constant is unsupportable.

The work in Chapter 4 shows that the model can reproduce the estimated avoidance rates from empirical studies. This study demonstrates that the model can provide insight into the effect of environmental conditions on collision risk which has been difficult to assess using empirical techniques (Section 4.5). In addition, it is shown that spatial considerations, such as the angle at which flocks approach a wind farm, can have a significant effect on avoidance (Section 5.3.2). The model provides a powerful tool in which these different social, environmental and engineering

scenarios can be explored, both pre- and post- construction, to predict situation specific avoidance rates and inform decisions regarding potential mitigation strategies. However, this relies on the availability of empirical data. In order to provide reliable quantitative predictions the model requires species specific parameters to characterise behaviour; these parameters are not site specific and once determined can be applied generally. In recent years stereoscopic vision techniques have been developed to track the motion of animals and provide the data necessary to identify such parameters. This technology has evolved and become more mobile, allowing the movements of even the smallest of animals, for example clouds of midges, to be observed and accurately tracked in their natural environment (Attanasi et al., 2014). This is critical for birds, such as geese, where it can be difficult to identify field sites with sufficient, repeatable activity.

One of the key observations from the model outlined in Chapter 4 is the similarity of movement patterns produced by groups with different underlying network structure; upon visual inspection there are no obvious characterising features which could be used to easily distinguish between movement patterns by network structure. It therefore seems reasonable to suggest that in the absence of individual level data, as is the case for radar studies typically used to investigate avoidance at wind farms, it is unlikely that the network structure of geese could be inferred with an degree of certainty. Empirical evidence has indicated that hierarchical interactions are likely to exist within groups of moving animals and models, including those presented in this thesis, have shown that these structures could have a significant impact on group movement. It is critical that these network structures be accurately determined in order to identify their impact on collision risk. The identification of social networks has become an emerging area of interest within studies of collective motion. Studies have exploited modern GPS technologies to observe social structure of birds in flight (e.g. Nagy et al., 2013). This technology is promising and could be implemented not only to identify these networks but to provide more accurate empirical data for the interaction of groups with obstacles.

6.2   Conclusions and further work

Whilst the models presented in this thesis have provided a rigorous platform for future research, it is clear that further detailed development is needed. In order to model birds more realistically it is necessary to consider movements in three-dimensions. This has always been a consideration throughout the development process and modelling decisions have been made in order to facilitate a simple transition to three-dimensional space without the need to alter the existing framework. These developments are important to investigate the effect of flight height on collisions where accurate empirical observation is difficult.

The results of model simulations have shown consistently that the presence of social interactions can have a large effect on the avoidance response of groups towards wind turbines. It must be concluded from this work that the simple assumption made by all collision risk models that avoidance rates are independent of social factors, such as group size, cannot be supported.

Crucially, the models presented have demonstrated an ability to test hypotheses about collision risk which are challenging to observe empirically, for example the effects of poor visibility where use of the visual techniques argued necessary to assess the behaviour of socially navigating groups would be seriously limited. This will be particularly important to supplement discussions relating to vertical avoidance at wind farms which currently relies upon human observation.

Despite having been explicitly developed to consider geese and wind farms the models are general and therefore not limited to this particular example of collective motion. The versatility of the modelling approach makes it a powerful tool to improve understanding of collective motion. The obstacle representation used throughout this work is widely applicable and can be introduced into other individual based model frameworks. An extension of these models could be used to explore the impact of other renewable technologies on socially navigating animals, for example fish interacting with tidal turbines, which is an area of growing concern amongst ecologists.

The study of collective motion has been largely exploratory, but there are many

important ecological problems where it can be applied. The application in this thesis is only an example, but has shown that the ideas that have been generated over the past decade provide a robust basis on which tools can be developed to address these issues. This perhaps signals the evolution of this field towards a more translational science.

List of references

M.V. Abrahams and P.W. Colgan. Risk of predation, hydrodynamic efficiency and their influence on school structure. *Environmental Biology of Fishes*, 13(3):195–202, 1985.

I. Aoki. An analysis of the schooling behavior of fish: internal organization and communication process. *Bulletin of The Ocean Research Institute, University of Tokyo (Japan)*, 12:1–62, 1980.

I. Aoki. A simulation study on the schooling mechanism in fish. *Bulletin of The Japanese Society of Fisheries Science*, 48(8):1081–1088, 1982.

A. Attanasi, A. Cavagna, L. Del Castello, I. Giardina, S. Melillo, L. Parisi, O. Pohl, B. Rossaro, E. Shen, E. Silvestri, and M. Viale. Collective behaviour without collective order in wild swarms of midges. *PLoS Computational Biology*, 10(7): e1003697, 2014.

I.L. Bajec and F.H. Heppner. Organized flight in birds. *Animal Behaviour*, 78(4): 777–789, 2009.

M. Ballerini, N. Cabibbo, R. Candelier, A. Cavagna, E. Cisbani, I. Giardina, V. Lecomte, A. Orlandi, G. Parisi, A. Procaccini, M. Viale, and V. Zdravkovic. Interaction ruling animal collective behavior depends on topological rather than metric distance: evidence from a field study. *Proceedings of the National Academy of Sciences*, 105(4):1232–1237, 2008a.

M. Ballerini, N. Cabibbo, R. Candelier, A. Cavagna, E. Cisbani, I. Giardina, A. Orlandi, G. Parisi, A. Procaccini, M. Viale, et al. Empirical investigation of starling flocks: a benchmark study in collective animal behaviour. *Animal Behaviour*, 76(1):201–215, 2008b.

W. Band. Windfarms and birds: calculating a theoretical collision risk assuming no avoiding action. Technical report, Scottish Natural Heritage, 2000.

W. Band, M. Madders, and D.P. Whitfield. Developing field and analytical methods to assess avian collision risk at wind farms. In M. De Lucas, G. Janss, and M. Ferrer, editors, *Birds and wind power*, pages 259–275. Lynx Edicions, Barcelona, Spain, 2005.

R.C. Banks. Human-related mortality of birds in the united states. Technical report, Washington, DC: US Fish and Wildlife Service, 1979. Special Scientific Report.

L. Barrios and A. Rodriguez. Behavioural and environmental correlates of soaring-bird mortality at on-shore wind turbines. *Journal of Applied Ecology*, 41(1):72–81, 2004.

G. Beauchamp. Individual differences in activity and exploration incluence leadership in pairs of foraging zerba finches. *Behaviour*, 137(3):301–314, 2000.

K. Bevanger. Biological and conservation aspects of bird mortality caused by electricity power lines: a review. *Biological Conservation*, 86(1):67–76, 1998.

D. Biro, R. Freeman, J. Meade, S. Roberts, and T. Guilford. Pigeons combine compass and landmark guidance in familiar route navigation. *Proceedings of the National Academy of Sciences*, 104(18):7471–7476, 2007.

N.W.F. Bode, J.J. Faria, D.W. Franks, J. Krause, and A.J. Wood. How perceived threat increases synchronization in collectively moving animal groups. *Proceedings of the Royal Society of London B: Biological Sciences*, 277(1697):3065–3070, 2010a.

N.W.F. Bode, D.W. Franks, and A.J. Wood. Making noise: emergent stochasticity in collective motion. *Journal of Theoretical Biology*, 267(3):292–299, 2010b.

N.W.F. Bode, D.W. Franks, and A.J. Wood. Limited interactions in flocks: relating model simulations to empirical data. *Journal of The Royal Society Interface*, 8(55): 301–304, 2011a.

N.W.F. Bode, D.W. Franks, and A.J. Wood. Social networks and models for collective motion in animals. *Behavioral Ecology and Sociobiology*, 65(2):117–130, 2011b.

N.W.F. Bode, A.J. Wood, and D.W. Franks. The impact of social networks on animal collective motion. *Animal Behaviour*, 82(1):29–38, 2011c.

N.W.F. Bode, D.W. Franks, and A.J. Wood. Leading from the front? social networks in navigating groups. *Behavioral Ecology and Sociobiology*, 66(6):835–843, 2012a.

N.W.F. Bode, D.W. Franks, A.J. Wood, J. Piercy, D.P. Croft, and E.A. Codling. Distinguishing social from non-social navigation in cohesive animal groups. *American Naturalist*, 179(5):621–632, 2012b.

N.W.F. Bode, A.J. Wood, and D.W. Franks. Social networks improve leaderless group navigation by facilitating long-distance communication. *Current Zoology*, 58 (2):329–341, 2012c.

N.W.F. Bode, A.U.K. Wagoum, and E.A. Codling. Human responses to multiple sources of directional information in virtual crowd evacuations. *Journal of The Royal Society Interface*, 11(91):20130904, 2014.

M. Botsch, L. Kobbelt, M. Pauly, P. Alliez, and B. Lévy. *Polygon mesh processing.* CRC press, 2010.

J. Bouguet. Camera calibration toolbox for Matlab$^{\circledR}$, September 2014. URL `http://www.vision.caltech.edu/bouguetj/calib_doc/index.html`.

R. Budgey. Three dimensional bird flock structure and its implications for birdstrike tolerence in aircraft. *Proceedings of the International Bird Strike Committee (IBSC)*, 24:307–320, 1998.

J. Buhl, D.J.T. Sumpter, I.D. Couzin, J.J. Hale, E. Despland, E.R. Miller, and S.J. Simpson. From disorder to order in marching locusts. *Science*, 312(5778):1402–1406, 2006.

A. Cavagna, I. Giardina, A. Orlandi, G. Parisi, A. Procaccini, M. Viale, and V. Zdravkovic. The starflag handbook on collective animal behaviour: 1. empirical methods. *Animal Behaviour*, 76(1):217–236, 2008.

A. Cavagna, A. Cimarelli, I. Giardina, G. Parisi, R. Santagati, F. Stefanini, and M. Viale. Scale-free correlations in starling flocks. *Proceedings of the National Academy of Sciences*, 107(26):11865–11870, 2010.

D.E. Chamberlain, M.R. Rehfisch, A.D. Fox, M. Desholm, and S.J. Anthony. The effect of avoidance rates on bird mortality predictions made by wind turbine collision risk models. *Ibis*, 148(s1):198–202, 2006.

O. Chepizhko, E.G. Altmann, and F. Peruani. Optimal noise maximizes collective motion in heterogeneous media. *Physical Review Letters*, 110(23):238101, 2013.

E.A. Codling and N.W.F. Bode. Copycat dynamics in leaderless animal group navigation. *Movement Ecology*, 2(1):11, 2014.

E.A. Codling, N.A. Hill, J.W. Pitchford, and S.D. Simpson. Random walk models for the movement and recruitment of reef fish larvae. *Marine Ecology Progress Series*, 279:215–224, 2004.

E.A. Codling, J.W. Pitchford, and S.D. Simpson. Group navigation and the "many-wrongs principle" in models of animal movement. *Ecology*, 88(7):1864–1870, 2007.

Commission of the European Communities. Renewable energy road map. renewable

energies in the 21st century: building a more sustainable future. Technical report, Commission of the European Communities, January 2007.

Committee on Climate Change. Renewable energy review. a report from the committee on climate change to the uk parliament. Technical report, Committee on Climate Change, May 2011.

L. Conradt, J. Krause, I.D. Couzin, and T.J. Roper. "Leading according to need" in self-organizing groups. *American Naturalist*, 173(3):304–312, 2009.

A.S.C.P. Cook, A. Johnston, L.J. Wright, and N.H.K. Burton. A review of flight heights and avoidance rates of birds in relation to offshore windfarms. *British Trust for Ornithology Research Report*, 618, 2012.

N. Correll, G. Sempo, Y. Lopez de Meneses, J. Halloy, J.L. Deneubourg, and A. Martinoli. Swistrack: a tracking tool for multi-unit robotic and biological research. In *Proceedings of Intelligent Robots and Systems (IROS)*, pages 2185–2191, 2006.

I.D. Couzin, J. Krause, R. James, G.D. Ruxton, and N.R. Franks. Collective memory and spatial sorting in animal groups. *Journal of Theoretical Biology*, 218(1):1–11, 2002.

I.D. Couzin, J. Krause, N.R. Franks, and S.A. Levin. Effective leadership and decision making in animal groups on the move. *Nature*, 433(7025):513–516, 2005.

D.P. Croft, R. James, and J. Krause. *Exploring animal social networks*. Princeton University Press, 2008.

S. Croft, R. Budgey, J.W. Pitchford, and A.J. Wood. The influence of group size and social interactions on collision risk with obstacles. *Ecological Complexity*, 16:77–82, 2013.

S. Croft, R. Budgey, J.W. Pitchford, and A.J. Wood. Obstacle avoidance in social

groups: new insights from asynchronous models. *Journal of The Royal Society Interface*, 12(106):20150178, 2015.

J.M. Cullen, E. Shaw, and H.A. Baldwin. Methods for measuring the three-dimensional structure of fish schools. *Animal Behaviour*, 13(4):534–543, 1965.

A. Czirók and T. Vicsek. Collective motion. In T. Vicsek, editor, *Fluctuations and scaling in biology*, pages 177–242. Oxford University Press, UK, 2001.

A. Czirók, M. Vicsek, and T. Vicsek. Collective motion of organisms in three dimensions. *Physica A: Statistical Mechanics and its Applications*, 264(1):299–304, 1999.

M. Desholm and J. Kahlert. Avian collision risk at an offshore wind farm. *Biology Letters*, 1(3):296–298, 2005.

M. Desholm, A.D. Fox, P.D.L. Beasley, and J. Kahlert. Remote techniques for counting and estimating the number of bird-wind turbine collisions at sea: a review. *Ibis*, 148(s1):76–89, 2006.

A.L. Drewitt and R.H.W. Langston. Collision effects of wind-power generators and other obstacles on birds. *Annals of the New York Academy of Sciences*, 1134(1): 233–266, 2008.

B. Dumont, A. Boissy, C. Achard, A.M. Sibbald, and H.W. Erhard. Consistency of animal order in spontaneous group movements allows the measurement of leadership in a group of grazing heifers. *Applied Animal Behaviour Science*, 95 (1):55–66, 2005.

L. Edelstein-Keshet, J. Watmough, and D. Grunbaum. Do travelling band solutions describe cohesive swarms? an investigation for migratory locusts. *Journal of Mathematical Biology*, 36(6):515–549, 1998.

R. Eftimie, G. de Vries, M.A. Lewis, and F. Lutscher. Modeling group formation

and activity patterns in self-organizing collectives of individuals. *Bulletin of Mathematical Biology*, 69(5):1537–1565, 2007.

C. Elphick. Editor's choice: New research on wind farms. *Journal of Applied Ecology*, 45(6):1840–1840, 2008.

J. Emmerton and J.D. Delius. Beyond sensation: Visual cognition in pigeons. *Vision, brain, and behavior in birds*, pages 377–390, 1993.

A.H. Fielding, D.P. Whitfield, and D.R.A. Mcleod. Spatial association as an indicator of the potential for future interactions between wind energy developments and golden eagles *Aquila chrysaetos* in scotland. *Biological Conservation*, 131(3):359–369, 2006.

J.C. Flack. Multiple time-scales and the developmental dynamics of social systems. *Philosophical Transactions of the Royal Society B: Biological Sciences*, 367(1597): 1802–1810, 2012.

A.D. Fox, M. Desholm, J. Kahlert, T.K. Christensen, and I.K. Petersen. Information needs to support environmental impact assessment of the effects of european offshore wind farms on birds. *Ibis*, 148(s1):129–144, 2006.

G.A. Frank and C.O. Dorso. Room evacuation in the presence of an obstacle. *Physica A: Statistical Mechanics and its Applications*, 390(11):2135–2145, 2011.

N.R. Franks, S.C. Pratt, E.B. Mallon, N.F. Britton, and D.J.T. Sumpter. Information flow, opinion polling and collective intelligence in house–hunting social insects. *Philosophical Transactions of the Royal Society of London B: Biological Sciences*, 357(1427):1567–1583, 2002.

R. Freeman, R. Mann, T. Guilford, and D. Biro. Group decisions and individual differences: route fidelity predicts flight leadership in homing pigeons (*Columba livia*). *Biology Letters*, 7(1):63–66, 2011.

S. Garthe and O. Hüppop. Scaling possible adverse effects of marine wind farms on seabirds: developing and applying a vulnerability index. *Journal of Applied Ecology*, 41(4):724–734, 2004.

D.T. Gillespie. Exact stochastic simulation of coupled chemical reactions. *The Journal of Physical Chemistry*, 81(25):2340–2361, 1977.

G. Grégoire and H. Chaté. Onset of collective and cohesive motion. *Physical Review Letters*, 92(2):25702, 2004.

V. Guttal and I.D. Couzin. Social interactions, information use, and the evolution of collective migration. *Proceedings of the National Academy of Sciences*, 107(37): 16172–16177, 2010.

W.D. Hamilton. Geometry for the selfish herd. *Journal of Theoretical Biology*, 31(2): 295–311, 1971.

J.L. Harcourt, T.Z. Ang, G. Sweetman, R.A. Johnstone, and A. Manica. Social feedback and the emergence of leaders and followers. *Current Biology*, 19(3):248–252, 2009.

R. Hartley and A. Zisserman. *Multiple view geometry in computer vision*. Cambridge University Press, UK, 2003.

Y. Hayakawa. Spatiotemporal dynamics of skeins of wild geese. *EPL (Europhysics Letters)*, 89(4):48004, 2010.

K. Healy, L. McNally, G.D. Ruxton, N. Cooper, and A.L. Jackson. Metabolic rate and body size are linked with perception of temporal information. *Animal Behaviour*, 86(4):685–696, 2013.

D. Helbing, I. Farkas, and T. Vicsek. Simulating dynamical features of escape panic. *Nature*, 407(6803):487–490, 2000.

C.K. Hemelrijk and H. Hildenbrandt. Some causes of the variable shape of flocks of birds. *PLoS ONE*, 6:e22479, 2011.

C.K. Hemelrijk and H. Hildenbrandt. Schools of fish and flocks of birds: their shape and internal structure by self-organization. *Interface Focus*, 2(6):726–737, 2012.

C.K. Hemelrijk and H. Kunz. Density distribution and size sorting in fish schools: an individual-based model. *Behavioral Ecology*, 16(1):178–187, 2005.

F.H. Heppner. Three-dimensional structure and dynamics of birds flocks. In J.K. Parrish and W.M. Hamner, editors, *Animal groups in three dimensions*, pages 68–89. Cambridge University Press, UK, 1997.

F.H. Heppner, J.L. Convissar, Jr. Moonan, D.E., and J.G.T. Anderson. Visual angle and formation flight in canada geese (*Branta canadensis*). *The Auk*, 102:195–198, 1985.

H. Hildenbrandt, C. Carere, and C.K. Hemelrijk. Self-organized aerial displays of thousands of starlings: a model. *Behavioural Ecology*, 21(6):1349–1359, 2010.

H. Hötker, K.M. Thomsen, and H. Jeromin. Impacts on biodiversity of exploitation of renewable energy sources: the example of birds and bats. Technical report, Nature and Biodiversity Conservation Union, 2006.

A. Huth and C. Wissel. The simulation of the movement of fish schools. *Journal of Theoretical Biology*, 156(3):365–385, 1992.

Y. Inada and K. Kawachi. Order and flexibility in the motion of fish schools. *Journal of Theoretical Biology*, 214(3):371–387, 2002.

G.F.E. Janss and M. Ferrer. Common crane and great bustard collision with power lines: collision rate and risk exposure. *Wildlife Society Bulletin*, pages 675–680, 2000.

K. Kawasaki. Diffusion and the formation of spatial distributions. *Mathematical Sciences*, 16(183):47–52, 1978.

A.J. King, C.M.S. Douglas, E. Huchard, N.J.B. Isaac, and G. Cowlishaw. Dominance and affiliation mediate despotism in a social primate. *Current Biology*, 18(23): 1833–1838, 2008.

D. Klem Jr, D.C. Keck, K.L. Marty, A.J. Miller Ball, E.E. Niciu, and C.T. Platt. Effects of window angling, feeder placement, and scavengers on avian mortality at plate glass. *The Wilson Bulletin*, 116(1):69–73, 2004.

J. Krause. Differential fitness returns in relation to spatial position in groups. *Biological Reviews*, 69(2):187–206, 1994.

J. Krause and G.D. Ruxton. *Living in groups*. Oxford University Press, UK, 2002.

J. Krause, R. James, D.W. Franks, D.P. Croft, et al. *Animal social networks*. Oxford University Press, UK, 2014.

M. Kshatriya and R.W. Blake. Theoretical model of the optimum flock size of birds flying in formation. *Journal of Theoretical Biology*, 157(2):135–174, 1992.

R. Kumar, J. Novak, and A. Tomkins. Structure and evolution of online social networks. In P.S. Yu, J. Han, and C. Faloutsos, editors, *Link mining: models, algorithms, and applications*, pages 337–357. Springer New York, 2010.

R.H.J.M. Kurvers, B. Eijkelenkamp, K. van Oers, B. van Lith, S.E. van Wieren, R. C. Ydenberg, and H.H.T. Prins. Personality differences explain leadership in barnacle geese. *Animal Behaviour*, 78(2):447–453, 2009.

J. Lamprecht. Variable leadership in bar-headed geese (*Anser indicus*): an analysis of pair and family departures. *Behaviour*, 122(1):105–120, 1992.

R. Langston and J.D. Pullan. *Wind farms and birds: an analysis of the effects of wind farms on birds, and guidance on environmental assessment criteria and site selection issues*. Council of Europe, 2003.

A.K. Larsson. The environmental impact from an offshore plant. *Wind Engineering*, 18:213–218, 1994.

N.E. Leonard, T. Shen, B. Nabet, L. Scardovi, I.D. Couzin, and S.A. Levin. Decision versus compromise for animal groups in motion. *Proceedings of the National Academy of Sciences*, 109(1):227–232, 2012.

M. Lindhe, P. Ogren, and K.H. Johansson. Flocking with obstacle avoidance: a new distributed coordination algorithm based on voronoi partitions. In *Proceedings of the IEEE International Conference on Robotics and Automation (ICRA)*, pages 1785–1790, 2005.

X. Lu, D. Colbry, and A.K. Jain. Three-dimensional model based face recognition. In *Proceedings of the 17th International Conference on Pattern Recognition (ICPR2004)*, volume 1, pages 362–366, 2004.

P.F. Major and L.M. Dill. The three-dimensional structure of airborne bird flocks. *Behavioural Ecology and Sociobiology*, 4(2):111–122, 1978.

G.R. Martin. Understanding bird collisions with man-made objects: a sensory ecology approach. *Ibis*, 153(2):239–254, 2011.

E.A. Masden, D.T. Haydon, A.D. Fox, R.W. Furness, R. Bullman, and M. Desholm. Barriers to movement: impacts of wind farms on migrating birds. *ICES Journal of Marine Science*, 66(4):746–753, 2009.

E.A. Masden, R. Reeve, M. Desholm, A.D. Fox, R.W. Furness, and D.T. Haydon. Assessing the impact of marine wind farms on birds through movement modelling. *Journal of The Royal Society Interface*, 9(74):2120–2130, 2012.

A. Mogilner and L. Edelstein-Keshet. A non-local model for a swarm. *Journal of Mathematical Biology*, 38(6):534–570, 1999.

M.L. Morrison. *Searcher bias and scavenging rates in bird/wind energy studies.* National Renewable Energy Laboratory Golden, CO, 2002.

M. Moussad, N. Perozo, S. Garnier, D. Helbing, and G. Theraulaz. The walking

behaviour of pedestrian social groups and its impact on crowd dynamics. *PLoS ONE*, 5(4):e10047, 2010.

M. Nagy, Z. Ákos, D. Biro, and T. Vicsek. Hierarchical group dynamics in pigeon flocks. *Nature*, 464(7290):890–893, 2010.

M. Nagy, G. Vásárhelyi, B. Pettit, I. Roberts-Mariani, T. Vicsek, and D. Biro. Context-dependent hierarchies in pigeons. *Proceedings of the National Academy of Sciences*, 110(32):13049–13054, 2013.

M. Newman. *Networks: an introduction.* Oxford University Press, 2010.

M.E.J. Newman. The structure and function of complex networks. *SIAM Review*, 45 (2):167–256, 2003.

H. Niwa. Newtonian dynamical approach to fish schooling. *Journal of Theoretical Biology*, 181(1):47–63, 1996.

M.A. Ogilvie. *Wild geese.* A & C Black, London, UK, 2011.

J.K. Parrish and L. Edelstein-Keshet. Complexity, pattern, and evolutionary trade-offs in animal aggregation. *Science*, 284(5411):99–101, 1999.

B.L. Partridge, T. Pitcher, J.M. Cullen, and J. Wilson. The three-dimensional structure of fish schools. *Behavioral Ecology and Sociobiology*, 6(4):277–288, 1980.

J.W. Pearce-Higgins, L. Stephen, A. Douse, and R.H.W. Langston. Greater impacts of wind farms on bird populations during construction than subsequent operation: results of a multi-site and multi-species analysis. *Journal of Applied Ecology*, 49 (2):386–394, 2012.

C. Pendlebury. *An appraisal of "A review of goose collisions at operating wind farms and estimation of the goose avoidance rate" by Fernley, J., Lowther, S. and Whitfield, P.* British Trust for Ornithology, 2006.

C.J. Pennycuick. *Modelling the flying bird.* Academic Press, Elsevier, London, UK, 2008.

N. Pinter-Wollman, E.A. Hobson, J.E. Smith, A.J. Edelman, D. Shizuka, S. de Silva, J.S. Waters, S.D. Prager, T. Sasaki, G. Wittemyer, J. Fewell, and D.B. McDonald. The dynamics of animal social networks: analytical, conceptual, and theoretical advances. *Behavioral Ecology*, 25(2):242–255, 2014.

T.J. Pitcher. *Behaviour of teleost fishes.* Chapman and Hall, London, UK, 1993.

P. Plonczkier and I.C. Simms. Radar monitoring of migrating pink-footed geese: behavioural responses to offshore wind farm development. *Journal of Applied Ecology*, 49(5):1187–1194, 2012.

H. Pomeroy and F.H. Heppner. Structure of turning in airborne rock dove (*Columba livia*) flocks. *The Auk*, pages 256–267, 1992.

H. Rackham. *Pliny's Natural History. Vol. X:XXXII.* Harvard University Press, Cambridge, Massachusetts, USA, 1933.

J.R. Raymond and M.R. Evans. Flocking regimes in a simple lattice model. *Physical Review E*, 73(3):036112, 2006.

C.W. Reynolds. Flocks, herds and schools: A distributed behavioral model. *SIGGRAPH Computer Graphics*, 21(4):25–34, 1987.

C.W. Reynolds. Not bumping into things. *Computer Graphics*, page G1, 1988.

T.O. Richardson, N. Perony, C.J. Tessone, C.A.H. Bousquet, M.B. Manser, and F. Schweitzer. A framework for extracting pairwise coupling information during collective animal motion. *ArXiv e-prints*, 1311.1417, 2014.

V.B. Scheffer. *Spires of form: glimpses of evolution.* Harcourt Brace Jovanovich, 1985.

Scottish Natural Heritage. Avoidance rates for wintering species of geese in scotland at onshore wind farms. Technical report, Scottish Natural Heritage, May 2013.

T.D Seeley, P.K. Visscher, T. Schlegel, P.M. Hogan, N.R. Franks, and J.A.R. Marshall. Stop signals provide cross inhibition in collective decision-making by honeybee swarms. *Science*, 335(6064):108–111, 2012.

T.D. Seeley et al. *Honeybee ecology: a study of adaptation in social life.* Princeton University Press, 1985.

E. Selous. *Thought-transference (or what?) in birds.* Constable & Company, 1931.

Siemens AG, April 2012. URL http://www.energy.siemens.com/hq/en/renewable-energy/wind-power/offshore.htm.

Siemens AG, February 2014. URL http://www.energy.siemens.com/hq/en/renewable-energy/wind-power/offshore.htm.

T. Stankowich. Marginal predation methodologies and the importance of predator preferences. *Animal Behaviour*, 66(3):589–599, 2003.

D. Strömbom. Collective motion from local attraction. *Journal of Theoretical Biology*, 283(1):145–151, 2011.

R.W. Sugg. An investigation into bird densities which might be encountered by an aircraft during take off and landing. Technical Report 6/65, Ministry of Aviation, London, UK, 1965.

D.J.T. Sumpter. The principles of collective animal behaviour. *Philosophical Transactions of the Royal Society B: Biological Sciences*, 361(1465):5–22, 2006.

W. Swaney, J. Kendal, H. Capon, C. Brown, and K.N. Laland. Familiarity facilitates social learning of foraging behaviour in the guppy. *Animal Behaviour*, 62(3):591–598, 2001.

R.W. Tegeder and J. Krause. Density dependence and numerosity in fright stimulated aggregation behaviour of shoaling fish. *Philosophical Transactions of the Royal Society of London B: Biological Sciences*, 350(1334):381–390, 1995.

C.M. Topaz, A.L. Bertozzi, and M.A. Lewis. A nonlocal continuum model for biological aggregation. *Bulletin of Mathematical Biology*, 68(7):1601–1623, 2006.

C.J. Torney, S.A. Levin, and I.D. Couzin. Specialization and evolutionary branching within migratory populations. *Proceedings of the National Academy of Sciences*, 107(47):20394–20399, 2010.

UK Renewables, April 2012. URL `http://www.bwea.com`.

UK Renewables, November 2013. URL `http://www.bwea.com`.

G.F. Van Tets. A photographic method of estimating densities of bird flocks in flight. *CSIRO Wildlife Research*, 11:103–110, 1966.

T. Vicsek. *Fluctuations and scaling in biology.* Oxford University Press, Oxford, UK, 2001.

T. Vicsek and A. Zafeiris. Collective motion. *Physics Reports*, 517(3):71–140, 2012.

T. Vicsek, A. Czirók, E. Ben-Jacob, I. Cohen, and O. Shochet. Novel type of phase transition in a system of self-driven particles. *Physical Review Letters*, 75(6):1226, 1995.

S.V. Viscido, J.K. Parrish, and D. Grnbaum. The effect of population size and number of influential neighbours on the emergent properties of fish schools. *Ecological Modelling*, 183(2):347–363, 2005.

A.J.W. Ward, D.J.T. Sumpter, I.D. Couzin, P.J.B. Hart, and J. Krause. Quorum decision-making facilitates information transfer in fish shoals. *Proceedings of the National Academy of Sciences*, 105(19):6948–6953, 2008.

D.J. Watts. The "new" science of networks. *Annual Review of Sociology*, 30(1): 243–270, 2004.

T. Wey, D.T. Blumstein, W. Shen, and F. Jordán. Social network analysis of animal behaviour: a promising tool for the study of sociality. *Animal Behaviour*, 75(2): 333–344, 2008.

H. Whitehead and S. Dufault. Techniques for analyzing vertebrate social structure using identified individuals: review. *Advances in the Study of Behavior*, 28:33, 1999.

A.J. Wood. Strategy selection under predation; evolutionary analysis of the emergence of cohesive aggregations. *Journal of Theoretical Biology*, 264(4):1102–1110, 2010.

A.J. Wood and G.J. Ackland. Evolving the selfish herd: emergence of distinct aggregating strategies in an individual-based model. *Proceedings of the Royal Society B: Biological Sciences*, 274(1618):1637–1642, 2007.

Z. Zhang. A flexible new technique for camera calibration. *IEEE Transactions on Pattern Analysis and Machine Intelligence*, 22(11):1330–1334, 2000.